PHILOSOPHICAL TRANSACTIONS OF THE ROYAL SOCIETY A MATHEMATICAL, PHYSICAL & ENGINEERING SCIENCES

Morphodynamics of Intertidal Dunes: A Year-Long Study at Lifeboat Station Bank, Wells-Next-the-Sea, Eastern England

J. R. L. Allen, P. F. Friend, Ann Lloyd and Helen Wells

Phil. Trans. R. Soc. Lond. A 1994 **347**, 291-344
doi: 10.1098/rsta.1994.0046

Morphodynamics of intertidal dunes: a year-long study at Lifeboat Station Bank, Wells-next-the-Sea, Eastern England†

By J. R. L. Allen[1], P. F. Friend[2], Ann Lloyd[1] and Helen Wells[1]

[1]*Postgraduate Research Institute for Sedimentology, The University, Reading RG6 2AB, U.K.*

[2]*Department of Earth Sciences, University of Cambridge, Cambridge CB2 3EQ, U.K.*

Contents

† This paper was produced from the authors' disk by using the TEX typesetting system.

Phil. Trans. R. Soc. Lond. A (1994) **347**, 291–345
Printed in Great Britain

10-2

Sand is driven clockwise by tidal currents round a diamond-shaped sand shoal in the entrance to the harbour at Wells-next-the-Sea. A population of dune bedforms occupying the ebb-dominated channel on the western side of the shoal was monitored for a year (October 1975 to October 1976) in terms of shape (height, wavelength, superimposed immature dunes), movement and bedform composition. Individual dunes and the population of dunes as a whole changed in response to sediment transport on astronomical tidal scales varying from the semi-diurnal to the equinoctial and in response to seasonal meteorological forcing. Most change occurred during the autumn and winter, when strong winds and gales created surges which, in some cases very significantly, enhanced the sediment transport due purely to the astronomical tide. Dune height was on average greatest during the winter, when the sea temperature was low, and least during the period of summer warmth. Dune height also varied substantially on a spring-neap tidal scale, an increase in height with the onset of many of the springs being followed by a gradual lowering. Dune wavelength showed little response to the spring-neap variation of sediment transport, but decreased significantly between winter and summer. Varying degrees of time-lag accompanied all changes in bedform characteristics in response to hydraulic change. Although individual dunes had surprisingly large lifespans and ebb-directed excursions, some change was noted in the composition and statistical attributes of the bedform population as the result of appearances and disappearances. The more vigorous episodes of sediment transport created immature (nascent) dunes, some of which grew large enough to become incorporated as new members into the population of mature forms. Internally, the dunes were dominated by ebb-oriented cross-bedding, complicated by a variety of intra-set discontinuities commonly associated with mud drapes. Some recorded the smoothing of crests during tidal reversal and others the immobility of the bedform over a number of tidal cycles (occasionally many). Other discontinuities expressed the 'capture' of immature dunes by the main bedform within the duration of a single ebb-tide. Because of the frequent perturbation of the (astronomical) tidal sediment transport by meterological events, little order to the horizontal arrangement of discontinuities within the sets was detected, in contrast to other reported cases.

1. Introduction

In what ways, and by what mechanisms, do bedforms respond to changing hydraulic conditions in natural sedimentary environments? Which responses to change become preserved within the bedforms, thus acquiring a further chance to become fossilized and exploited as environmental criteria? To contribute to these important and challenging questions, we return to Lifeboat Station Bank on the Norfolk coast (Allen & Friend 1976 *a*, *b*), and in this paper describe an intensive, year-long (1975–1976), and closely integrated study of a field of intertidal dunes.

Field studies of the changeability of bedforms in modern tidal environments were pioneered by Cornish (1901). Subsequent work has revealed a bewildering variety of responses but as yet no firm generalizations (Pretious & Blench 1951; G.P. Allen *et al.* 1969; Boothroyd & Hubbard 1974; Nasner 1974; Elliott & Gardiner 1981; Langhorne 1982; Langhorne *et al.* 1985; Terwindt & Brouwer 1986; Ehlers 1988; Kostaschuk *et al.* 1989; Davis & Flemming 1991). Useful insights into some of the mechanisms of change, however, have come from laboratory experiments (Simons & Richardson 1962; Gee 1975; Nakagawa *et al.* 1978; Nakagawa & Tsujimoto 1983; Wijbenga & Klassen 1983; Tsujimoto & Nakagawa 1984; Sawai 1988) and mathematical modelling (Allen 1974, 1976 *a–e*, 1978 *a*, *b*; Fredsøe 1979, 1981; Tsujimoto & Nakagawa 1984), drawing partly on concepts of population dynamics in biology under which change can occur through the operation of birth–death processes (Allen 1973). Otherwise, change among sandy bedforms is dependent on sediment transport, and consequently lags in some degree the change in hydraulic conditions which forces it. The degree of lag, however, varies with, among other things, the bedform cross-sectional area (roughly proportional to square of wavelength), and so may be difficult to detect, calling for dense time-series of data, in the case of comparatively small bedforms in the more energetic of environments (see Gabel 1993).

Boersma (1969), Klein (1970), and De Raaf & Boersma (1971) were the first to describe from tidal bedforms the internal structures due specifically to hydraulic change. Highly ordered structural patterns may result under simple tidal régimes (Terwindt 1975, 1981; Visser 1980; Boersma & Terwindt 1981; Kohsiek & Terwindt 1981; Van den Berg 1982; De Mowbray & Visser 1984; Allen 1985; De Boer *et al.* 1989), but it is now clear that a considerable variety of responses in the shape of internal structural features and arrangements is possible (Langhorne 1982; Dalrymple 1984), depending on bedform scale, tidal hydraulics and meteorological conditions. It remains uncertain to what extent the general models of internal structure proposed for tidal bedforms by Reineck (1963), McCave (1971), Allen (1980) and Stride (1982) are applicable in the field.

Our work represents a case-history that provides further critical evidence of the nature, preservation and causes of the responses of tidal bedforms to a complex sequence of hydraulic changes. Field data were gathered by A. L. and H. W., with guidance and assistance provided by J. R. L. A. and P. F. F.; laboratory work and data analysis were carried out by P. F. F. and J. R. L. A.

PHILOSOPHICAL TRANSACTIONS OF THE ROYAL SOCIETY A MATHEMATICAL, PHYSICAL & ENGINEERING SCIENCES

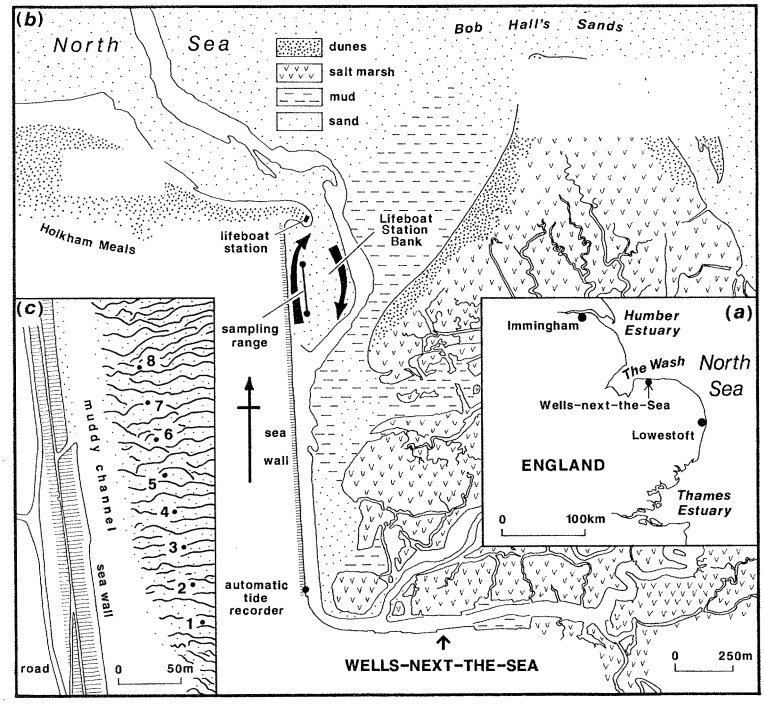

Figure 1. Lifeboat Station Bank and its context.

2. General setting

(a) *Morphology and sampling*

Lifeboat Station Bank (Brit. Nat. Grid Ref. TF 91 45) is an intertidal sand shoal within the main estuarine channel at Wells-next-the-Sea (see figures 1*a*, *b* and 2). This roughly diamond-shaped shoal measures approximately 600 m by 275 m, the western side adjoining the sea wall being the longest and also nearly straight. The crest ranges close to the southeastern edge of the bank before curving inward northwestward and then northward toward the Lifeboat Station. On the east the bank is skirted by the broad permanently flooded channel which ranges from the sea across Bob Hall's Sands toward the land. On the west, against the sea wall, lies a shallower channel drying at low tide.

Our dunes lay toward this western channel, where we studied their responses to changing tidal conditions by counting and measuring the features encountered on a fixed straight sampling range 208.1 m long defined by eight securely anchored buoys nominally 30 m apart (see figure 1*c*). Those bedforms intersected by this line of buoys constitute the population of dunes we describe below. Observations were made at most low-waters and cover 609 of a total of 719 tidal cycles; powerful lamps were used at night. We consequently sampled the population of three-dimensional bedforms in the channel two dimensionally, obtaining measurements on the sampling line of the horizontal position of elevation maxima (crests), together with the vertical elevation differences (local crest heights) between these maxima and the minima of elevation (troughs) next downstream (see figure 3). For practical reasons, horizontal measurements were based on crests, which were

Figure 2. Oblique aerial view of Lifeboat Station Bank looking north past the sea wall and Lifeboat Station to Bob Hall's Sands (see also figure 1). The distance across the foreground measures about 300 m, and across the background about 1 km. Arrows show facing direction of bedforms, as observed at low tide.

easily identified, rather than on troughs, which were difficult to locate accurately even when free from water. At each tide measurements began at the crest immediately south of buoy 1 and stopped at the first crest to north of buoy 8. Horizontal distances were measured to 0.05 m using a tape stretched taut between the buoys, the sideways deviation being no more than about 0.05 m from the straight-line position, even on the windiest days. Vertical distances were measured to 0.01 m using a graduated staff and a stiff rod fitted with a spirit level. These measurements were not applied to what were classed visually as nascent dunes (see § 4*b*), which were recorded separately. All bed features were described qualitatively during each low-water survey, and we paid special attention to indications on or near the range of the presence of new bedforms, and to signs of the spanwise migration of established structures. Hence we have a long time-series of precise, quantitative data about the bedforms in vertical two-dimensional profile, and some qualitative to semi-quantitative information concerning their three-dimensional character.

(*b*) *Tides*

The tidal streams circulate around Lifeboat Station Bank as is the case generally (Robinson 1960). The flood sweeps its eastern flank, leaving at low tide flood-oriented dunes east and north of the crest (see figure 2). The shoal elsewhere

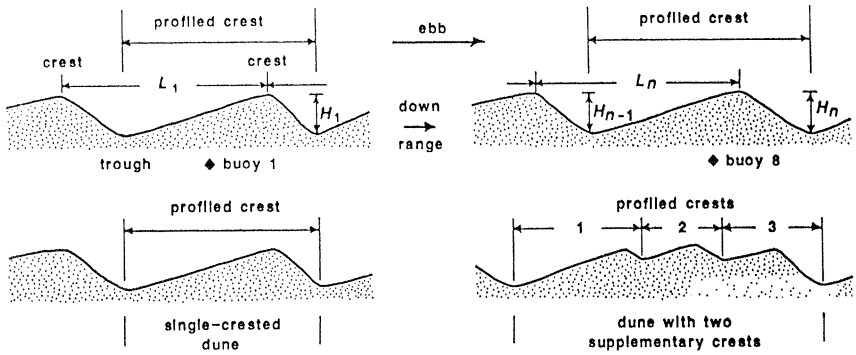

Figure 3. Definition diagram for field measurement of bedforms.

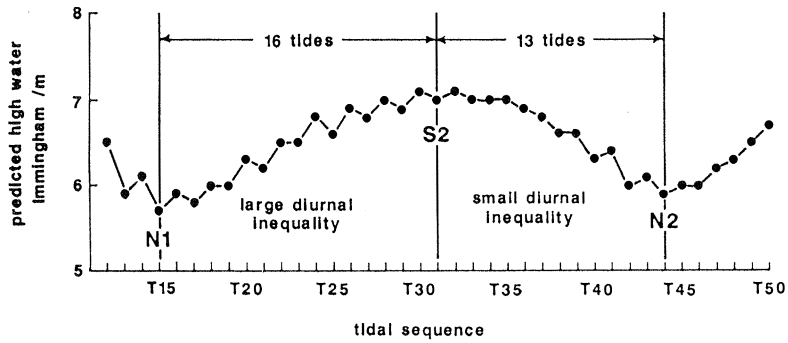

Figure 4. A representative spring-neap cycle of predicted tides at Immingham (11–31 October 1975).

carries ebb-oriented dunes driven by the ebb stream as it follows the shallower western channel containing the sampling range. These dunes survive the subordinate, flood tide (except for, at times, a slight rounding of the crests), and the field they occupy appears not to vary with seasonal changes in tidal conditions.

The régime is barely macrotidal (Davies 1964), semidiurnal, and with a marked diurnal inequality. Our study covered a total of 719 twice-daily cycles, from the high water at 0702 h GMT on 6 October 1975 to the cycle commencing at the high water of 2030 h GMT on 11 October 1976. These tides we number T1–T719. The sets of spring and neap tides included within the observation period are coded respectively S1–S26 and N1–N25. Spring-neap cycles are numbered SN1–SN26.

Wells-next-the-Sea (latitude 52° 57′ N, longitude 0° 51′ E) has no accredited tidal station, and tidal predictions are based on the standard port of Immingham (latitude 53° 58′ N, longitude 0° 11′ W) (see figure 1*a*). Here the extreme tidal range is 8.1 m, while that for mean spring tides is 6.4 m. Mean high water springs at Wells Harbour (landward of Lifeboat Station Bank) rise to −3.7 m of the predicted level at Immingham, both measured relative to chart datum, which at Wells is −0.75 m OD. Continuous measurements of actual water levels at Wells Harbour are made by the Anglian Water Authority's automatic tide recorder, positioned on the channel approximately 1.35 km south of our sampling range (see figure 1*b*). The stilling well of this gauge is a vertical concrete pipe, 2 m in diameter and 8 m long, connected to the channel by a 0.05 m diameter outlet pipe. The Anglian Water Authority generously gave us copies of the weekly charts.

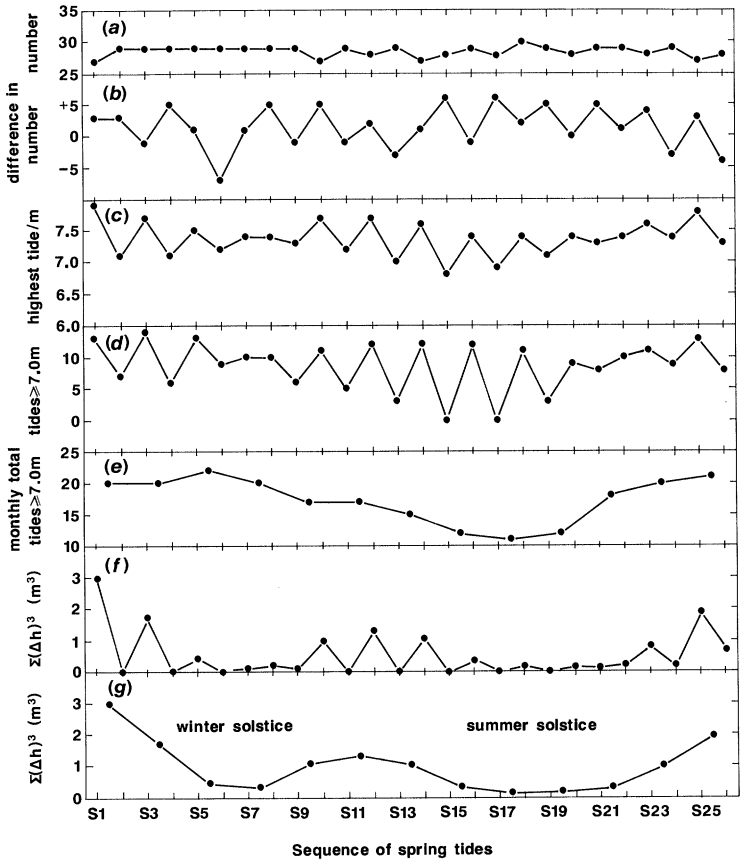

Figure 5. Summary of the predicted tides at Immingham over the period of the survey and their expected influence on sand transport. (*a*) Total of tides in spring-neap cycle. (*b*) Difference in number of tides between rising and falling limbs in a spring-neap cycle. (*c*) Height of highest tide in a spring-neap cycle. (*d*) Number of tides equal to or greater than 7.0 m in height in a spring-neap cycle. (*e*) Monthly total of tides equal to or greater than 7.0 m in height. (*f*), (*g*) Proxy quantities for total sediment transport on spring-neap and lunar monthly cycles respectively (see text for details).

Referring to Immingham, the astronomical tidal régime is unsteady: (i) within each twice-daily tide; (ii) on a nearly 25 h period between successive tidal cycles (diurnal inequality); (iii) on a roughly 14 d period between springs and neaps (spring-neap cycle); (iv) on an approximately 29 d period between alternate springs (lunar monthly inequality); and (v) on a roughly equinoctial period. In a representative run of predicted astronomical tides (SN2) at Immingham (see figure 4), there are two lengthy intervals over which a diurnal inequality of up to 0.3 m (approximately 0.15 m at Wells) is predicted. The spring-neap cycle SN2 is asymmetrical, the straight envelope of the rising limb being 16 tides long, whereas the descending limb is convex-upward and shorter. As the peak tidal-current velocity increases approximately linearly with tidal height, and the sand transport rate increases steeply nonlinearly with velocity, any sediment transport could be concentrated in the last half of such a cycle.

Figure 5 summarizes the predicted tide at Immingham. Spring-neap cycles

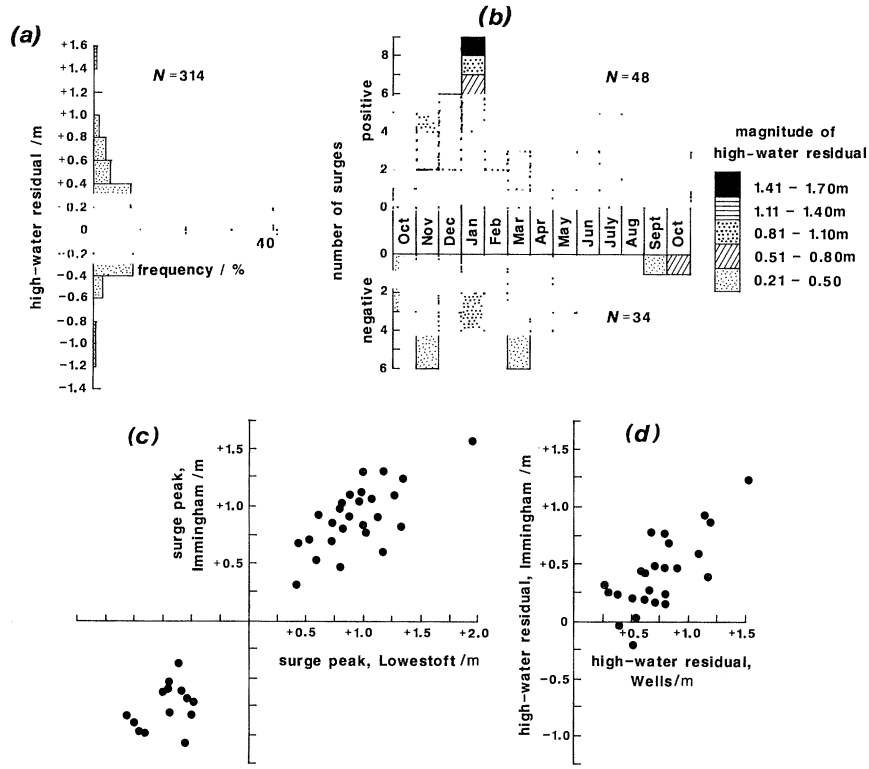

Figure 6. Summary of meteorological influences on observed tides at Wells-next-the-Sea over the survey period. See text for full explanation. (*a*) Frequency distribution of differences (residuals) between observed and predicted high-water levels. (*b*) Seasonal distribution of positive and negative surges. (*c*) Correlation of surge peaks between Immingham and Lowestoft. (*d*) Correlation between high-water residuals at Immingham and Wells-next-the-Sea.

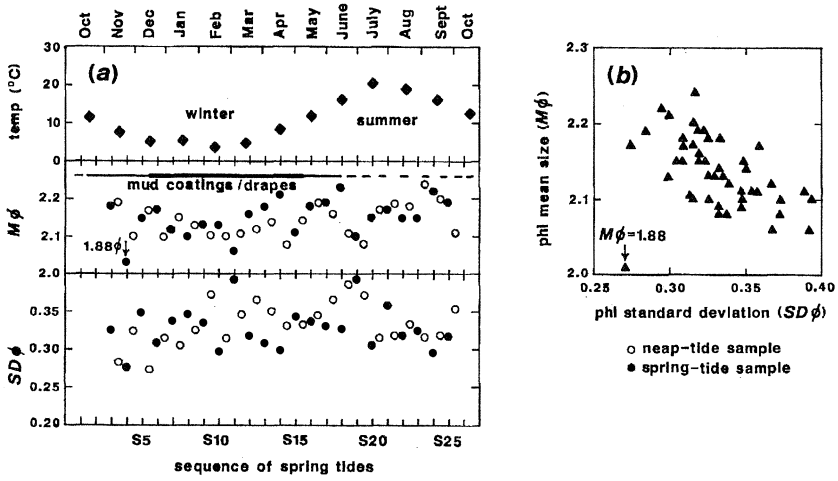

Figure 7. Sea temperature measured at Brancaster over the survey period and sediment grain size at Lifeboat Station Bank. $M\phi$ is the phi mean particle size and $SD\phi$ is the phi standard deviation.

average 28.6 tides (range 27–30 tides)(see figure 5*a*). Their asymmetry is indicated in figure 5*b* as the difference between the number of tides on the rising and falling limbs. Eight cycles have the opposite asymmetry to SN2 (see figure 4) and one is symmetrical in number terms. There is no clear correlation between the kind and the degree of cycle asymmetry and long-period tidal patterns. The height of the greatest predicted tide in each spring-neap cycle varies through the sampling period (see figure 5*c*), the springs being highest at about the equinoxes and lowest shortly after solstices. They also vary on a monthly scale. Defining convenient lunar months, the first springs (new-moon tides) rise higher than the second (full-moon tides) from a little before the autumnal equinox to the winter solstice, whereas the second springs (full-moon tides) are dominant from broadly the winter solstice to almost the autumnal equinox. An Immingham tide of 7.0 m causes just perceptible dune activity on Lifeboat Station Bank. The numbers of tides equalling or exceeding this height in each cycle and lunar month vary in a similar manner to the greatest heights themselves (see figure 5*d*, *e*). Hence, astronomically, most sand transport and dune activity should typify equinoctial periods, particularly the autumnal equinox. Figure 5*f*, *g* shows the sum in each spring-neap cycle and lunar month of the cube of the difference between the level of a predicted high water in excess of 7.0 m and the critical level itself. We use the cube exponent for this illustration because the bedload transport rate is widely thought to increase as the excess velocity cubed.

(*c*) *Storms and surges*

The tides we actually encountered (see § 3) are the astronomical ones modified meteorologically by wind stress and pressure systems. Storm surges, chiefly positive (water level heightened), occur often in the southern North Sea (Suthons 1963; Harding & Binding 1978; Summers 1978), and are mainly linked to depressions travelling either eastward from northern Scotland to Denmark or southeastward from Shetland to the Low Countries (see, for example, Rossiter 1954; Harding & Binding 1978; Steers *et al.* 1979). Negative surges (water level lowered) are almost as common and as large in magnitude as positive ones. A positive surge of order 1 m occurs on average annually. These meteorological events may significantly affect sand transport and dune behaviour at Lifeboat Station Bank; a positive surge, for example, should augment transport.

We explored their incidence by calculating the difference (high-water residual) at Wells Harbour between the measured (Anglian Water Authority gauge) and astronomically predicted high water in the case of 314 spring tides (see figure 6*a*). A zero residual was obtained for 27 occasions. Positive differences marginally exceed negative ones, and small residuals are more frequent than large differences. For the present, we designate any residual of a magnitude greater than 0.2 m as a surge. We consequently identify a total of 82 significant meteorological events, of which 48 are positive surges, numbering them in sequence from M1–M82. Surges were frequent during the autumn and winter, but significant events also occurred during spring and summer (see figure 6*b*).

The Meteorological Office's Storm Tide Warning Service told us of 40 tides that they considered to have been affected by surges between the October and March and in the subsequent September and October of our study. Their data for Immingham and Lowestoft appear in figure 6*c*, where the surge peak is the largest difference over the tidal cycle between measured and predicted tidal levels. In

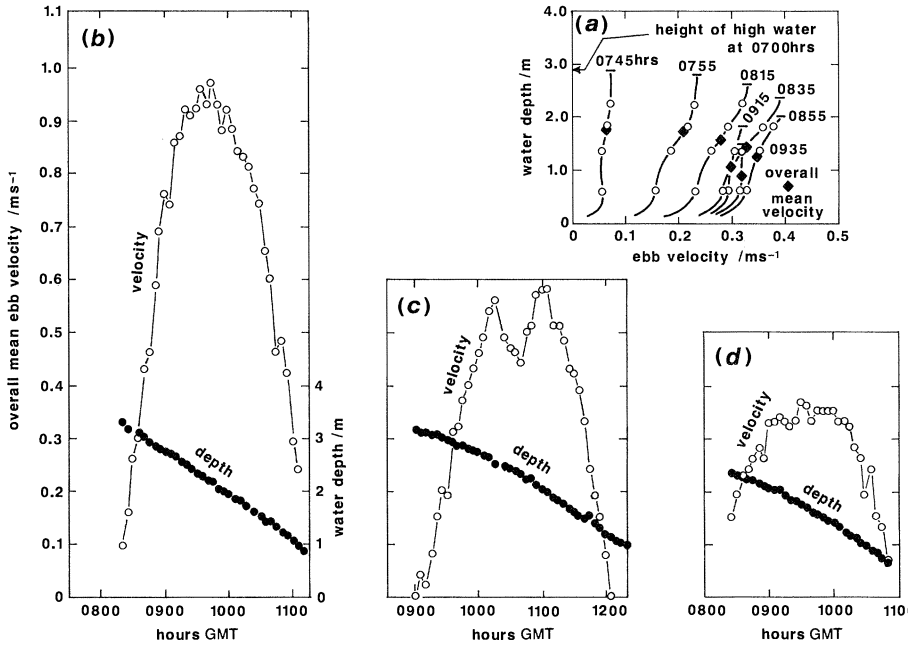

Figure 8. Representative tidal current velocity and depth patterns. (*a*) Vertical profiles of velocity measured over the ebb of T59. (*b*)–(*d*) Mean velocity and depth pattern measured over the ebb of T687, T206 and T148 respectively.

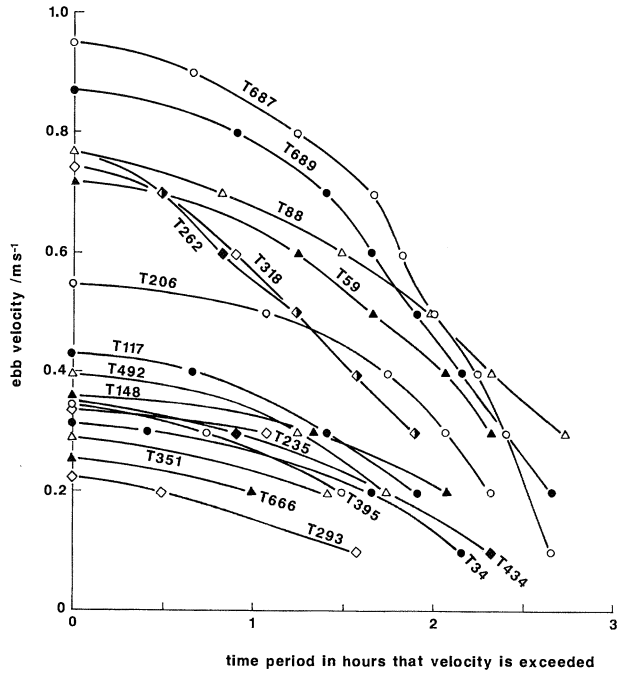

Figure 9. Representative patterns of velocity exceedance.

PHILOSOPHICAL TRANSACTIONS OF THE ROYAL SOCIETY A MATHEMATICAL, PHYSICAL & ENGINEERING SCIENCES

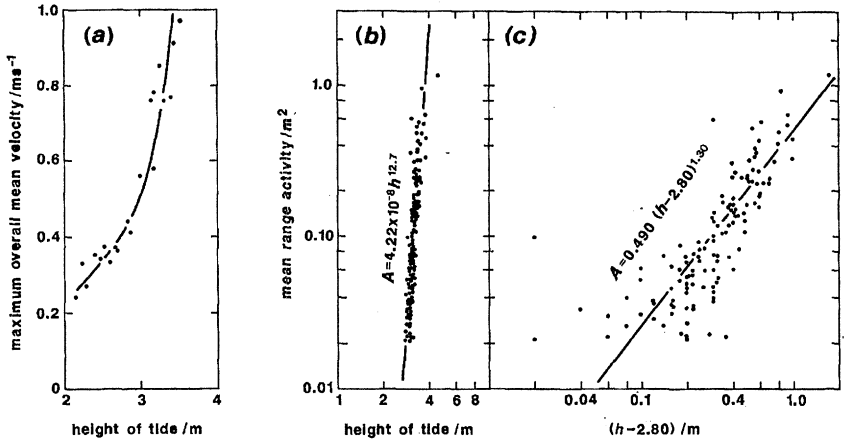

Figure 10. Relation of (*a*) maximum overall mean tidal velocity, and (*b*), (*c*) total sediment transport per tidal cycle (mean range activity) to measures of tidal high-water stage.

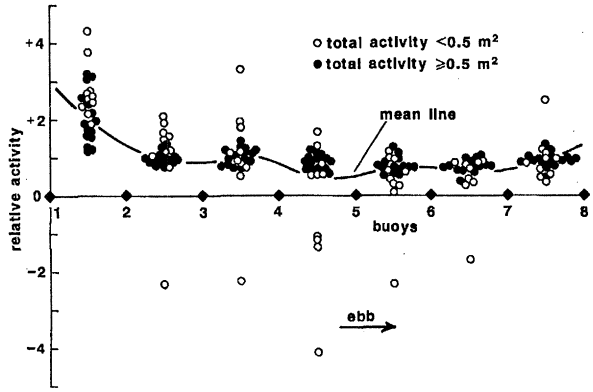

Figure 11. Variation of sediment transport (relative activity) with position on the sampling range. To display them individually, data points have been plotted so as largely not to overlap. See text for full explanation.

figure 6*d* we compare our positive surges at Wells Harbour to their available high-water residuals at Immingham. Residuals at Wells are about 0.3 m larger than at Immingham, and as figure 6*c*, *d* present a similar scatter, we feel confident about the residuals derived from our non-accredited gauge. During our autumn and winter, moderate surges coincided with S1(M1 +ve; M2, 3 −ve), S3(M5–7 −ve), S4(M8, 12 −ve; M9–11, 13, 14 +ve) and S5(M16 −ve; M17, 18, 22 +ve). The gale of 3–5 January 1976 (Shaw *et al.* 1976; Harding & Binding 1978; Flather & Davies 1978; McIntyre 1979) accompanied S7 and caused two large negative (M27, 30) and four moderate to very large positive surges (M25, 28, 29, 31). The high-water residual for M29 was 1.44 m, coinciding with the largest astronomical tide of the set. Moderate to large surges similarly attended S8(M33 −ve; M34–37, 38 +ve). February was a quiet month, and S9 and S10 saw only a few, chiefly small surges. Mainly small surges accompanied S11(M44 +ve, M45–47 −ve), S12(M48–50 −ve), S13(M51–53 +ve), S14(M54–57 −ve), S15(M58 −ve), S16(M59 +ve; M60, 61 −ve), S17(M62 +ve), S18(M63 +ve) and S19(M64 +ve). There were no detectable

surges during either S20 or S22 in the summer. In late July, S21 was affected by numerous small surges (M65–69 +ve), as was S23 near the end of August (M70–74 +ve). Surges attended S24(M75 −ve, M76–78 +ve) and S26(M79 −ve, M80–82 +ve), but S25 in late September was unaffected.

(*d*) *Wave activity*

Dunes on Lifeboat Station Bank are susceptible to wave attack during the ebb. Our sampling range (see figure 1*b*) is sheltered from the west (a deliberate choice), but is more open to the north, east and south. Wave heights were estimated during 20 representative ebb tides using a graduated staff fixed to the current-meter frame (see § 3*a*). Heights were mostly less than 0.1 m, but northerly and easterly winds at times made waves as tall as 0.5 m. Only on the windiest days, however, did any significant rounding and smoothing of dune crests result.

(*e*) *Sea temperature*

We did not measure this property, but were kindly given data from the entrance to Brancaster Harbour, 12 km west of Wells, by Dr S.R. Jones (MAFF Fisheries Laboratory, Lowestoft)(see also Jones 1981; Jones & Jeffs 1991). Here there is a fluctuation in sea temperature of the general order of 0.5 °C on a timescale of a few days. The most important variation, however, is seasonal (see figure 7*a*), the temperature changing by about 15 ° between winter and high summer.

(*f*) *Sediments*

Lifeboat Station Bank consists of well-sorted, fine grained quartz sand with some sand-grade shell debris and, towards its seaward end, a little flint and shell gravel. Southwest of the crest, the surface sand includes, locally and at times, small numbers of granules and pebbles of mud torn from deposits accumulated as drapes and coatings, particularly in dune troughs, and from eroding mudflats east of the main channel. These coating and drapes are least conspicuous during the summer (see figure 7*a*) when the sea is clearest (see, for example, Visser 1970; Eisma & Kalf 1979).

The sand on our range (see figure 1*c*) varied slightly in texture, on the basis of sieved composite samples collected at springs and neaps between S3 and S25 (see figure 7). Curiously, it seemed finer grained at springs than neaps during the long period when mud coatings and drapes were most evident (see figure 7*a*), the sorting (phi standard deviation) worsening with increasing mean sand size. The main textural fluctuations correlate best with sea temperature (i.e. with viscosity), pointing to a seasonal effect on sediment entrainment and transport.

3. Kinetics of tidal flows and associated sand transport

(*a*) *Equipment and methods*

We measured water velocity during the ebb phase of twenty tidal events, chosen to sample the full range of predicted high-water levels over the year. On each occasion, a steel frame had been assembled and secured to the sand during a previous low tide, on a site a few metres west of buoy 4 (see figure 1*c*). The frame supported a vertical rod on which four horizontally-mounted Braystoke Current Flow Meters (BFM 001) aligned parallel with the channel axis were positioned.

PHILOSOPHICAL TRANSACTIONS OF THE ROYAL SOCIETY A MATHEMATICAL, PHYSICAL & ENGINEERING SCIENCES

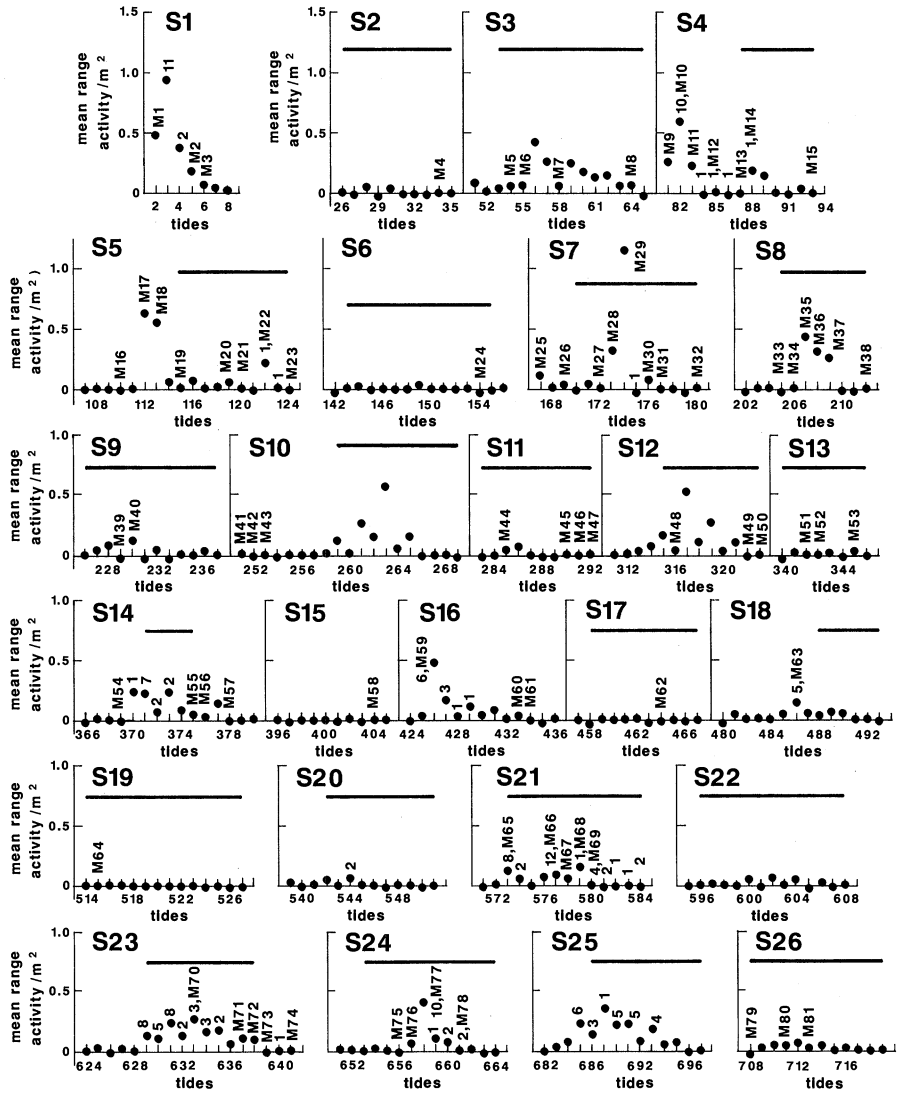

Figure 12. Sediment transport (mean range activity) at the sampling site on a tide-by-tide basis for each of 26 spring-neap cycles. Tides accompanied by significant meteorological surges (e.g. M59) are identified, together with the numbers of nascent dunes seen at low water. The horizontal solid lines define the periods of predicted diurnal inequality in the predicted tides.

It also supported a vertical scale allowing the depth of water above the sediment surface to be read directly, using field glasses, from the sea-wall about 75 m away. Each rotation of one of the 5 in (127 mm) plastic impellors caused a reed switch to open and close within the meter, sending electrical pulses along a multicored cable to revolution counters that we manned on the sea wall. During each ebb phase, the number of revolutions of each current meter was counted for one minute in every five, the counts then being converted into velocity values using calibration tables (Valeport Developments, Dartmouth, Devon, U.K.).

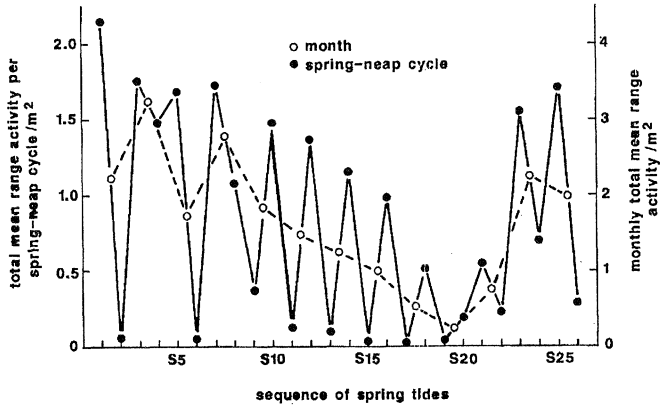

Figure 13. Total sediment transport (total mean range activity) at the sampling site in terms of spring-neap and lunar monthly cycles.

(*b*) *Vertical velocity profiles*

Figure 8*a* shows vertical ebb velocity profiles measured at stated times during a representative tidal event (T59 of S3). For each time, an overall mean velocity was estimated as the velocity interpolated at a height above the sediment surface of 0.6 times the water depth.

The local velocity tends to increase upward at almost all times in our measured flows. In many cases, however, there is a particularly sharp rise above a point 1–1.5 m above the bed, suggesting a measure of water stratification.

(*c*) *Mean velocity variation during the tidal ebb*

In most measured flows, as shown by selected representative tides (see figure 8*b–d*), the overall mean velocity tends to oscillate during the period of strongest ebb flow, perhaps reflecting the episodic falling out of play of major creeks in the area drained by the channel. We smoothed out these oscillations in estimating a maximum overall mean velocity for each chosen ebb.

The overall mean velocity-time curves also tell us for how long each of the measured flows exceeded particular velocity values. Earlier (Allen & Friend 1976*a*), a threshold velocity for dune activity was estimated as $0.6\,\mathrm{m\,s^{-1}}$ using interpolations for a point 0.6 m above the bed. In this study, with the velocity interpolated for a point 0.6 times the depth, we estimate that the dune threshold is an overall mean of about $0.65\,\mathrm{m\,s^{-1}}$. Our plot of the time periods in each ebb over which particular velocities were exceeded varies unpredictably in form (see figure 9). Some tides flowed at an intermediate velocity for much longer than others attaining the same peak value. We are so far unable to explain this effect.

A nonlinear relation holds between the maximum overall mean velocity of the ebb tide and the gauged height of the preceding high water (see figure 10*a*). This effect appears to be related to the tidal volume to be discharged which, because of the triangular cross-sections of the major channels, and the presence of many 'perched' creeks and gullies in the marshes, together with the floodplain-like character of the marshes at Wells, grows increasingly steeply with tidal height.

PHILOSOPHICAL TRANSACTIONS OF THE ROYAL SOCIETY A MATHEMATICAL, PHYSICAL & ENGINEERING SCIENCES

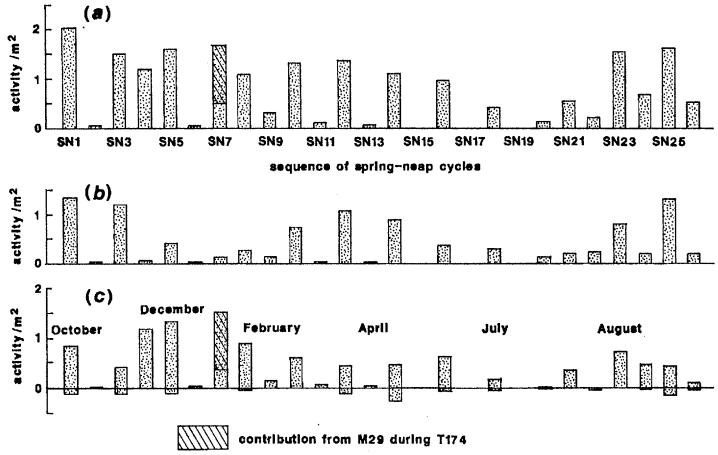

Figure 14. Relative contribution of astronomical and meteorological tides to sediment transport on the sampling range. (*a*) Net (observed) total sediment activity per spring-neap cycle. (*b*) Predicted astronomical component. (*c*) Predicted meteorological component (positive and negative surges).

(*d*) *General sand transport activity and its variation*

We used our detailed knowledge of the movement-history and height of dunes on the range (see § 5*a*) to obtain an estimate of the sand transport as bedforms. We measure this as the bedform activity, defined for any tide as the product of the distance moved by a feature (positive, northward along the range) and its height averaged over that tide. This product is the area swept by the bedform as it advances, and equals the true total sediment transport per unit width per tide when multiplied by the sediment bulk density and a dune shape coefficient. The latter—generally not known exactly—varies with shape but is close to one-half (Simons *et al.* 1965*a*). For each tide the activity was calculated for one bedform randomly selected between each of the seven pairs of buoys on our range (see figure 1*c*). The mean range activity for that tide was then calculated as the average of the seven values.

Sand transport on the range varies spatially as well as temporally. The variation in relative activity, defined as the total between-buoy activity for each set of springs normalized by the total averaged over the whole range for that set, is shown in figure 11. The southern end of the range shows more activity than average, confirming our general impression that dune movements here are greater and begin earlier than elsewhere. Dune heights tend also to increase southward. We infer that the flow in our ebb channel (see figure 1*b*) is slightly non-uniform. The temporal pattern of sediment transport is complex, as can be seen from a plot of the mean range activity for each tide within each set of springs (see figure 12), and of the total mean range activity for each set of spring tides throughout the year (see figure 13). A further smoothing is achieved in figure 13 by plotting monthly totals. Sand transport in dune bedforms clearly peaks in autumn-winter but is a minimum in mid summer.

Figure 10*b*, *c* shows how the mean range activity varies with the observed height of the preceding high water. We took activities greater than 0.02 m^2 to have involved significant sand transport; this occurred only for tides with heights greater

PHILOSOPHICAL TRANSACTIONS OF THE ROYAL SOCIETY A MATHEMATICAL, PHYSICAL & ENGINEERING SCIENCES

Figure 15. Vertical air photograph of dunes on the sampling range at Lifeboat Station Bank. The black discs (arrowed) mark the buoys at the ends of the range. The photograph shows an area measuring approximately 260m × 300m. See also figure 1.

than about 2.8 m, although a little sand was moved by lesser tides. We had earlier found that 2.6 m was the threshold tidal height for dune movement (Allen & Friend 1976*a*). This difference from our present finding is small enough to be explained by natural changes at Lifeboat Station Bank over the three years between the two studies (a gradual weakening of the régime in the ebb channel is suspected). Introducing the new threshold value into one of the formulae, the activity and tidal height vary as

$$A = 4.22 \times 10^{-8} h^{12.8} \quad \text{and} \quad A = 0.490(h - 2.80)^{1.30},$$

where A is the activity and h the gauged height of the preceding high water (see figure 10*b*, *c*). The variation of sand grade with water temperature (see figure 7*a*) made us suspect a seasonal shift in the activity-height relation but, taking the data two months at a time, we could not establish an effect with certainty.

(*e*) *Tide and storm influence on sand transport*

Because we have a continuous record of both the predicted (astronomical) and actual (astronomical and meteorological) tidal heights, we are able, on a

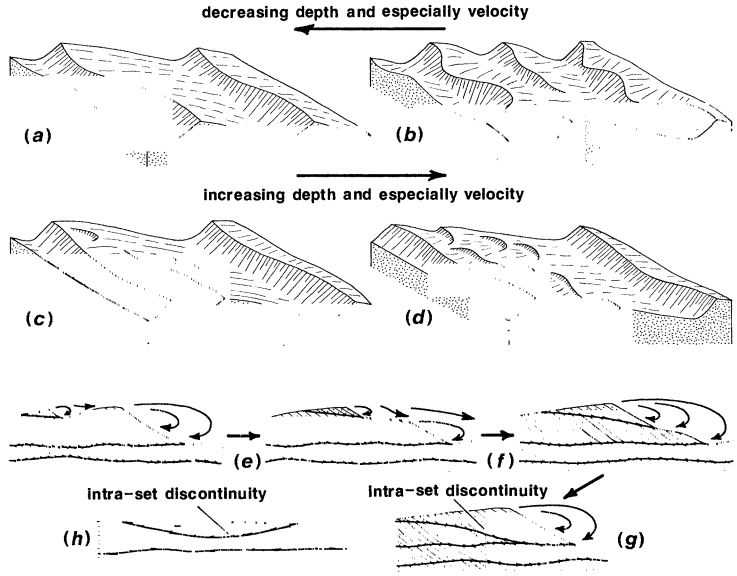

Figure 16. Idealized bedform geometry and internal structures at Lifeboat Station Bank. (*a*) Low-energy type of dune. (*b*) High-energy type of dune. (*c*) Dune with supplementary crest. (*d*) Dune with superimposed nascent dunes. (*e*)–(*g*) Streamwise sections, with the current from left to right, illustrating the formation of an intraset discontinuity by the more rapid advance of a supplementary crest or nascent dune. (*h*) Transverse section through an intraset discontinuity generated by a nascent dune or short supplementary crest.

semidiurnal timescale, separately to estimate and then compare the astronomical and meteorological components of the observed total sand transport. We do this (see figure 14) by evaluating (i) actual tidal heights less 2.8 m all raised to the power 1.30, and (ii) predicted (astronomical) tidal heights less 2.8 m all raised to this power (see second formula above). The difference on each tide is a measure of the meteorological contribution to sediment transport, through either a positive or a negative surge.

We estimate over the year that only 50.4% of the dune-related sand transport apparently resulted from the astronomically generated flows, chiefly during alternate sets of spring tides in the autumn and spring equinoctial periods (see figure 14), as suggested theoretically in figure 5*f*, *g*. The remaining 49.6% of the transport was due to storm surges; the main January event (M29, see figure 12) alone contributed 5.5% of the annual total. Positive surges by themselves would have caused 55% of the sediment transport, if this effect had not been offset by a 5.4% lowering by negative ones. Thus the meteorological events, individually with a diurnal timescale, combined to 'infill' the sediment-transport minimum which would otherwise have accompanied the winter solstice (see figure 5*g*), and the actual sediment transport varied on twice the expected period (see figure 13).

(*f*) *Sand transport and diurnal inequality*

In view of the high frequency (see figure 6), relatively short duration, and substantial effect on sediment transport (see figure 14) of meteorological events at Lifeboat Station Bank, it is important in connection with the internal structural

PHILOSOPHICAL TRANSACTIONS OF THE ROYAL SOCIETY A MATHEMATICAL, PHYSICAL & ENGINEERING SCIENCES

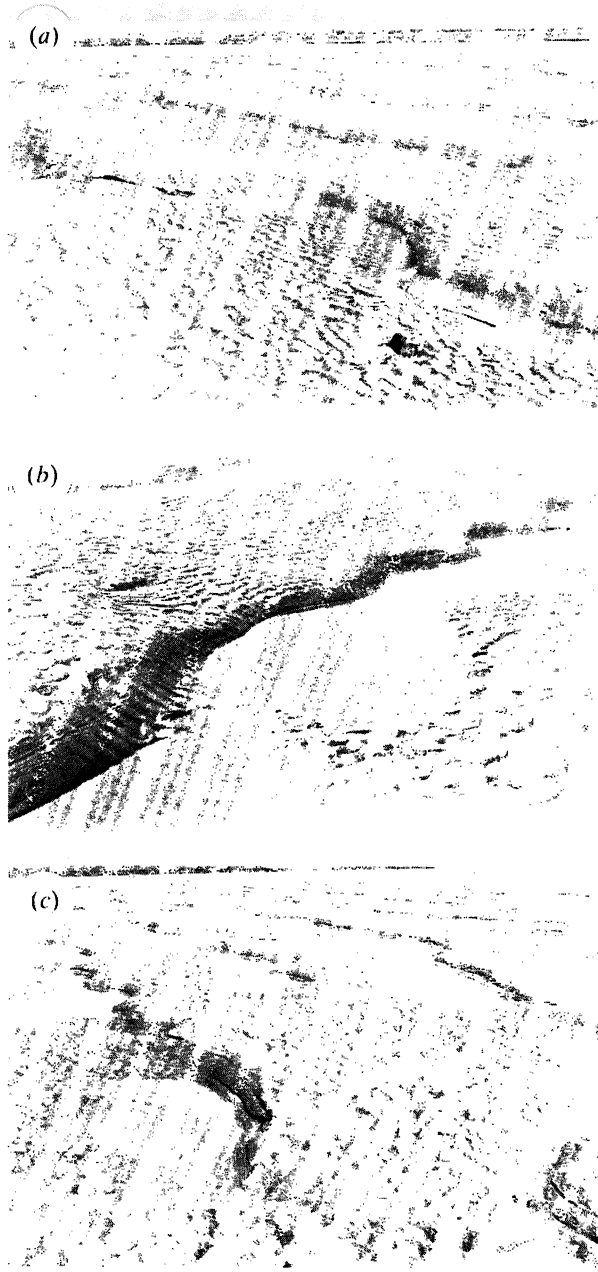

Figure 17. (*a*) Low-energy mature dunes. Flow from upper right. Current ripples have wavelength of about 0.15 m. (*b*) Low-energy mature dunes. Flow from upper left. Wavelength of current ripples about 0.15 m. (*c*) High-energy mature dunes. Flow from upper right. Wavelength of current ripples about 0.15 m.

PHILOSOPHICAL TRANSACTIONS OF THE ROYAL SOCIETY A MATHEMATICAL, PHYSICAL & ENGINEERING SCIENCES

Table 1. *The effect of meteorological tides (surges) on the degree of expression through sediment transport (measured activity difference) of predicted diurnal inequalities (height difference)*
(See text for full explanation.)

set of tides	number of tides	correlation coefficient activity difference on height difference	variance explained (%)
S1	6	0.920	84.6
S2	8	0.517	26.7
S3	14	0.622	38.7
S4	8	0.079	0.6
S5	15	0.031	0.1
S6	13	0.285	8.1
S7	13	0.735	54.0
S8	10	0.531	28.2
S9	11	0.823	67.7
S10	12	0.967	93.5
S11	9	0.492	24.2
S12	12	0.891	79.4
S13	7	−0.783	61.3
S14	13	0.329	10.8
S16	12	0.046	0.2
S18	12	0.140	2.0
S20	12	0.692	47.9
S21	11	0.465	21.6
S22	13	0.976	95.3
S23	13	0.904	81.7
S24	12	0.583	34.0
S25	13	0.826	68.2
S26	11	0.700	49.0
all tides	260	0.648	42.0

patterns of the dunes (see § 6*c*) to examine the extent to which the tidal diurnal inequality (see figures 4 and 12) was blurred.

We accordingly correlated over each set of spring tides two quantities standing for sand transport on the scale of the diurnal inequality. One quantity—the activity difference—is the difference between the $(n+1)$th and the nth tides in the observed mean range activity. This quantity measures the actual change due to all causes in the sediment transport from one tide to the next. The second quantity—the height difference—is the difference of the predicted (astronomical) tidal height, each less 2.80 m and raised to the power 1.30, between the $(n+1)$th and the nth tides. It stands as proxy for the expected difference in the sediment transports between tides, in the absence of any meteorological effect. The strength of the positive correlation between the two differences suggests the likely quality of internal structural patterns within the dunes as records of diurnal changes in sand transport of astronomical origin.

A significant meteorological disturbance of the diurnal sediment transport pattern is to be expected in most sets of spring tides (see table 1). Excluded from the analysis, however, are S15, S17 and S19, when there was almost no sand transport (see figure 13). Low transports, affecting the reliability of the correlation through large measurement errors, also marked S2, S6, S11 and S13.

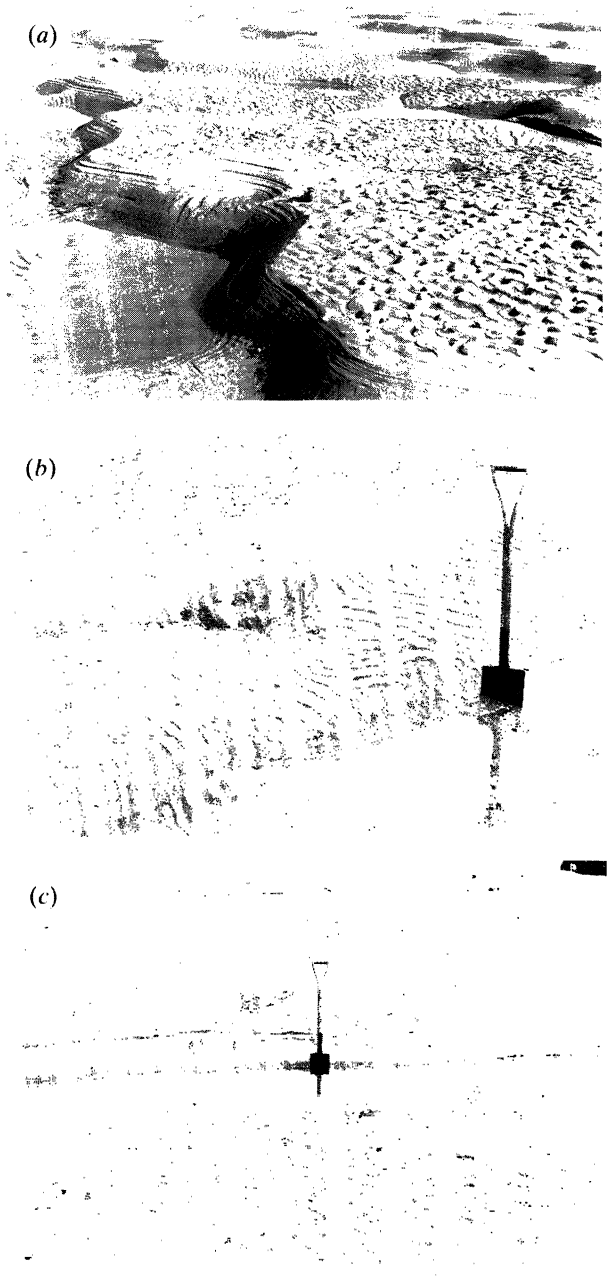

Figure 18. (*a*) High-energy mature dunes. Flow from upper right. Current ripples have wavelength of about 0.15 m. (*b*) Mature dune with a supplementary crest, viewed from leeward. Current from upper left. Spade about 0.9 m tall. (*c*) Mature dune with superimposed nascent forms, viewed from leeward. Flow toward observer. Spade about 0.9 m tall.

PHILOSOPHICAL TRANSACTIONS OF THE ROYAL SOCIETY A MATHEMATICAL, PHYSICAL & ENGINEERING SCIENCES

4. General bedform morphology

(*a*) *Dunes*

We describe as mature dunes (Allen 1982) those three-dimensional asymmetrical sand ridges marked by a (i) comparatively long transverse crest, typically measured in tens of metres, (ii) wavelength measured in metres, (iii) height of several decimetres, and (iv) persistence in time of at least one spring-neap cycle and normally of many cycles. Although changing diurnally and from one spring-neap cycle to the next, as well as spatially within the ebb-affected area, mature dunes are bedforms which we found were easily recognized as individuals from tide to tide on Lifeboat Station Bank. The dunes (see figure 15), facing northward with the ebbing tide, run nearly east-west and roughly straight over most of their length, but bend sharply southward over the crest of the bank. As is widely observed (Allen 1968), some dunes split at the slip face to form a Y-shaped structure, whereas others gradually fade away on stoss slopes. Judging from the alignment of features in their dark-toned troughs (see figure 15), the ebb stream fans out northward in the expanding area between the bank crest and the sea wall. Consequently, as the bank shoals but little in this direction, the general strength of the ebb stream should gradually decline northward over the sampling range (see also figure 11).

The main kinds of dune found at low water are epitomized in figure 16*a*–*c*, and we emphasize that, in terms of our intensive observations on Lifeboat Station Bank, they define a morphological continuum in both space and time. Forms associated with periods of low to moderate sediment transport (see figure 17*a*, *b*) (i) are relatively flat, (ii) vary little to moderately in height along their span, (iii) have a smoothly curved crest, and (iv) comprise lobes and saddles (Allen 1968) of a similar curvature along the crest in plan. They closely resemble Allen's (1968) 'sinuous large-scale ripples', the 'sand waves' and some of the 'megaripples' of Boothroyd & Hubbard (1974), the 'type 1 megaripples' of Dalrymple *et al.* (1978) and Elliott & Gardiner (1981), the '2D dunes' of Costello & Southard (1981), the '2D sandwaves' of Terwindt & Brouwer (1986), Ashley's (1990) '2D simple dunes', and the '2D megaripples' of Dalrymple *et al.* (1990). As the flow depth, velocity, and sand transport grow over the ebb-dominated area, the dunes become increasingly steep, variable in height along their span, and three-dimensional in character (see figures 17*c* and 18*a*). The crests grow increasingly irregular in plan, although retaining their general length and straightness. The leeward sides comprise groups of deeply embayed lobes which intersect at sharply curved to cusped saddles. Sharp-crested spurs extend from the saddles downstream across the dune trough, dividing up the latter into a spanwise chain of deep, water-filled hollows, the 'scour pits' or 'scour holes' of other workers (see, for example, Boothroyd & Hubbard 1974; Elliott & Gardiner 1981). Hence these dunes resemble some of Allen's (1968) catenary forms, the 'megaripples' of Boothroyd & Hubbard (1974), the 'type 2 megaripples' of Dalrymple *et al.* (1978) and Elliott & Gardiner (1981), Costello & Southard's (1981) '3D dunes', the '3D sandwaves' of Terwindt & Brouwer (1986), Ashley's (1990) '3D simple dunes', and the '3D megaripples' of Dalrymple *et al.* (1990).

The dunes are single-crested during most spring-neap cycles but at the more powerful springs may display locally as many as two further crests, although one additional feature is most common (see figure 16*c* and figure 18*b*). These supple-

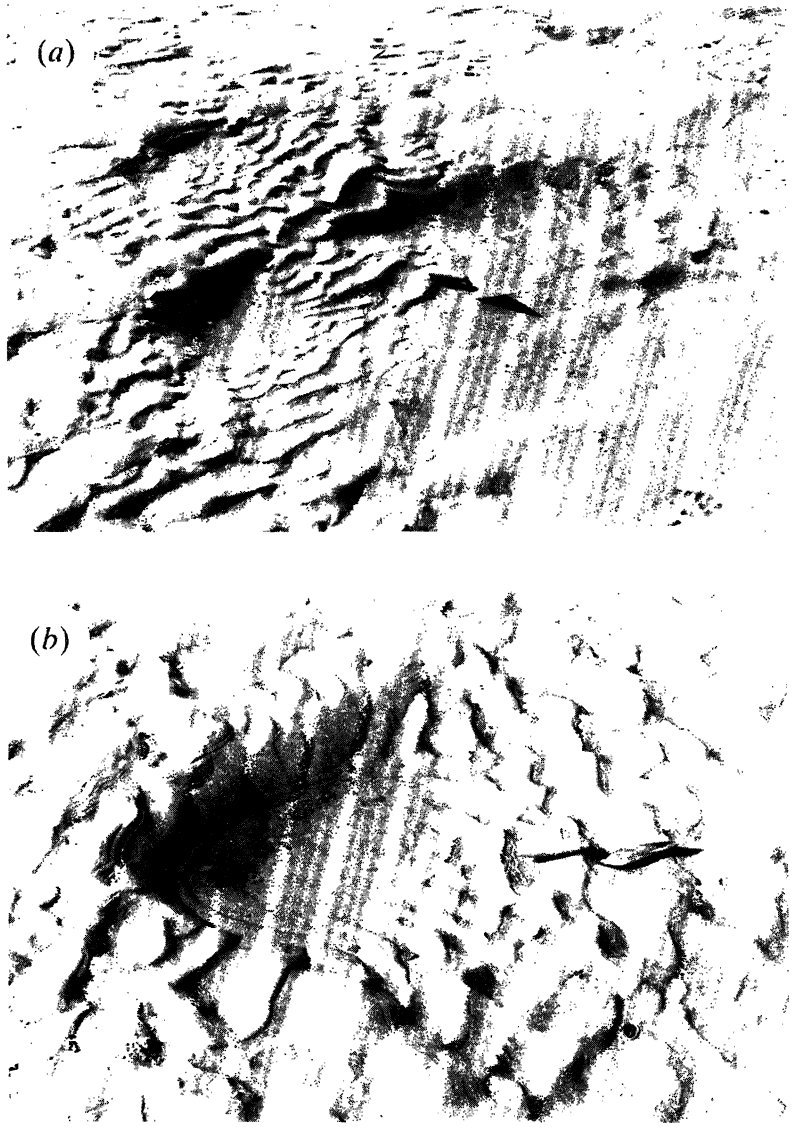

Figure 19. Forms of nascent dune. Current from upper left in (*a*), (*c*), (*d*) and from left in (*b*). Trowel about 0.28 m long.

mentary crests, shorter than the dune itself and perched high on the bedform, are comparatively straight and lie not far back from the main leading crest. With continuing sediment transport, each supplementary crest in turn advances forward to degrade and replace the previously leading crest (see § 5*d*).

Although the dunes vary mainly in time, we found some differences at most times between the upstream (southern) and downstream (northern) parts of the range, due to the slightly non-uniform flow and transport activity (see figure 11). As the tides strengthen and then wane, strongly three-dimensional dunes appear earliest at the upstream end and remain longest here.

PHILOSOPHICAL TRANSACTIONS OF THE ROYAL SOCIETY A MATHEMATICAL, PHYSICAL & ENGINEERING SCIENCES

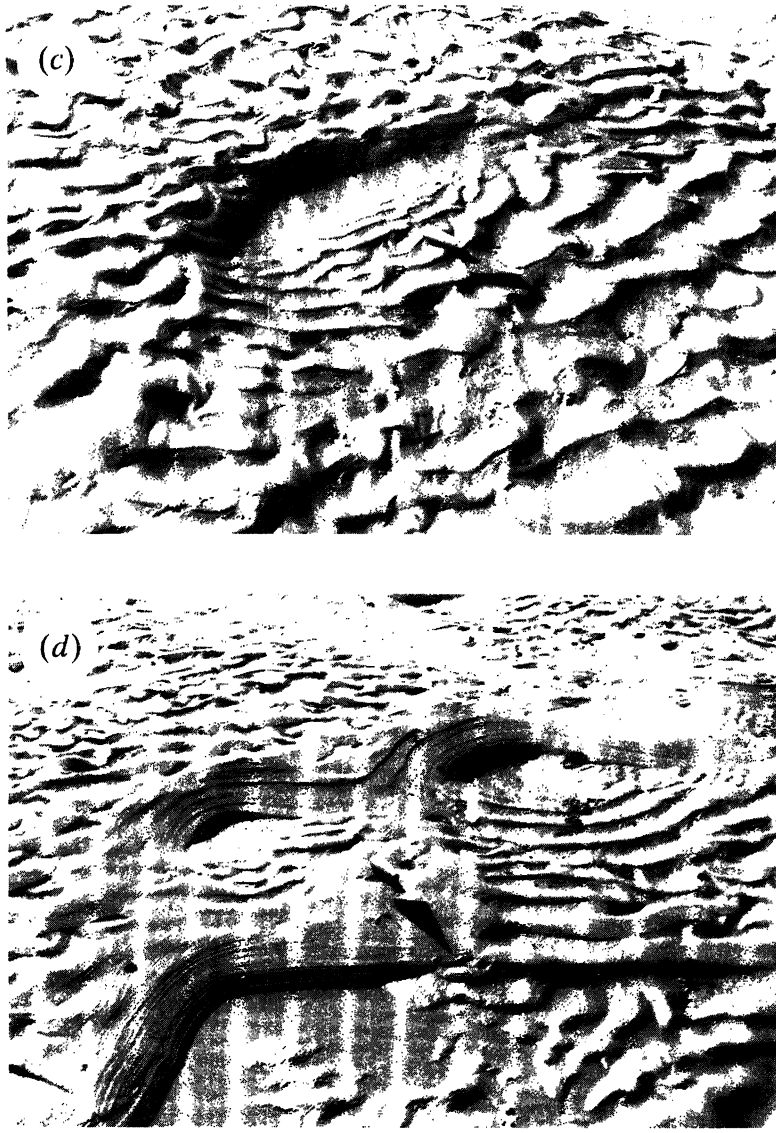

Figure 19. Continued.

(*b*) *Nascent dunes*

Dune-like bedforms intermediate in size between current ripples and mature dunes (as described above) suddenly appeared at times on the range. These structures, here called nascent dunes, correspond to our earlier 'minor dunes' (Allen & Friend 1976*a*) and the 'smaller-scale isolated megaripples' of Elliott & Gardiner (1981). We explain their character and then our choice of terminology.

Nascent dunes are mainly negative features superimposed on mature dunes but restricted to the downstream two-thirds to one-half of their stoss slopes (see figure 16*d*, and figure 18*c*). As seen after ebb, the smallest nascent dunes (see

PHILOSOPHICAL TRANSACTIONS OF THE ROYAL SOCIETY A MATHEMATICAL, PHYSICAL & ENGINEERING SCIENCES

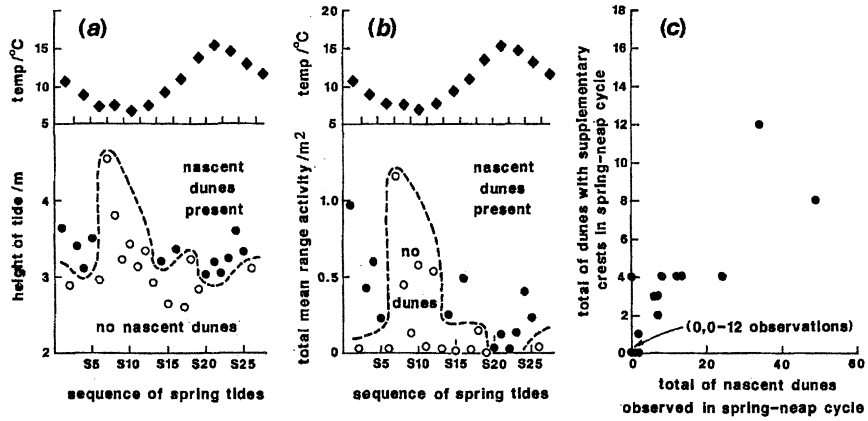

Figure 20. Nascent dunes at Lifeboat Station Bank. (*a*) Occurence during the survey period in relation to sea temperature (at Brancaster) and tidal height. (*b*) Occurence in relation to sea temperature and activity. (*c*) Relation to total of mature dunes with supplementary crests.

figure 19*a*) are isolated, oval to crescentic pits 0.3–0.5 m across and up to about 0.1 m deep. Typically, the upstream side is a steep, ebb-facing avalanche slope, and the downstream surface a gentler, largely convex-up slope carrying a fan of current ripples (Allen 1968). Larger examples have a symmetrical to asymmetrical crescentic form (see figure 19*b*, *c*), with a corresponding ripple-fan, but are up to 0.25 m deep and 2–3 m wide. The sharp-rimmed avalanche face at the upstream end typically reveals overlapping sand-flow tongues. Nascent dunes of small to intermediate size range widely over the stoss sides of mature forms, whereas large examples occur only near to the crests. Here, because of their relative size, nascent dunes may interfere and fuse laterally (see figures 18*c* and 19*d*).

Generally speaking, our nascent dunes moved and changed too rapidly to be individually recognizable from tide to tide. From the few exceptions, however, we conclude that nascent dunes (i) advance faster than the crest of the mature dune supporting them, and (ii) grow in size while approaching the crest of this dune.

Nascent dunes are triggered by tides rising higher than those driving mature forms. Earlier we found that tides of 2.8 m would create nascent forms (Allen & Friend 1976*a*), but this threshold, determined for the brief period August–September 1973, now requires revision. Figure 20 shows the high-water level and activity of the tide at which nascent dunes first appear in a spring-neap cycle; during cycles when the bed lacks these forms, the largest activity and tidal height are recorded. Each form of threshold—largest during the autumn and winter—varies antithetically with sea temperature at Brancaster (see figure 7*a*), pointing to a control from viscosity. In harmony, nascent dunes proliferate in spring and summer, when powerful tides are few or lacking (see figure 12).

We now justify the term nascent dunes. These forms are accepted as immature dunes because of their (i) dune-like scale and slip face, (ii) increase in size with increasing duration of sediment transport (see Raichlen & Kennedy 1965; Jain & Kennedy 1974; Yalin 1975; Tsujimoto & Nakagawa 1984), (iii) lateral fusion into long-crested features, and (iv) predominance during spring tides, when mature dunes are most active.

PHILOSOPHICAL TRANSACTIONS OF THE ROYAL SOCIETY A MATHEMATICAL, PHYSICAL & ENGINEERING SCIENCES

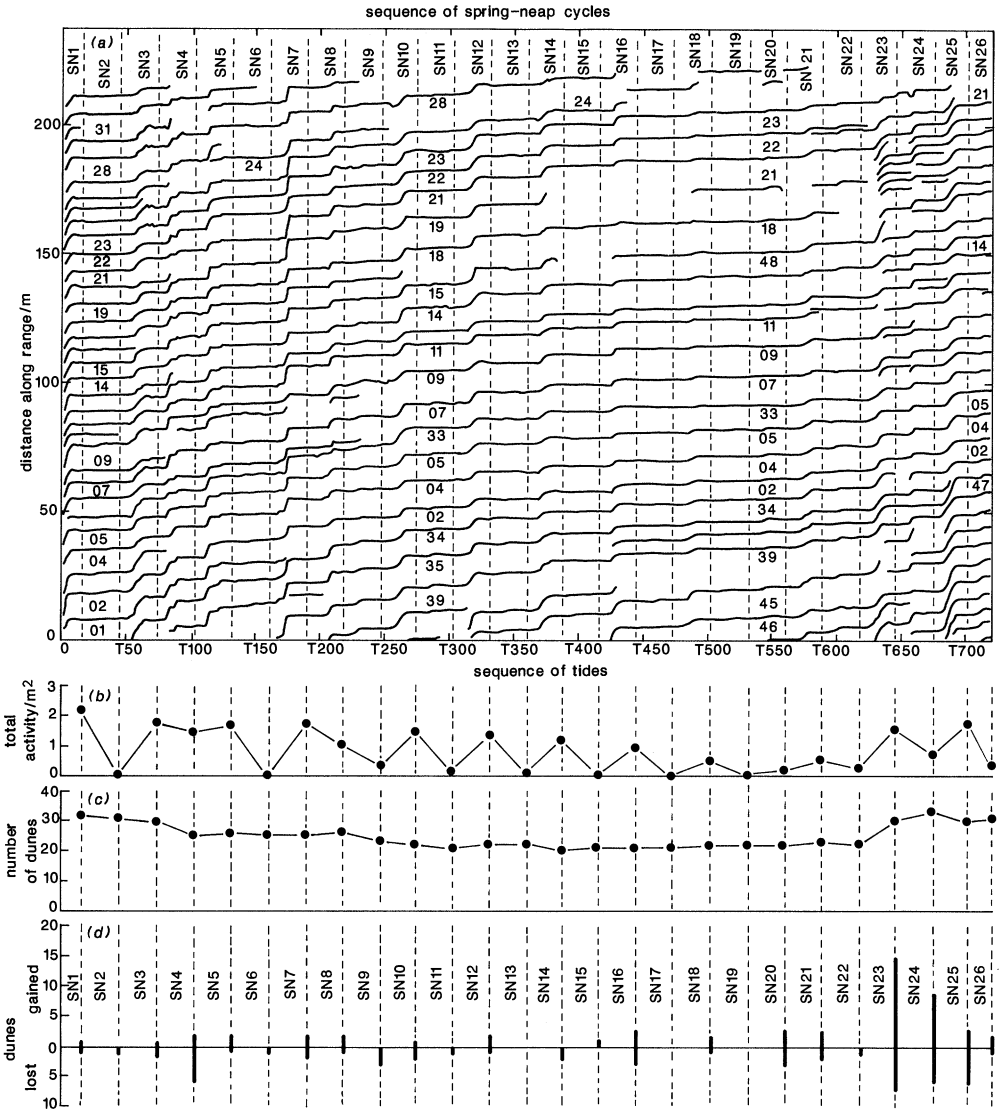

Figure 21. Mature dunes and their behaviour. (*a*) Time-distance graph for mature dunes (crest positions) over the period of the survey. Dunes numbered (selection only shown) from uprange to downrange and thereafter in order of appearance on the range. (*b*) Total activity per spring-neap cycle. (*c*) Number of mature dunes per spring-neap cycle. (*d*) Numbers of dunes gained and lost in each spring-neap cycle.

(*c*) *Current and wave ripples*

Ebb-oriented current ripples abound at low tide on Lifeboat Station Bank, decorating, in places and at times, even the leeward slopes of the dunes studied. The ripples, varying from straight-crested to (mainly) linguoid, take various orientations relative to dune crests. The ripples on the stoss sides of some dunes have almost the same orientation as the dune crests, and seem to have been formed by ebb flows that kept to one direction as depth declined. In other cases, particularly

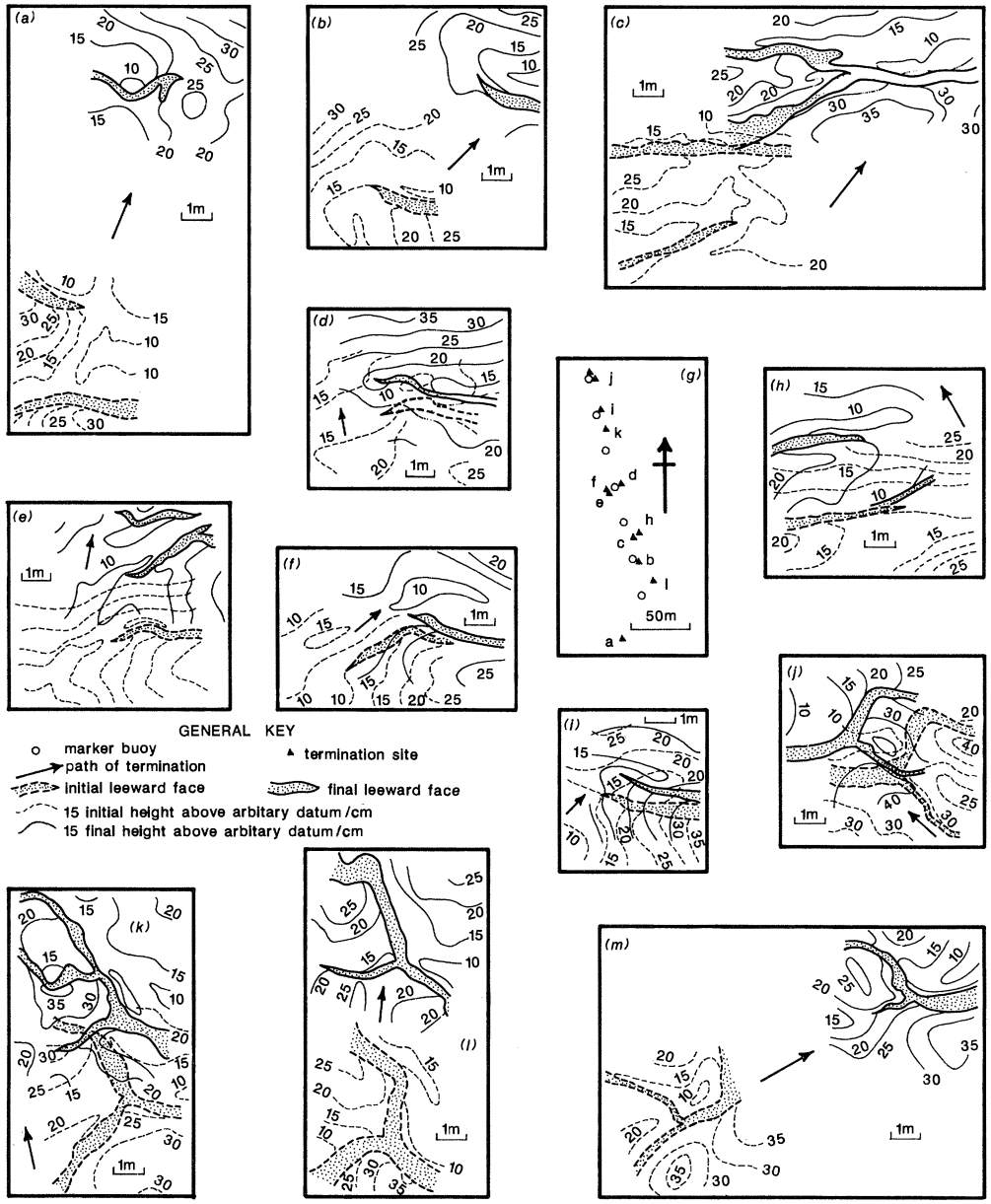

Figure 22. Behaviour of crest terminations on or near the sampling range over a set of spring tides. The vertical borders of each map are oriented parallel with the general direction of bedload transport. (*a–c*, *e*, *k*, *l*) S21. (*d*) S23. (*f*), (*h*) S22. (*i*), (*j*) S26. (*m*) S24. (*g*) Location relative to the range of the terminations surveyed. See also figure 1*c*.

where the leeward slopes of the dunes are affected, ripple and dune crests differ widely in trend, pointing to late-ebb flows that became partly channelized along dune troughs. Except in these cases, ripple-fans abound in the dune troughs, taking a pattern and orientation controlled by the trend and shape of the dune crest upsteam. Tucker (1973) sees ripple-fans as features of 'late-stage run-off',

and Elliott & Gardiner (1981) also treat them as reflecting 'falling stage conditions rather than active bedform migration'. These interpretations do not apply at Lifeboat Station Bank, because (i) current-ripple and dune hydraulic existence fields overlap significantly (Simons *et al.* 1965*b*; Allen 1982), (ii) the reverse bottom current in the separated flow at a dune is weak (although much unsteadier) compared to the external stream (Allen 1968, figs 9.20, 10.10), and (iii) we saw many cases of ripple-fans undergoing discordant burial by dune avalanche deposits, implying that fans and dunes are simultaneously active.

Symmetrical to near-symmetrical wave ripples with long, straight, regular crests appear on Lifeboat Station Bank only on the windiest days. They seem to be late-ebb, shallow-water features, as the structures are normally imprinted on current ripples, particularly those arranged in ripple-fans.

5. Behaviour of dunes as individuals and as an ensemble

(*a*) *Assessing bedform character and behaviour*

Though the dunes on Lifeboat Station Bank are bedforms in three-dimensional space, we emphasized in § 2*a* that, at the quantitative level, we sampled them only two-dimensionally on the buoyed range. Excepting the nascent dunes, our measurements suffice only to define an operational unit, which we informally call a profiled crest (see figure 3), composed of an upstream (southern or stoss) slope, a summit, and a downstream (northern or leeward) slope. Each profiled crest, with a certain height and wavelength (see § 2*a* for practical details), is a functional entity, for it advances along the range by erosion on the stoss and deposition to lee. A profiled crest is not a dune in the sense of a bedform in three-dimensional space, but merely one possible cross-section through either a mature form or some significant part of a form. There is an exact correspondence only between single-crested mature dunes and profiled crests. Dunes with supplementary crests (see § 4*a*), developed in response to the highest tides, contribute more than one of our profiled crests. Each sample (one tide) obtained from the range consists of all the profiled crests encountered at that time, together with the profiled crests which overlap the range at its ends (see figure 3), the nascent dunes being ignored, as already noted. The full space-time graph of the tide-by-tide movement of all the 331 profiled crests which appeared on the range, of which 37 occurred at the start, is too complex to give here (but see figure 25 below). The corresponding figure 21*a*, however, summarizes the behaviour of the 83 mature dunes to which these crests belonged. The numbers of profiled crests and dunes vary with time partly because of (i) the spanwise movement of bedforms on to and off the range, and (ii) interactions between profiled crests.

(*b*) *Spanwise movement of bedform terminations*

The mature dunes show two main kinds of spanwise termination (Allen 1968) (see figure 15). In the open type the leeward face gradually dies out along the stoss of a neighbouring dune. The other kind involves the joining of crests and leeward slopes to form a buttress or Y-shaped triple-junction.

We attempted to map 16 terminations over selected spring-neap cycles, by lowering a weighted measuring tape on to the sand from graduated rigid rods levelled and supported on moveable upright stakes. Resurvey was successfully completed

PHILOSOPHICAL TRANSACTIONS OF THE ROYAL SOCIETY A MATHEMATICAL, PHYSICAL & ENGINEERING SCIENCES

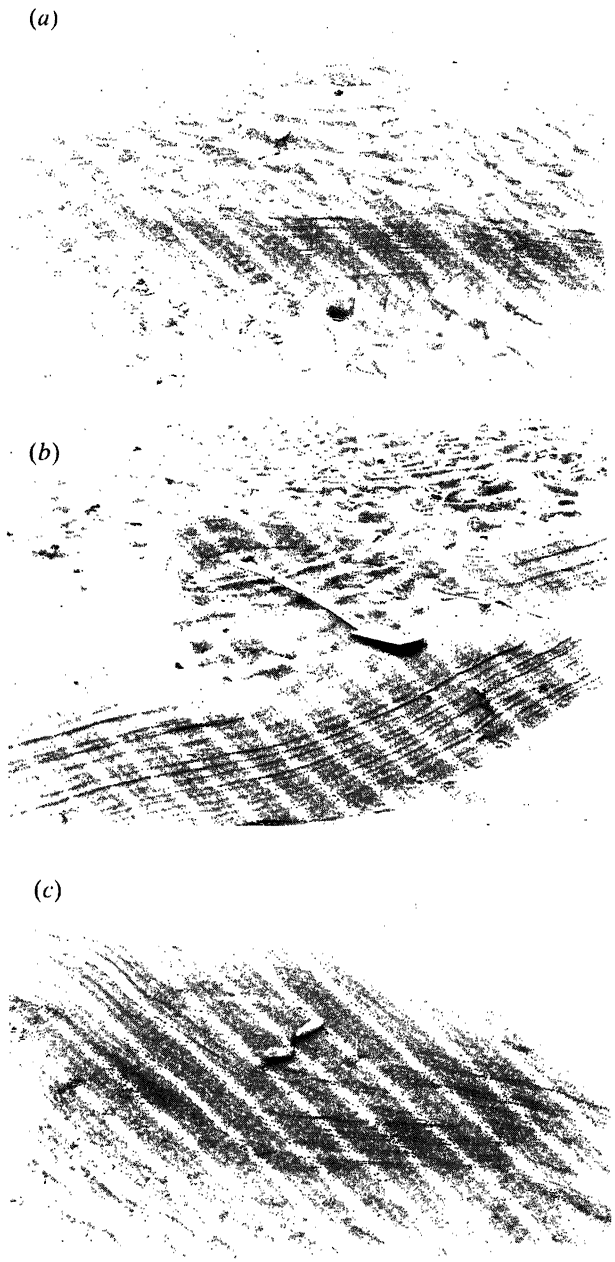

Figure 23. Photographs of selected nascent dunes to illustrate the progressive replacement of a portion of the crest of a mature dune by the crest of a nascent dune advancing upon it from upstream. See also figure 16*e*–*g*. Trowel (0.28 m) and spade (0.94 m) point in current direction.

in twelve cases, but in the remainder the termination had either disappeared or was unrecognizable. Most of the sites lie a little upslope from the range (see figure 22*g*) and therefore in a slightly more active part of the dune field. There are eight open terminations (see figure 22*a*–*i*) and four triple-junctions (see figure 22*j*–

PHILOSOPHICAL TRANSACTIONS OF THE ROYAL SOCIETY A MATHEMATICAL, PHYSICAL & ENGINEERING SCIENCES

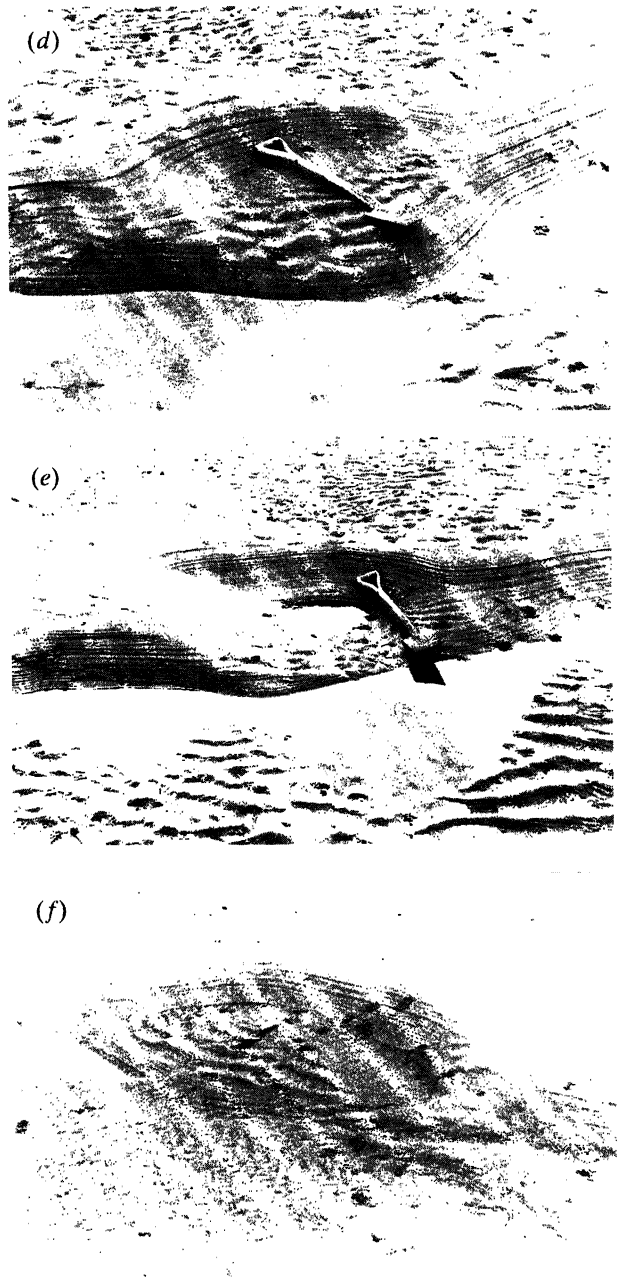

Figure 23. See opposite for caption.

m). All of the terminations showed some evidence of change. Open terminations proved capable in a set of spring tides of a lateral migration either side of the local average sand-transport direction of between a few decimetres and 3.5 m. One advanced to join the dune next downstream (see figure 22*c*). Triple-junctions showed an even greater degree of movement perpendicular to the direction of

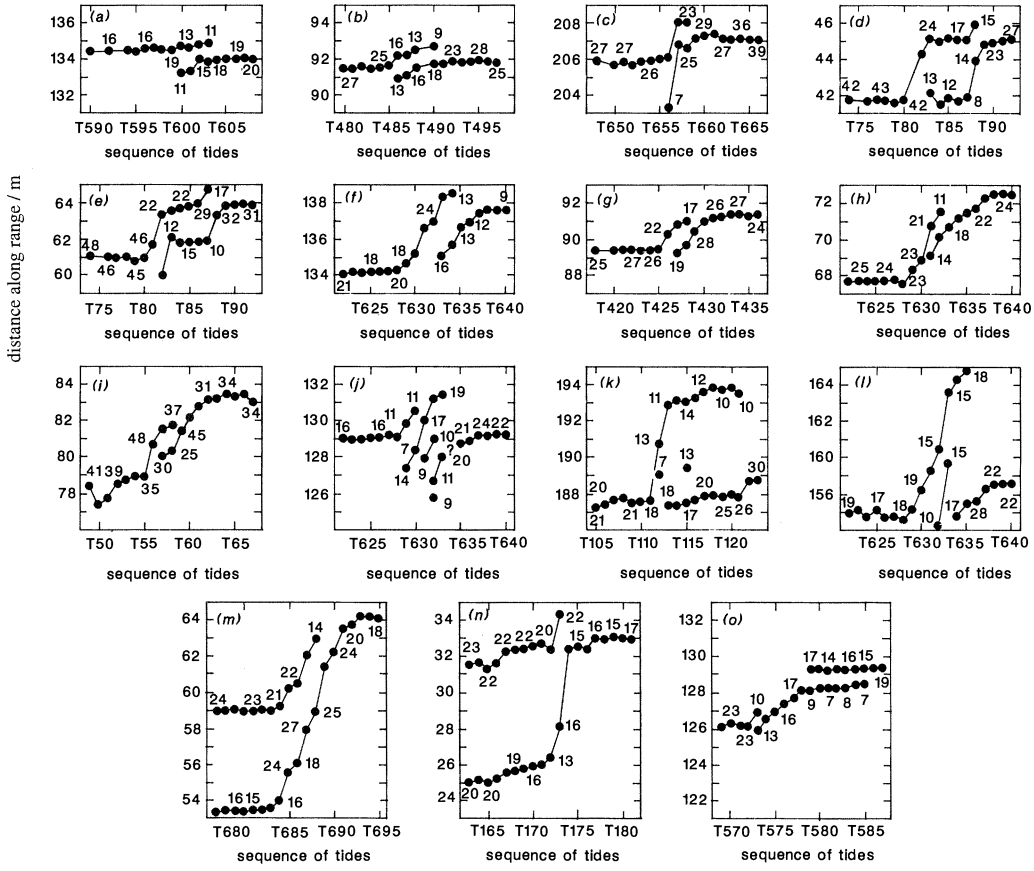

Figure 24. Interactions between mature dunes illustrated by respresentative time-distance plots of crests. Crest height in centimetres given beside selected dune positions.

sand transport. One migrated 7.6 m to the right of the transport direction while advancing 3.8 m (see figure 22*m*).

(*c*) *Interactions involving nascent dunes*

As nascent dunes are highly mobile, because of their small size, we are not in general sure of their identity from tide to tide, but nevertheless judge the morphological evidence to indicate their involvement in at least two kinds of interaction.

We often saw features (see figure 18*c* and 19*a*) suggesting that two or more nascent features grew to interfere and fuse laterally while advancing abreast toward the crest, single or supplementary, of a mature dune. The resulting bedform has a relatively long and sinuous to straight crest, but is subordinate in scale to the mature dune on which it is superimposed. Hence many supplementary crests, locally and intermittently developed on mature dunes, probably arose by the growth, spanwise fusion and straightening of nascent forms, a view supported by the positive correlation between the frequencies of supplementary crests and nascent dunes (see figure 20*c*).

The second interaction involves single nascent dunes and the crests of mature

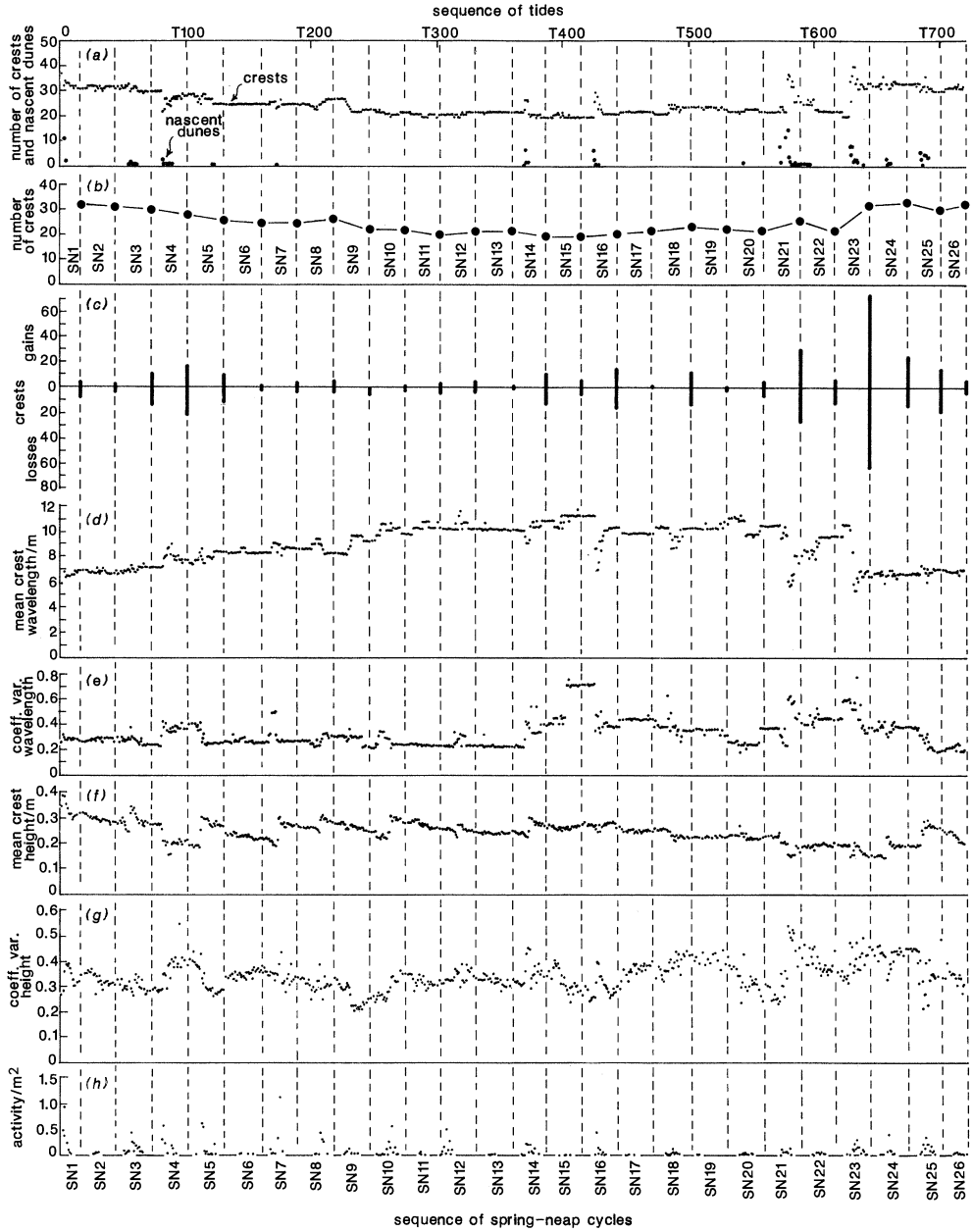

Figure 25. Summary of behaviour and properties of profiled crests. (*a*) Total crests and nascent dunes on a tide-by-tide basis. (*b*) Number of crests per spring-neap cycle. (*c*) Gains and losses of crests per spring-neap cycle. (*d*) Mean crest wavelength on a tide-by-tide basis. (*e*) Coefficient of variation of crest wavelength on a tide-by-tide basis. (*f*) Mean crest height on a tide-by-tide basis. (*g*) Coefficient of variation of crest height on a tide-by-tide basis. (*h*) Tide-by-tide activity.

dunes. We could not trace it through time, for reasons already stated, but at many spring-tide low-waters saw what we claim are stages in a morphological continuum compatible with the interaction. The earliest stage (see figure 23*a*)

PHILOSOPHICAL TRANSACTIONS OF THE ROYAL SOCIETY A MATHEMATICAL, PHYSICAL & ENGINEERING SCIENCES

sees the advance of a nascent dune to within 1-2 m upstream of the crest of a mature dune. As the two forms travel further, the nascent one at the faster rate, the dune crest becomes lowered and forward-bulging, at first only moderately (see figure 23*b*, *c*) but later more severely (see figure 23*d*). At an advanced stage (see figure 23*e*, *f*), the crest and leeward slope of the mature dune are almost obliterated, while the nascent dune is increased in height virtually to that of the original mature feature. Thus the nascent form, by simultaneously driving forward and obliterating a section of the crest and lee of the mature dune, locally replaces that dune, becoming locally in its turn the mature form. The latter 'captures' the nascent dune only in the restricted sense that for a while it holds the ends of the nascent form. What we describe may occur widely amongst tidal bedforms. Elliott & Gardiner (1981) note that their isolated megaripples (nascent dunes) 'migrate faster than the bedform on which they are superimposed, and eventually intersect and locally deflate the main slipface'. Dalrymple (1984) describes a related interaction between his sandwaves and superimposed megaripples. A similar process seems to have affected the 3D sandwaves of Terwindt & Brouwer (1986, fig. 9).

Our second interaction has important implications for the internal structure of the mature dunes affected (see § 6*d* below). The more rapid advance of the nascent form, and the accompanying progressive deflation of the crest and leeward slope of the mature dune, should create an erosional discordance eventually preserved through burial within the final bedform, as conjectured earlier (Allen 1968, fig. 5.16; Allen 1973, fig. 3) and partly shown experimentally (McCabe & Jones 1977). The developmental sequence (see figure 16*e*–*g*) indicates a discordance that is probably convex-up to semi-sigmoidal in streamwise profile and certainly less steep than the underlying and overlying avalanche laminae. Because of the laterally restricted shape of the nascent dune, however, the discordance should be slightly concave-up in spanwise profile (see figure 16*h*).

(*d*) *Interactions involving mature dunes*

Analysis of our detailed, tide-by-tide record of bedform movements showed that five kinds of interaction can occur during the more vigorous tides, involving either the principal and supplementary crests of a mature dune or, less often, two mature forms. Sixty-eight interactions in all were noted during the survey period.

Interactions of type A (48 examples) see the replacement of a length of the leading crest of a dune by a single supplementary crest, in a similar manner to the nascent forms but on a front many metres long (see figure 24*a*–*i*). Having appeared on the dune stoss, the supplementary crest maintains during the interaction a relatively constant distance upstream from the leading crest. The separation varies between roughly 1 and 3 m and tends to grow with bedform height at the start of interaction. Typically, the height of the supplementary crest increases fairly steadily, while that of the principal crest tends to decline. The interaction is completed in 2–7 tides; the supplementary crest gradually obliterates a substantial length of the principal crest, itself becoming the crest of a locally renewed single-crested bedform. The new crest, however, invariably lies slightly upstream from the last detectable line of the old. Internally, the final bedform should preserve a discordance similar to that resulting from a nascent dune (see figure 16*e*–*h*), but perhaps less steep and certainly flatter spanwise.

Type B interactions (3 examples, all in S23) resemble those of type A, but see

the advance and replacement of a series of crests of which generally only two, one supplementary (upstream) and the other principal (downstream), are visible at any one tide (see figure 24*j*).

Type C interactions (5 examples) involve mature dunes with open terminations, occuring as the latter shift across the path of sediment transport either in the same direction at different rates, or in opposite directions (see figures 22 and 24*k*, *l*). The characteristic signature shows one dune suddenly advancing quickly in anticipation of the appearance of the other. Height is lost as the termination passes across and off the range. Conversely, a dune passing on to and across the range appears to gain in height.

Interactions of type D (11 examples) also affect mature dunes (see figures 22 and 24*m*, *n*). They occur whenever there is a spanwise movement of either a triple-junction or of an openly terminated dune positioned near an inflection point on the crest (in plan) of a second bedform.

We recorded one example of a fifth interaction which we call type E (see figure 24*o*). It involved three dunes, two with open terminations, that joined east of the range in a Y-shaped arrangement, the 'stem' of which pointed eastward. The southernmost dune shrank eastward across the range, while the open termination on the northern dune moved to the west.

(*e*) *Number of mature dunes*

The number of mature dunes (see figure 21*a*) on the range gradually fell from 32 at the end of SN1 to a minimum of 20 at the close of SN14, remaining near that level until the end of SN22 (see figure 21*c*). The next cycle, however, saw an abrupt increase to 30 (see figure 21*a*) followed in SN24 by the largest recorded total of 33 dunes. Thirty-one mature dunes existed at the end of the study, compared to 32 a year earlier (see figure 21*c*).

The number of mature dunes (see figure 21*c*) is the net change of dune appearances and disappearances (see figure 21*d*). Change of both kinds is mostly associated with SN4 and especially with SN22–SN24, when gains significantly exceeded losses. Appearances on the range are of three kinds: (i) entrance at the upstream (southern) end; (ii) spanwise growth on to the buoyed line; and (iii) appearance at the downstream (northern) end, due to the counting method (see figure 2). Disappearances are of two kinds: (i) exit downstream; and (ii) from within the range. Conservation requires that

$$\begin{aligned}\text{dunes at start (32)} + \text{dunes entering upstream (13)} + \text{dunes appearing within range (37)} + \text{dunes appearing downstream (1)} \\ = \text{dunes at finish (31)} + \text{dunes exiting downstream (7)} + \text{dunes disappearing within range (45)},\end{aligned}$$

where the numbers are the respective totals (excluding reappearances and subsequent disappearances of the same dune downstream). Hence annual dune turnover on the range is approximately twice the average size of the sample.

(*f*) *Numbers of profiled crests and nascent dunes*

The number of recorded profiled crests fluctuates markedly on a tide-by-tide basis (see figure 25*a*), but on a longer scale drifts downward to a minimum in SN14 and SN15, subsequently rising to a sustained peak in SN23–25. The number

PHILOSOPHICAL TRANSACTIONS OF THE ROYAL SOCIETY A MATHEMATICAL, PHYSICAL & ENGINEERING SCIENCES

at the end of a spring-neap cycle is much less variable and shows a similar pattern (see figure 25*b*) to the variation of mature dunes (see figure 21*c*).

Many profiled crests appeared and disappeared within a single spring-neap cycle (see figure 25*c*), especially during SN21 and SN23 and to some extent during SN3–SN5, SN14, SN16 and SN25. As with mature dunes

$$\begin{matrix}\text{crests at}\\ \text{start (37)}\end{matrix} + \begin{matrix}\text{crests entering}\\ \text{upstream (14)}\end{matrix} + \begin{matrix}\text{crests appearing within}\\ \text{range and downstream (280)}\end{matrix}$$

$$= \begin{matrix}\text{crests at}\\ \text{finish (32)}\end{matrix} + \begin{matrix}\text{crests exiting}\\ \text{downstream (16)}\end{matrix} + \begin{matrix}\text{crests disappearing}\\ \text{within range (283)}\end{matrix},$$

the brackets enclosing the respective totals. Hence the annual crest turnover is about 12 times the sample average (cf. mature dunes, § 5*e*).

Nascent dunes (see also figure 12) are most plentiful during spring tides and the warmer months (see figure 25*a*). The largest numbers accompany SN21, SN23 and SN25.

(*g*) *Wavelength and height of profiled crests*

The ensemble mean profiled-crest wavelength varies antithetically with number through the unfolding sequence of tides (see figure 25*d*). The value increases comparatively steadily up to a maximum of about 11 m in SN13; sharp but temporary falls below this ceiling mark SN14, SN16, SN18 and SN21 which follow. Another sharp fall in SN23 leads a sustained drop in the ensemble mean to about 7 m, roughly the starting value. The population tends to be most disordered in association with spring tides, as shown by coefficients of wavelength variation (ensemble standard deviation divided by ensemble mean) in excess of the general level (see figure 25*e*).

In figure 25*f* we show that, on the longer term, the ensemble mean profiled-crest height gradually drifts downward from the start up to SN21, with some increase toward early values in SN25. Superimposed on this trend, within each spring-neap cycle, is a sharp rise followed by a gradual recovery, except during the summer (SN17–SN21). Cycles yielding many nascent dunes (see figure 25*a*), and in which numerous profiled crests appear and disappear (see figure 25*c*), generally see a sharp but temporary fall in the ensemble mean. As shown by the coefficient of height variation (ensemble standard deviation divided by ensemble mean), height also is generally most variable during spring tides (see figure 25*g*).

(*h*) *Persistence and excursion of mature dunes and profiled crests*

In figure 21*a*, we have effectively characterized our mature dunes individually in terms of their persistence and excursion; our detailed records allow the profiled crests to be similarly analysed. The persistence (lifespan of Allen 1974) of a bedform is the interval of time, in units of an appropriate tidal period, over which it was recognisable on the range. The excursion (Allen 1974) is the streamwise distance travelled by the form during this interval.

Figure 26 should not be regarded as a complete characterization of our bedform population. Although our survey lasted a little over a year, no less than seven mature dunes on the range at the start survived to the close. The furthest-travelled dune, lying closest to the southern end of the range, covered only 66.6 m (about eight average dune wavelengths), taking 21 spring-neap cycles in the pro-

PHILOSOPHICAL TRANSACTIONS OF THE ROYAL SOCIETY A MATHEMATICAL, PHYSICAL & ENGINEERING SCIENCES

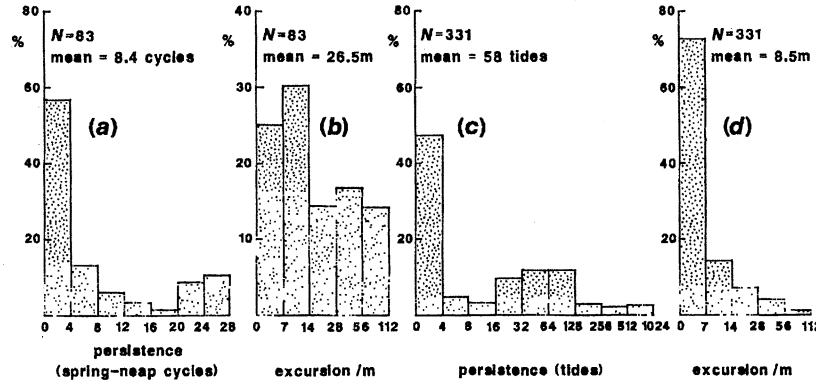

Figure 26. Mature dunes: (*a*) persistence and (*b*) excursion. Profiled crests: (*c*) persistence and (*d*) excursion.

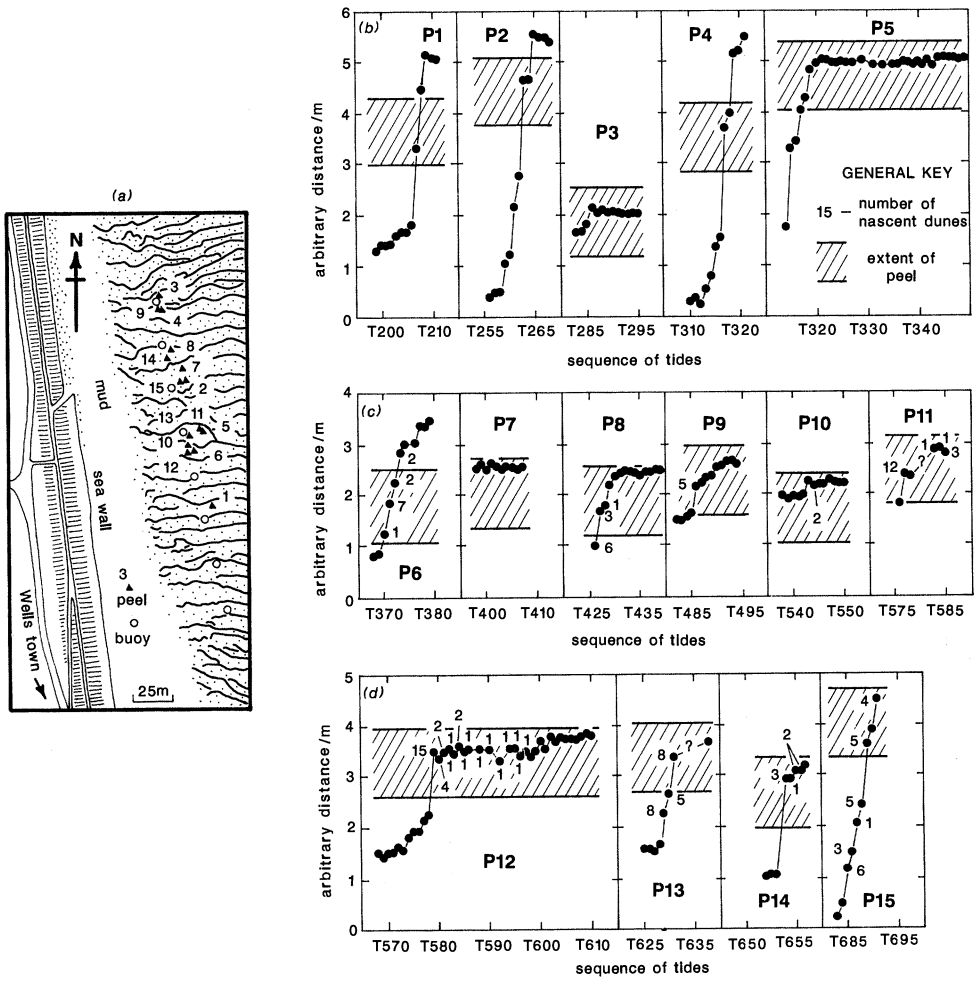

Figure 27. Behaviour of dunes from which peels (relief casts) were made. (*a*) Location of sampled dunes relative to the range, together with representative dune crests. (*b*)–(*d*) Time-distance graphs of the crests of the selected dunes.

cess; the other six dunes travelled shorter distances, commensurate with their initial positions on the buoyed line. Consequently, we do not know how far, and for how long, these severn bedforms would have travelled had a longer period for observation been available. It is nevertheless clear that mature dunes have a life, in terms of excursion and persistence, at least several times longer than that of profiled crests, which at times appear more than one to a dune and become engaged in the interactions described. In a field study of small dunes in the Calamus River, Gabel (1993) measured minimum excursions between 4.5 and 7 dune lengths. Under laboratory experimental conditions, dunes have been found to have excursions of only 1–2 wavelengths (Wijbenga & Klaasen 1983).

6. Internal sedimentary structures

(*a*) *Sampling*

To link internal bedding with sand transport patterns, we sampled internally at the end of each of 15 spring tides a selected dune bedform, the movement of which had been monitored (see figure 21). Stakes were emplaced upstream and downstream of the chosen dune just before the onset of the springs. The position of the dune relative to the stakes was measured at all subsequent tides until the springs were over (see figure 27). Across the stoss was then inserted a continuous row of five Reineck boxes (each approximately 0.26 m long by 0.4 m deep). These samples gave relief casts (peels) when treated with a pre-catalysed cold-setting polyester resin. During some tides the dune was lightly sprayed with differently coloured paints, or dusted with plaster of Paris, as a further means of linking internal structure to bedform movement. We used these potentially disruptive procedures sparingly and cautiously, however, recognizing that they could affect the subsequent response of the dunes to currents.

(*b*) *Scope of the peels*

Our peels are another record of the evolving morphology of the dunes. Some because of vigorous sand transport tell only of the most recent few dune-moving tides (see figure 27, P1, P2, P4, P14, P15), whereas others document longer sequences, but nonetheless of recent tidal flows (see figure 27, P6, P7, P11, P13). Long sequences of tides, commonly reaching back to earlier spring-neap cycles, are recorded in peels made at times of moderate or low sediment transport (see figure 27, P3, P5, P8, P9, P10, P12). Many peels in their lower parts contain laminae or beds that represent events on the bank probably antedating any that we observed (see figure 27, P3, P4, P8–10, P12–14).

The peels reveal in streamwise section arbitary portions of cross-bedding sets which, because they lie within active dunes, have not yet been incorporated into the population of sets preserved within Lifeboat Station Bank below the surface defined by the dune troughs. These more permanently preserved sets, because of dune truncation, could be substantially thinner than the sets we record in figure 28. Moreover, the preserved sets, again because of truncation, could have lost their upper levels, in which topset laminae and a variety of complex discordant features can occur (see below). The streamwise lengths of the preserved sets are unknown but, in terms of the crest and dune excursions measured, could amount to many wavelengths.

PHILOSOPHICAL TRANSACTIONS OF THE ROYAL SOCIETY A MATHEMATICAL, PHYSICAL & ENGINEERING SCIENCES

(*c*) *Cross-bedding*

Internally, the dunes are dominated by ebb-orientated cross-bedding (see figures 28 and 29). Cross-lamination with a flood-oriented component of dip, relating to ripple-scale bedforms, occurs in many peels but only to a very minor extent (see figure 28, P5, P7, P9–15). Curved bedding that formed as drapes in shallow troughs downcurrent from, but continuous with, cross-bedding occurs in several peels (see figure 28, P3, P7, P10, P11, P13, P14), affording gentle flood-directed dips. People digging or walking on the bank probably triggered the soft-sediment folding seen in three peels (see figure 28, P2, P9, P10), two of which date from the summer holiday-period.

Most foreset beds grade down into bottom-set strata. The rate of this transition, and the relative length of the bottomsets, vary substantially, but few peels (see figure 28, P11) lack bottomsets altogether. The cross-beds in many peels have been truncated in their relatively steep (26°–33°) and planar upper parts. One peel (see figure 28, P8) reveals an increase in foreset dip from about 30° to nearly 40° with decreasing tidal activity, and another (see figure 28, P13) shows foresets that appear to be oversteepened to about 45° at their upper ends, perhaps due to slight soft-sediment deformation. Rarely, a transition between foreset and top-set beds is evident (see figure 28, P2, P4, P5, P11, P14), recording the presence of a crestal shoulder on the dune (Allen 1968). In these cases, at a comparatively well defined brink point, the foresets pass up into lower angle but still ebb-oriented parallel laminations.

(*d*) *Intra-set discontinuities*

Without exception, the cross-bedding sets in our peels are interrupted along their length by a range of intra-set discontinuities (see figure 30) also, but less satisfactorily, called 'reactivation surfaces' or 'pause planes' (Collinson 1970; Klein 1970; Boersma & Terwindt 1981; De Mowbray & Visser 1984). These record a variety of events during bedform movement (see § 6*e* below). In streamwise spacing, the discontinuities range from much less than one set thickness apart, to a separation of several thicknesses, depending on the activity (see figures 27 and 28).

Discontinuities of type A are rolling to almost stepped, planar or convex-up erosional surfaces which truncate the bedding below and are buried by overlapping discordant laminae above. The breaks invariably commence either high up within, or at the top of, the set, but may descend to an intermediate height or even scoop down below the established set base. There are no detectable lithological changes across them. Partly because they are seen only in two-dimensions, these discontinuities cannot be interpreted unambiguously in the absence of constraining data on tidal flows. The convex-up to planar ones in particular suggest interactions between nascent dunes or supplementary crests and the main bedforms. An especially vigorous interaction is suggested by discontinuities that cut the set base, perhaps the result of storms or the most energetic of spring tides. Planar to rounded discontinuities could also arise during tidal reversals or through wave action during bedform ebb exposure.

Type B discontinuities, restricted to the lower part of a set, are concave-up erosional surfaces which cut bottomsets and scour below the established set base. There is again no accompanying change in lithology. These discontinuities also point to the rejuvenation of the bedform by some vigorous event, but are puzzling

PHILOSOPHICAL TRANSACTIONS OF THE ROYAL SOCIETY A MATHEMATICAL, PHYSICAL & ENGINEERING SCIENCES

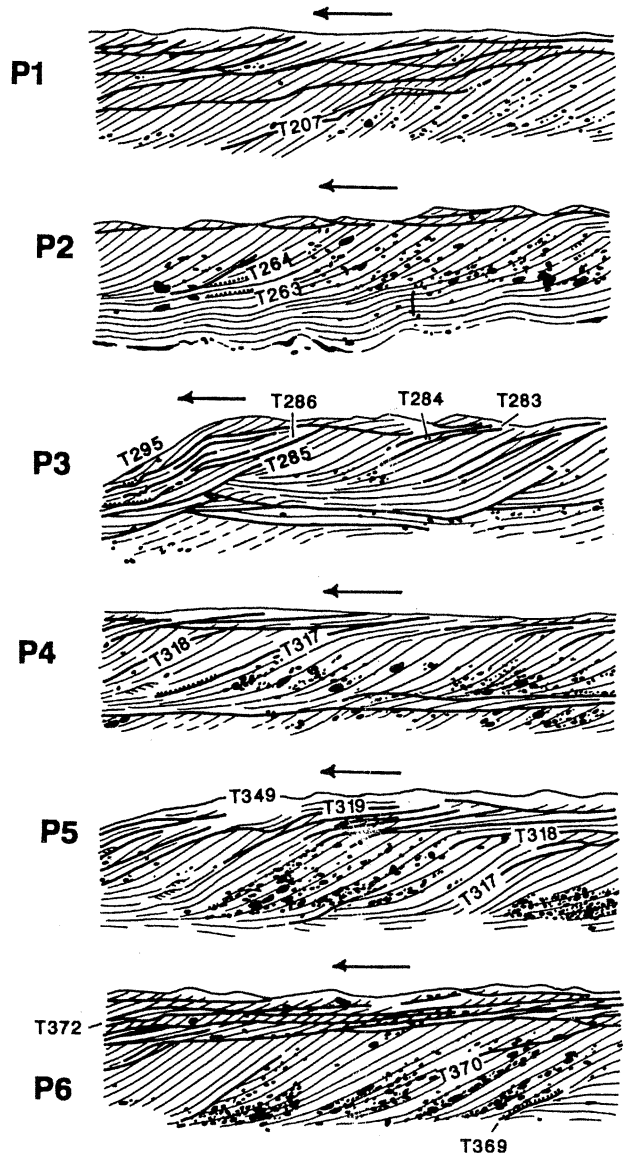

Figure 28. Internal sedimentary structure of selected mature dunes as shown by peels (relief casts) representing vertical sections parallel with the ebb tide. Features identified with particular tides are marked. See also figures 31 and 33.

in that there is apparently no evidence for the reshaping of the upper part of the dune. Type C discontinuities resemble them, but fail to cut the set base and fade out amongst the bottomsets. The origin of type C discontinuities is obscure, except where a stepped profile is visible, suggesting wave activitiy on water ponded in the dune troughs.

Discontinuities of type D involve a lithological change expressed as a planar to concave-up mud drape that either overlies an erosional surface or passes up-

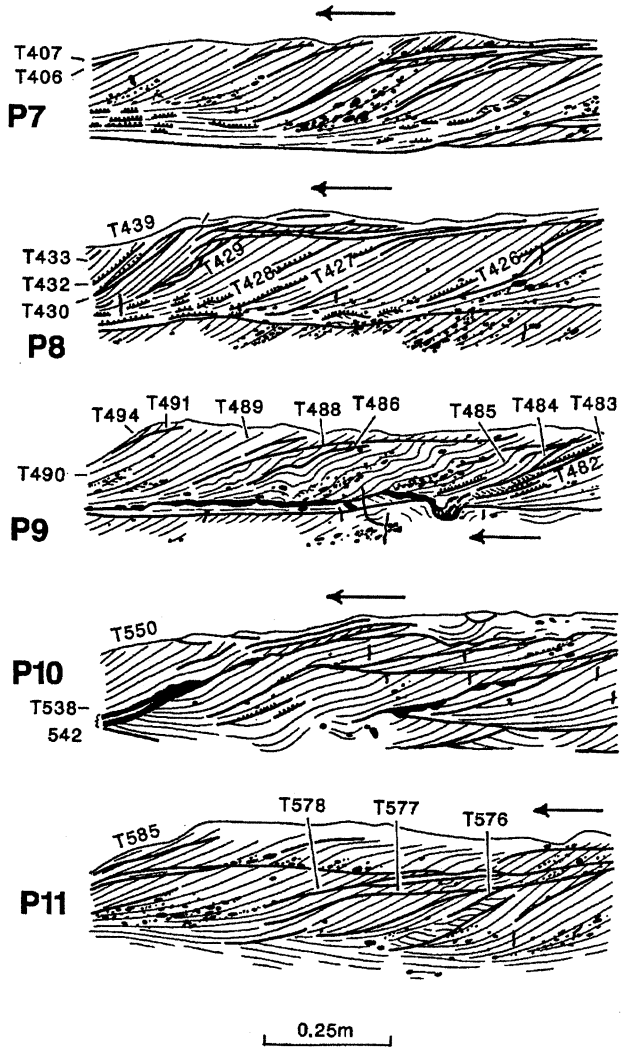

Figure 28. Continued.

ward into one. In some cases, the drape amongst the bottomsets smothers one or more internally cross-laminated ripple marks that faced the dune. Very rarely current ripples overlie the drape. Where flood-facing ripples, a mud drape, and an erosional discontinuity are combined, we are confident that tidal reversal and high-water slack are indicated. Draped ripples alone in the lower part of the set, however, need not record other than the ponding of muddy water in the dune trough at low tide.

Some peels disclosed our painted or powdered surfaces, but associated with neither a detectable erosional break nor a mud drape. These marked laminae clearly record the cessation of dune movement, but we accept that the coating, no matter how lightly applied, may have stabilized the sand sufficiently that an aberrant response to the tidal flow resulted.

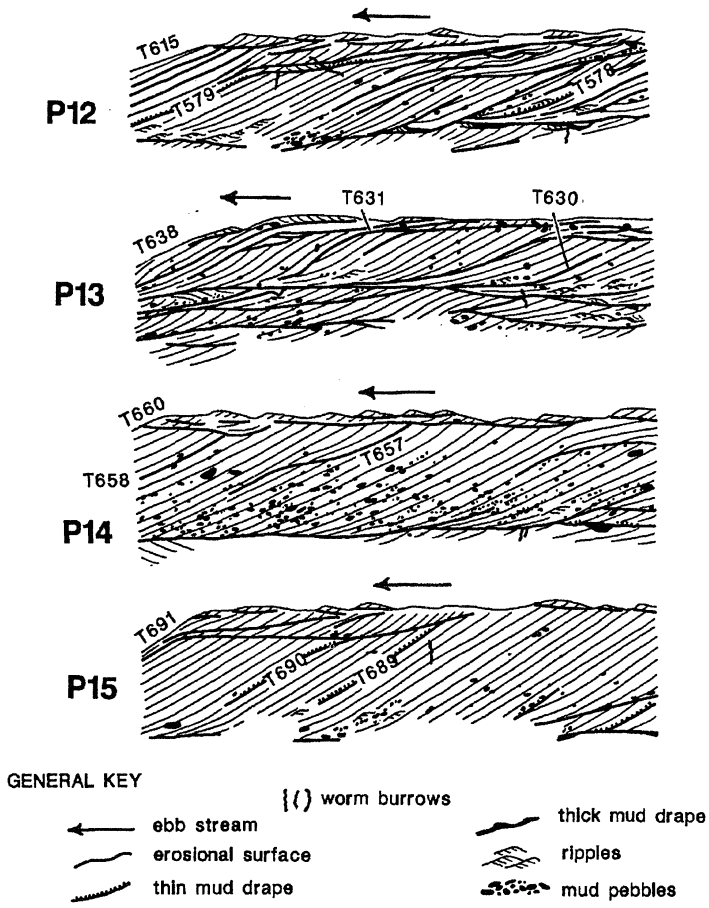

Figure 28. Continued.

(*e*) *Notes on individual peels*

Figure 28 illustrates the bedding patterns and relations mapped on to photographs after close inspection of the peels (see also figure 29).

Peel 1 records a cross-bedding set shaped by vigorous surge-augmented tides (see figure 12 and table 1). Several gently inclined type-A discontinuities are present. The stepped form of the surface attributable to T207—the only tide recorded in the peel—recalls the profile of a dune at a late stage of interaction with either a nascent dune (see figure 23) or supplementary crest, although no nascent forms were seen at the subsequent low water (see figures 12 and 27). Judging from the time-distance graph (see figure 27), the other discontinuities represent superimposed bedforms active during ebb, and not dune exposure as might under other circumstances be inferred.

Vigorous spring tides also shaped peel 2 (see figures 12 and 27). T263 and T264 are recorded by short mud drapes, perhaps formed at low tide in the dune trough. Judging from the time-distance graph, the subsequent type-C discontinuity represents an erosional event early in the ebb of T265. The absence from

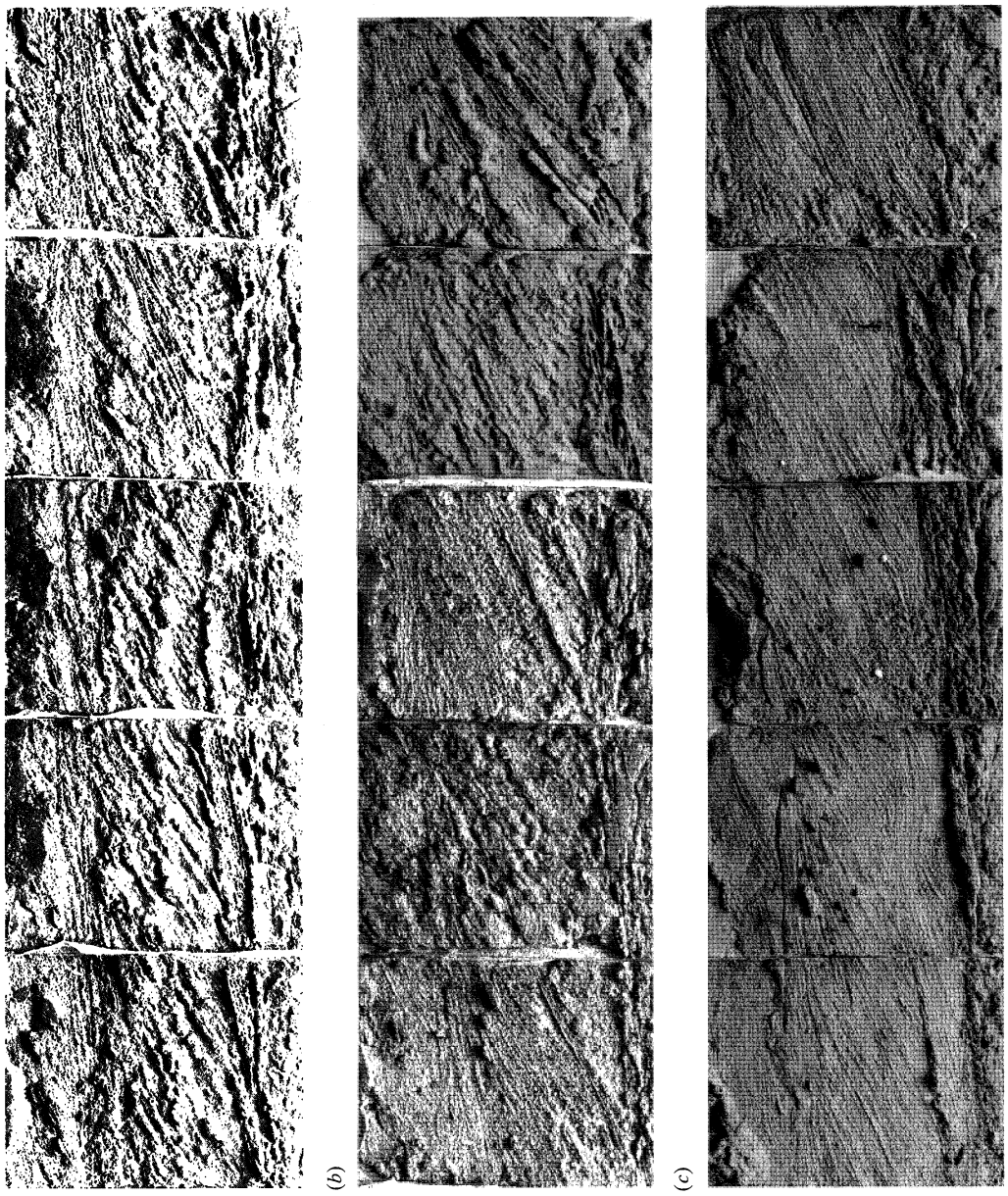

Figure 29. Sets of photographs of representative relief casts (to be read from left to right). (*a*) P4, (*b*) P8, (*c*) P12. Each composite peel is approximately 1.3 m long. See also figure 28.

the set of further breaks is compatible with the restricted diurnal inequality (see figures 12 and 27).

Peel 3 records weak springs (see figures 12 and 27). T283 and T284 are represented each by a short type-A discontinuity, formed either during late ebb or, less probably, as the subsequent flood drowned the surface. The succeeding eleven

PHILOSOPHICAL TRANSACTIONS OF THE ROYAL SOCIETY A MATHEMATICAL, PHYSICAL & ENGINEERING SCIENCES

tides gave only six detectable breaks, two involving mud drapes (low tide), three of type A (including the surface at the time of sampling), and one of type B.

Peel 4 (see also figure 29*a*) was shaped by energetic springs with a marked and little-perturbed diurnal inequality (see figures 12 and 27, and table 1). T317 is represented by a convex-up erosional discordance that passes down-dip into a mud drape beginning high enough up to record the following high-water slack. T318 appears as a sigmoidal drape-less scour. The other three type-A discontinuities probably record nascent dunes, although none were evident at low water (see figures 12 and 27).

Peel 5 represents a dune tracked over weak springs (S13) and consequently has additional features, interpreted from the movement of the mature form nearest on the range, dating from the preceding S12 (see figures 12 and 27), but it is uncertain what events they reflect. Only four discontinuities are identifiable from the long interval T319–T349. All but two of the earlier discontinuities are attributable from figure 27 to interactions with nascent dunes.

The dune in peel 6 advanced approximately 2.6 m during S14, when nascent dunes were plentiful on the nearby range (see figures 12 and 27). T369, T370 and T371 are recorded by respectively type-D, type-A and type-C discontinuities. T372 is hesitantly identified amongst gently dipping type-A discontinuties mainly attributable to supplementary crests and/or nascent dunes.

Peel 7 represents a dune that was almost stationary during the sampled spring tides (S15), and which consequently has structures dating from the preceding S14 (see figures 12 and 27). These are mainly type-A and some type-D discontinuities, the impression of a representation of the diurnal inequality being misleading (see table 1). Flood-oriented current ripples overlie the low-tide mud drape contributing to the second break. Flood-tide rounding may therefore be recorded.

A dune lightly painted every low tide appears in peel 8 (see figures 18*c* and 29*b*). T426, T427, T428 and T432 each gave a long mud drape that conceals a coloured surface, allowing these type-D discontinuities to be assigned to the following flood tides (rise and/or high-water slack). T429, T430 and T433 are recorded as type-A breaks. A few breaks cannot be assigned to either the exposure or drowning of the bedform, and so must record probably nascent dunes. The apparent diurnal inequality is of purely meteorological origin (see figure 12 and table 1).

Moderately vigorous tides shaped peel 9, disturbed by holiday-makers (see figures 12 and 27). Long mud drapes record the high-water slacks following T482 and T483, and the two shorter (possibly low-tide) drapes may represent earlier tides. T486, T488 and T491 are seen as type-A discontinuities, and T484, T485, T487, T489 and T490 as coloured but uneroded surfaces. The remaining breaks probably record interactions with nascent dunes, many of which were seen after T486 (see figure 27).

Peel 10 represents perhaps three sets of springs (see figures 12 and 27), the first (S18) of moderate activity and the last two weak (S19, S20). T538-542 are recorded as partly superimposed painted surfaces and by a thick and complex mud drape attributable to N19. The preceding thick drape probably represents N18.

A dune active during moderate but surge-disturbed tides is seen in peel 11 (see figures 12 and 27, table 1). T576 (painted surface), T577 and T578 are recorded as type-A discontinuities. The structures between T578 and the final surface (T585) suggest the repeated advance of supplementary crests and/or nascent

PHILOSOPHICAL TRANSACTIONS OF THE ROYAL SOCIETY A MATHEMATICAL, PHYSICAL & ENGINEERING SCIENCES

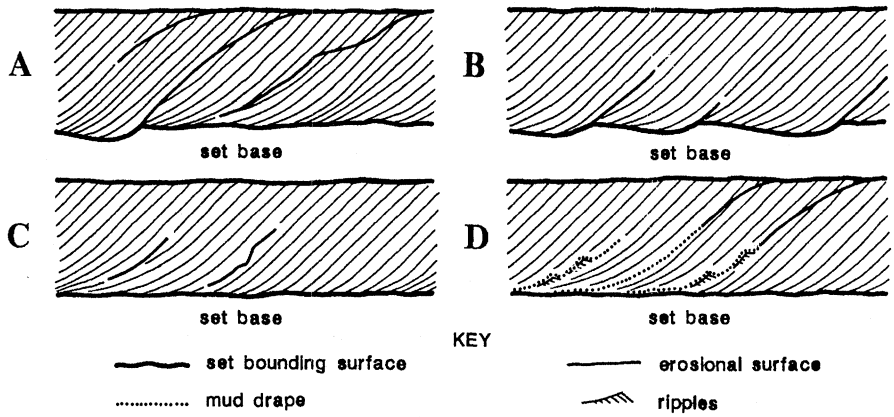

Figure 30. Sketch of kinds of intra-set discontinuity encountered in peels from mature dunes at Lifeboat Station Bank.

dunes (recorded in large numbers from the range over that period), and some of these lesser forms seem themselves to have been reactivated.

Peel 12 (see also figure 29*c*), sampled at the end of S22, includes many features due to S21 (see figures 12 and 27). T578 is recorded by a short low-tide mud drape and T579 by a long drape deposited during the subsequent high-water period. Five intervening type-A breaks testify to the action of supplementary crests and/or nascent dunes. T579–T615, however, failed to yield any large total of these subordinate forms.

Peel 13 records a vigorous set of springs (see figures 12 and 27). T630 is represented by a type-B discontinuity and T631 by a break of type A. The two intervening discontinuities point to interactions with supplementary crests and/or nascent dunes, both kinds of feature occuring on the bank at low water (see figures 12 and 27). In number, the breaks in the set between T631 and T638 fall short of the tides.

Moderately energetic surge-disturbed springs formed peel 14 (see figures 12 and 27, table 1). T657 and T658 are identifiable, but the earlier breaks represent superimposed smaller bedforms active during the ebb. Some nascent dunes were recorded nearby.

The set in peel 15 was also shaped by vigorous tides (see figures 12 and 27). Long slack-water mud drapes represent T689 and T690. Nascent dunes appeared in numbers on the range during these springs, and breaks attributable to them occur between T690 and T691. The diurnal inequality is clearly recognizable.

(*f*) *Comparison with other records*

The internal structural patterns displayed by our dune bedforms would be difficult to interpret unambiguously if preserved, say, in the rock record, in the absence of direct information on the sequence of tidal heights and sand transports. One reason is that our bedforms are at times comparatively immobile (cf. Dalrymple 1984; Dalrymple *et al.* 1990), so the indicative features can be inseparably crowded (e.g. some mud drapes). It is, secondly, difficult to distinguish discontinuities due to the activities of nascent dunes and/or supplementary crests within one phase of the tide (i.e. the ebb) from features due to tidal reversal, that is, the change from the ebb to the flood phase. The third reason is the considerable

disorder introduced at Lifeboat Station Bank by the frequent, largely seasonal meteorological events. The diurnal inequality, for example, is seldom expressed by an orderly spacing of discontinuities. In other contexts, however, the structural expression within cross-bedding sets of shorter-term tidal patterns, including the diurnal inequality, seems to be almost perfect (see, for example, Terwindt 1981; De Boer *et al.* 1989).

7. Bedform properties in a complex unsteady flow

(*a*) *Properties under uniform steady conditions*

Our main aim was to learn more about the response of bedforms to changes in natural hydraulic conditions. Ideally, the tidal flows and bedforms at Lifeboat Station Bank constitute a nonlinear dynamical system of some complexity (but apparently not chaotic), such as occur widely in the biological and physical worlds (May 1973; Thompson & Stewart 1986; for semi-popular reviews see Gleick 1988; Stewart 1990). In our example, the tidal variations of water depth drive the tidal streams, which in turn create the sediment transports enabling the bedforms to respond, through alterations in their size, shape and relative position, to the unfolding temporal sequence of fluid and flow properties (themselves influenced by the bedforms that are present). This multi-periodic situation is perturbed by quasi-periodic meteorological effects. An insight into the deterministic 'rules' underpinning our system, together with the sources of its nonlinearity, comes from laboratory work on dunes and current ripples in uniform steady flows.

Under uniform steady conditions, the ensemble properties of a bedform population remain statistically stable, at levels determined by the fluid (density, viscosity), flow (strength, depth), and bed material (solids density, grain size, sorting). Individual bedforms, however, change in size, shape and relative position as the local sand-transporting currents remodel them, and they, simultaneously, affect the local pattern and strength of flow over the bed. This stochastic behaviour is well established for both current ripples (Ashida & Tanaka 1967; O'Loughlin & Squarer 1967; Allen 1968, 1973; Squarer 1970; Taylor 1971; Nordin 1971; Pratt & Smith 1972; Jain & Kennedy 1974) and dunes (Nordin & Algert 1966; Ashida & Tanaka 1967; Fukuoka 1968; Hino 1968; Crickmore 1970; Taylor 1971; Nordin 1971; Annambhotla *et al.* 1972; Pratt & Smith 1972; Shen & Cheong 1976). Not only do individual bedforms change once established, but new individuals arise to replace those being destroyed, in what amounts to a birth-death process (see, for example Allen 1973; Gabel 1993). Hence, when flow conditions change, the bedform population is itself in some measure able to respond. The ability of the bed to change, however, depends on there being a redistribution and transport of sand over the bed. As the bedforms increase in size—the cross-sectional area is broadly proportional to the square of the wavelength—their ability to respond to a given change must decline. Inevitably, therefore, the change in ensemble properties will increasingly lag a change in flow.

The sediment transport is one major source of nonlinearity in a system such as we discuss. We have demonstrated at Lifeboat Station Bank (see figure 10) that both flow strength (maximum overall mean velocity), and particularly a measure of sediment transport (mean range activity), are nonlinearly increasing functions of tidal height.

A second important source of nonlinearity in a dune population is the variation in wavelength and height with flow depth, as perceived under a range of uniform steady conditions. Empirically, ensemble mean wavelength broadly increases with flow depth and is roughly six times the depth (Allen 1982, fig. 8-18). For constant depth, however, ensemble wavelength and bed sediment coarseness are inversely related (USWES 1935; Simons *et al.* 1965*b*; Guy *et al.* 1966). The variation of ensemble mean height with depth is more complex (Shinohara & Tsubaki 1959; Stein 1965; Guy *et al.* 1966; Williams 1970). The relative height is a maximum at about the middle of the broad range of hydraulic conditions appropriate to dunes (see Allen 1982, figs 8-21, 8-24), but smallest near the boundaries with the current ripple and plane-bed fields. A similar nonlinear relation, expressed as a bell-shaped curve, describes the way dune steepness (ensemble height/wavelength) varies with flow strength (Fredsøe, 1975, 1982; Yalin & Karahan 1979). Although dunes will increase in wavelength with increasing flow depth and decreasing sediment size, they may not similarly increase in height.

Apparently like current ripples (Allen 1969, 1977; Banks & Collinson 1975), dunes become increasingly three dimensional with growing flow strength, as is clear experimentally (see Guy *et al.* 1966) as well as from the field (see Rubin & McCulloch 1980; Terwindt & Brouwer 1986). This trend in dunes is mainly expressed internally as a change from tabular to trough cross-bedding.

(*b*) *Change on short and intermediate timescales*

Our chosen site on Lifeboat Station Bank offers both gains and disadvantages for the study of bedforms in unsteady flows. Wind-generated waves and river floods can be ignored, and the flows that constitute the only significant dune-changing events are unidirectional, although tidally generated. Storm surges at times either enhance or diminish the effectiveness of these flows (see figure 14), but without changing their unidirectional character. However, the unsteadiness develops on an extensive hierarchy of timescales, such as is lacking in rivers. On Lifeboat Station Bank, dunes are active within a relatively small number of short, pulse-like periods during certain of the ebb tides. These semi-diurnal, crest-moving events are the basic component flow events in the hierarchy. Above them come two levels of astronomical variation of either a short or intermediate timescale: diurnal and semi-monthly (spring-neap cycle). Above these again are monthly (lunar monthly inequality), semi-annual (equinoctial), and annual variations. Superimposed on this complex but predictable unsteadiness are quasi-periodic variations due to the frequent and often potent storm surges (see figures 6 and 14).

Crest-moving flows are the only tidal events that can change the dune population. Although many ebb tides nudge the bedforms forward a little, it is only when the mean range activity reaches about 0.15 m^2 that change in our sense becomes possible. The frequency distribution of measured mean range activities is exceptionally skewed and only 42 tides (5.84%) of the total of 719 caused activities in excess of the above (see figure 31*a*). The longest of these events probably occupied about 2.5 hours (20%) of a semi-diurnal cycle. However, because of the marked variation in form of the time–velocity graphs for tides of equal height (see figure 9), we cannot be certain about the duration of crest-moving events, but think that a duration of roughly one hour is about average. On this basis, crest-moving events defined in terms of the above activity level occupied only

PHILOSOPHICAL TRANSACTIONS OF THE ROYAL SOCIETY A MATHEMATICAL, PHYSICAL & ENGINEERING SCIENCES

1–2% of the whole year. The dunes, for the vast majority of the time, were inactive as such.

In figure 31*b* we summarize in phase space the sequences of tides (see also figure 25) which created the most important changes in our population of profiled crests. Eleven single-tide events raised the ensemble mean crest height by more than 0.04 m. In eight such cases the observed tidal height was more than 0.2 m higher than the preceding one. Two other increases coincided with decreases in the number of profiled crests, but may simply have been a result of the preferential loss of crests with lesser heights. Five single-tide events saw decreases of more than 0.04 m in the ensemble mean crest height. Two in SN4 were events in which tidal height was lower than the preceding tidal heights. A single event in late July (T573 in SN21) was associated with a strongly increased tidal height. Another in late August (T632 in SN23), also accompanied by a sharply increased tidal height, stands out within a lengthy burst of almost catastrophic change in the long quiescent population (see figures 21*a* and 25). Turning to the number of profiled crests (see figure 25), with an inverse relation to the ensemble mean wavelength (see figure 25*a*, *d*), 18 single-tide events changed the total population by more than four crests. These pulse-like events in some respects resemble the sudden imposition, as by an experimenter, of a steady dune- or ripple-forming flow on an artificially flattened sand bed (see Tsujimoto & Nakagawa 1984). Over a short initial period, ensemble height, wavelength and steepness increase very rapidly, while bedform number (over some fixed bed length) declines. High transport activities at Lifeboat Station Bank generally see the appearance of the comparatively small nascent dunes (see figures 12, 21 and 25*a*), as well as supplementary crests, swelling the profiled total. These comparatively small features seem to correspond to the bedforms seen early on after the imposition of the experimental flow to which we allude. The various accompanying interactions involving nascent dunes and supplementary crests on the scale of single-tide events leave a range of imprints internally within our bedforms (see figures 16, 24 and 28). The intra-set discontinuities that record these interactions have a good chance of permanent preservation, provided that the bedforms containing them are not truncated too deeply by their successors (see also Langhorne *et al.* 1985).

The diurnal inequality, involving a variation of high-water levels of the order of 0.15 m, is another small-scale tidal periodicity which can be reflected in bedform movements (Allen 1985; De Boer *et al.* 1989). There is occasionally evidence for it in the form of alternations of crest migration amounts during springs (see figure 27), as well as in patterns of internal discontinuities (especially those with mud drapes)(see figure 28), but at Lifeboat Station Bank it is generally blurred by the effects of surges (see table 1).

Speaking generally, unsteadiness on the spring-neap scale completely dominated change in the bedform population (see figures 25 and 31). These periods saw anything from a maximum of ten significant events to minima, notably during the late spring and summer, when there was no detectable crest movement. Numbers of profiled crests tend to increase and then decrease during the springs, but not necessarily to the initial levels. The ensemble mean height may either increase and then decrease (SN1, 5, 10, 14, 24, 25), decrease and then increase (SN4, 12, 15), simply decrease (SN21), or vary in some other and generally more complex way (SN3, 7, 8, 22, 23). In the case of both crest number and height, the change tends to lag the variation in flow properties.

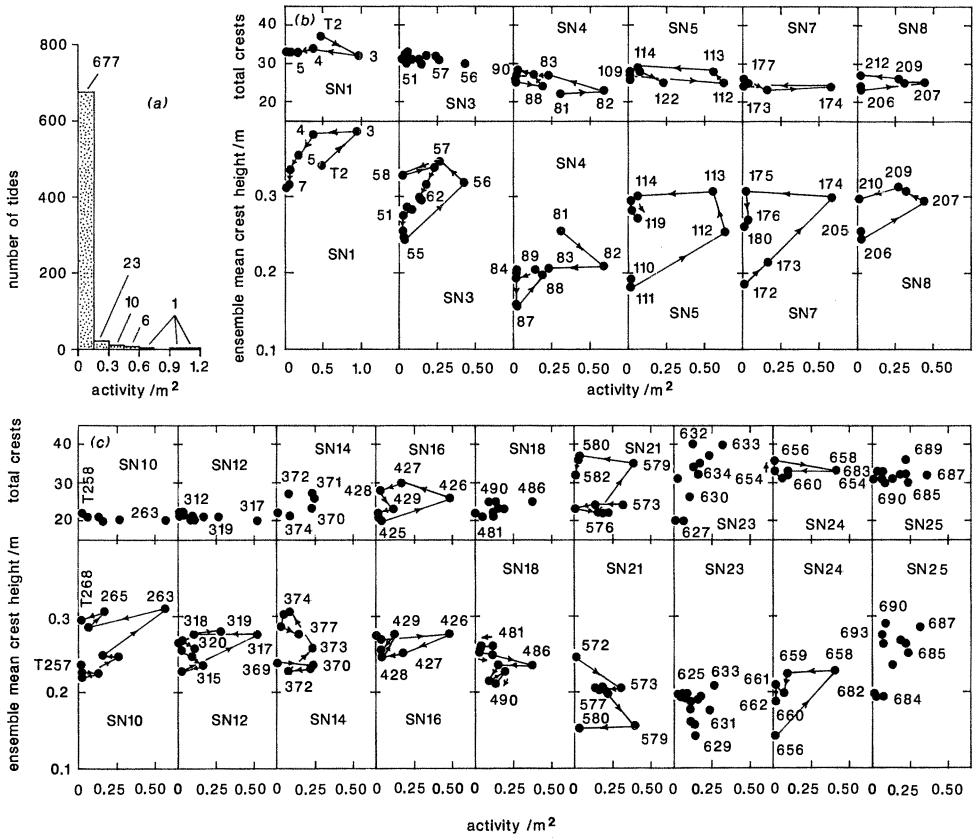

Figure 31. Ensemble properties of population of profiled crests as a function of activity and implicit time over selected spring-neap cycles. (*a*) Frequency distribution of activity values. (*b*), (*c*) Behaviour of total of crests and crest height. Data points are connected to show the flow of time where there is considered to be a clear pattern resembling a limit cycle.

Other populations of large tidal bedforms are known to change on the spring-neap scale, at least over time-series up to a few cycles long. Cornish's (1901) and Elliott & Gardiner's (1981) dunes moved most and were steepest during springs but became flattened at neaps. G.P. Allen *et al.* (1969) found, over two spring-neap cycles, that the ensemble mean height and wavelength varied systematically with tidal height, but with a variable lag (hysteresis) depending on the general strength of the springs (see also Allen 1974, 1976*a*). Some evidence for lag was also detected by Langhorne *et al.* (1985). Terwindt & Brouwer (1986), working over three spring-neap cycles, discovered that dune ensemble mean height and wavelength increased during the more vigorous tides, but with delays relative to the flow. At the height of the changes, short-wavelength features apparently similar to our supplementary crests tended to appear. The system at Lifeboat Station Bank, however, is not in general as dynamic as any of these.

(*c*) *Change on long timescales*

Unsteadiness on the lunar monthly cycle is clearest in the alternation of spring-neap cycles with large and small total activities (see figure 13), but finds lit-

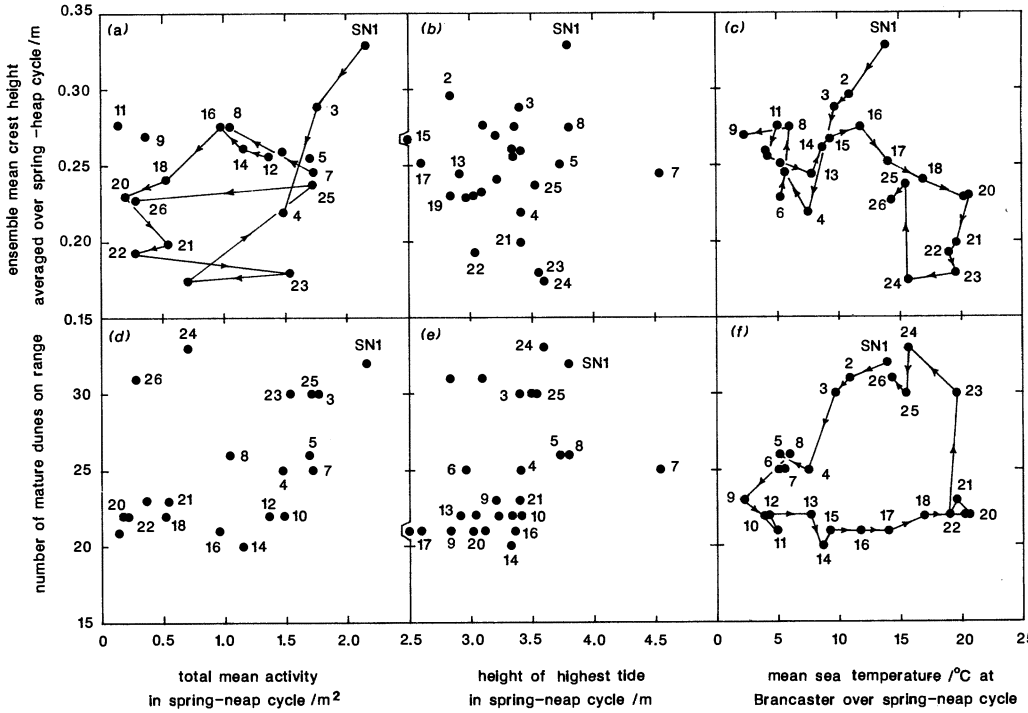

Figure 32. Ensemble properties of population of bedforms (a characteristic profiled crest height; number of mature dunes) as a function of (*a*), (*d*) total mean activity per spring-neap cycle (*b*), (*e*) height of highest tide in spring-neap cycle, and (*c*), (*f*) mean sea temperature at Brancaster over spring-neap cycle. Data points are connected to show the flow of time where there is considered to be a clear pattern resembling a limit cycle.

tle systematic expression in the properties of the bedforms (see figure 25). One preservable structural expression, however, is the close bundling of intra-set discontinuities during the weaker spring-neap cycles (see figure 28). A consideration of the astronomical tides suggested that there should also be change on an equinoctial timescale (see figure 5). The frequent storm surges during the winter, however, caused extra sediment transport sufficient to eliminate change on this period (see figures 13 and 14). Hence the system in this respect came to resemble most rivers, which vary in discharge on a 12-monthly cycle.

The most striking expressions of unsteadiness on a long timescale are to be seen in the variation of a characteristic dune height (ensemble mean averaged over a spring-neap cycle) and the number (inverse of wavelength) of mature dunes on the range. Height seems to change on limit cycles with activity and water temperature but appears to be independent of tidal height (see figure 32*a*–*c*). The general effect of increasing sea temperature is to decrease the general bedform height. The number of mature dunes varies with activity according to a rather confused, anticlockwise limit cycle (see figure 32*d*), with SN23 witnessing the major recruitment to the population after the spring and summer fall. As with dune height, the number of dunes appears to be independent of tidal height, but changes on a well-defined limit cycle with sea temperature (see figure 32*e*, *f*). We have already noted than an increase in temperature sees a noticeable decrease in the coarseness of the sand on Lifeboat Station Bank (see figure 7*a*). These

PHILOSOPHICAL TRANSACTIONS OF THE ROYAL SOCIETY A MATHEMATICAL, PHYSICAL & ENGINEERING SCIENCES

annual patterns of variation are driven by the level of sediment transport but apparently governed by sea temperature. The activity is greatest from August to April, and it is over this period that the mature dunes decline in number from about 32 to 22, while the temperature falls from 20 °C to about 4 °C. The fluid viscosity correspondingly increases by about 60%, lowering the settling velocity of bed grains by a similar degree, and in effect reducing the coarseness of the sandy bed material. The effects of temperature change on the scale of the bedforms at Lifeboat Station Bank, albeit a lagged response, does not seem incompatible with the conclusions of Allen (1982) and of Southard & Boguchwal (1990*a*, *b*) derived from steady-state experiments, if it is accepted that the system is effectively operating in the lower part of the range of stream powers appropriate to dunes.

Ours is the only reported study of bedforms in a purely tidal environment that show a delayed variation in properties on an annual scale. Long term lagged responses to flow changes, however, have been described from dunes in the river-dominated tidal reaches of the Fraser (Pretious & Blench 1951; Kostaschuk *et al.* 1989; see also Allen 1974, 1976*a*) and Weser (Nasner 1974; see also Allen 1974, 1976*a*, *d*). Dunes in rivers beyond the reach of tides also respond with a variable lag to seasonal and other patterns of flow (Carey & Keller 1957; NEDECO 1959; Stückrath 1969; Peters 1971; Jackson 1976; Gabel 1993). Indeed, the lagged response of aqueous bedforms seems universal where fluid and/or flow properties are changeable, although the particulars of the pattern, almost invariably expressible as limit cycles, vary greatly from case to case (see Allen 1982, for review).

8. Conclusions

We conclude as follows as the result of monitoring for a year, in an ebb-dominated channel at Wells-next-the-Sea, the response of dune bedforms to changing tidal conditions.

1. Some stratification commonly being evident, the local and depth-mean tidal current velocity increase and then decrease during the tidal ebb. The peak current tends to increase steeply nonlinearly with increasing high-water height, but there are substantial differences in the peak velocity between tides of the same height.

2. The sediment bedload transport rate, estimated from the scale and movement of the dune bedforms, increases steeply nonlinearly with tidal height and velocity. The observed variations in the rate reflect the presence in the astronomical tidal régime of the diurnal inequality, spring-neap cycle, lunar-monthly inequality, and equinoctial cycle, as well as the presence of meteorological influences (negative or positive surges). Meteorological effects contribute significantly to the observed sediment transport. Because of autumn–winter winds and storms, the sediment transport effectively varies on an annual scale, rather than on the equinoctial period required by a purely astronomical tidal régime.

3. Sea temperature varies over a 15 °C range between winter and summer. Although temperature has no detectable influence on the bedload transport rate, the sand composing the dune bedforms coarsens slightly as the sea cools.

4. The dune bedforms on Lifeboat Station Bank are similar in scale and appearance to dunes described from other intertidal sand shoals. They vary from three-dimensional in character at times of vigorous sand transport to two-dimensional when the tidal conditions dictate a comparatively low rate. Commonly, during periods of vigorous transport, the dunes become multiple-crested as the result of

PHILOSOPHICAL TRANSACTIONS OF THE ROYAL SOCIETY A MATHEMATICAL, PHYSICAL & ENGINEERING SCIENCES

the development on their upper stoss slopes of what we call supplementary crests. Small, crescentic, dune-like features, or 'nascent dunes', also appear on the backs of the larger forms during vigorous tides. Nascent dunes, their occurrence triggered by a temperature-related threshold, are most plentiful during spring and summer. The evidence of our tide-by-tide survey suggests that nascent dunes evolve into supplementary crests, and that both nascent and supplementary features, by advancing faster than the main crest of the bedform, are able locally to replace the main crest. The bedform population seems to be operating toward the lower end of the range of stream powers appropriate to dunes.

5. The dune bedforms are cross-bedded (ebb-oriented) internally, the sets being broken along their length by a variety of intra-set discontinuities (e.g. erosion surfaces, mud drapes) which record such events as tidal reversal or the differential movement within the span of a single ebb tide of nascent dunes and supplementary crests. The frequent disturbance of the sediment transport régime by surges further ensures that there is little pattern in the spacing of these discontinuities.

6. Individual dunes can be recognized over long periods at Lifeboat Station Bank, while changing in character in response to the unfolding pattern of tidal flows and sediment transports. Simultaneously, the dune population changes in composition as the result of recruitment through the creation and development to maturity of new forms, in which nascent dunes and supplementary crests are implicated, and the destruction of existing features.

7. The ensemble characteristics of the dune bedforms change with various time delays on a number of periodicities related to sediment transport and sea temperature. The ensemble mean height varies on both spring-neap (sediment-transport) and annual (sea temperature) scales; the height does not in every spring-neap cycle increase with growing tidal height. The ensemble mean wavelength is insensitive to change on the spring-neap scale but varies on an annual basis, apparently in response to changes in sea temperature.

This work was made possible by a grant from the Natural Environment Research Council, which is gratefully acknowledged. We thank the Wells Harbour Commissioners (Mrs C.R. Able, Clerk) for their interest and support; the Institute of Terrestrial Ecology (Mr W.B.E. Avisen) for the use of its equipment store at Wells; the former Anglian Water Authority (Mr K.A. Bokley, Mr L.F. Fillenham and Mr H.F. Messon) for data from the Wells Harbour tide gauge; the Cambridge University Committee for Aerial Photography for special flights; the Bidston Observatory of the Institute of Oceanographic Sciences (Mr G.W. Lennon, Mrs S.M. Shaw) for tidal data; the Taunton Laboratory of the Institute of Oceanographic Sciences (Dr D.N. Langhorne) for the loan of echo-sounder equipment; the MAFF Fisheries Laboratory, Lowestoft (Dr S.R. Jones) for data on sea temperature; and the Storm Tide Warning Service of the Meteorological Office for information on storm surges. We are grateful to our families, and especially to Jean, Jenny and Peter, for their support and help in the field.

References

Allen, G. P., Deresseguier, A. & Klingebiel, A. 1969 Évolution des structures sédimentaire sur un banc sableux d'estuaire en fonction de l'amplitude des marées. *C. r. hebd. Séanc. Acad. Sci., Paris* D**269**, 2167–2169.

Allen, J. R. L. 1968. *Current ripples.* Amsterdam: North-Holland.

Allen, J. R. L. 1969 On the geometry of current ripples in relation to stability of water flow. *Geogr. Annlr* A**51**, 61–96.

Allen, J. R.L. 1973 Features of cross-stratified units due to random and other changes in bed forms. *Sedimentol.* **29**, 189–202.

Allen, J. R. L. 1974 Reaction, relaxation and lag in natural sedimentary systems: general principles, examples and lessons. *Earth Sci. Rev.* **10**, 263–342.

Allen, J. R. L. 1976*a* Computational models for dune time-lag: general ideas, difficulties and early results. *Sediment. Geol.* **15**, 1–53.

Allen, J. R. L. 1976*b* Computational models for dune time-lag: population structures and the effects of discharge pattern and coefficient of change. *Sediment. Geol.* **16**, 99–130.

Allen, J. R. L. 1976*c* Computational models for dune time-lag: an alternative boundary condition. *Sediment. Geol.* **16**, 255–279.

Allen, J. R. L. 1976*d* Time-lag of dunes in unsteady flows: an analysis of Nasner's data from the R. Weser, Germany. *Sediment. Geol.* **15**, 309–321.

Allen, J. R. L. 1976*e* Bed forms and unsteady processes: some concepts of classification and response illustrated by common one-way types. *Earth Surface Proc.* **1**, 361–374.

Allen, J. R. L. 1977 The plan shape of current ripples in relation to flow conditions. *Sedimentol.* **24**, 53–62.

Allen, J. R. L. 1978*a* Polymodal dune assemblages: an interpretation in terms of dune creation-destruction in periodic flows. *Sediment. Geol.* **20**, 17–28.

Allen, J. R. L. 1978*b* Computational models for dune time-lag: calculations using Stein's rule for dune height. *Sediment. Geol.* **20**, 165–216.

Allen, J. R. L. 1980 Sand waves: a model of origin and internal stucture. *Sediment. Geol.* **26**, 281–328.

Allen, J. R. L. 1982 *Sedimentary structures*, vol. 1. Amsterdam: Elsevier.

Allen, J. R. L. 1985 *Principles of physical sedimentology.* London: Allen & Unwin.

Allen, J. R. L. & Friend, P. F. 1976*a* Changes in intertidal dunes during two spring-neap cycles, Lifeboat Station Bank, Wells-next-the-Sea, Norfolk (England). *Sedimentol.* **23**, 329–346.

Allen, J. R. L. & Friend, P. F. 1976b Relaxation time of dunes in decelerating aqueous flows. *J. geol. Soc. Lond.* **132**, 17–26.

Annambhotla, V. S. S., Sayre, W. W. & Livesey, R. H. 1972 Statistical properties of Missouri River bedforms. J. WatWays Harb. Div. Am. Soc. civ. Engrs **98**, 489–510.

Ashley, G. M. 1990 Classification of large-scale aqueous bedforms: a new look at an old problem. *J. sedim. Petrol.* **60**, 160–172.

Banks, N. L. & Collinson, J. D. 1975 The size and shape of small-scale current ripples: an experimental study using medium sand. *Sedimentol.* **22**, 583–599.

Boersma, J. R. & Terwindt, J. H. J. 1981 Neap-spring tide sequences of intertidal shoal deposits in a mesotidal estuary. *Sedimentol.* **28**, 151–170.

Boersma, J. R. 1969 Internal structure of some tidal megaripples on a shoal in the Westerschelde Estuary, The Netherlands. Report of a preliminary investigation. *Geol. Mijnb.* **48**, 409–414.

Boothroyd, J. C. & Hubbard, D. K. 1974 Bed form development and distribution pattern, Parker and Essex estuaries, Massachusetts. *Misc. Pap. U.S. Army Corps Engrs Cstl Engng Res. Center* 1-74, 1–39.

Carey, W. C. & Keller, M. D. 1957 Systematic changes in the beds of alluvial rivers. *J. Hydraul. Div. Am. Soc. civ. Engrs* **83**, 1–24.

Collinson, J. D. 1970 Bedforms of the Tana River, Norway. *Geogr. Annlr* A**52**, 31–56.

Cornish, V. 1901 On sand waves in tidal currents. *Geogr. J.* **18**, 170–200.

Costello, W. R. & Southard, J. B. 1981 Flume experiments on lower-flow-regime bed forms in coarse sand. *J. sedim. Petrol.* **51**, 849–864.

Crickmore, M. J. 1970 Effect of flume width on bed-form characteristics. *J. Hydraul. Div. Am. Soc. civ. Engrs* **96**, 473–496.

Dalrymple, R. W. 1984 Morphology and internal structure of sandwaves in the Bay of Fundy. *Sedimentol.* **31**, 365–382.

Dalrymple, R. W., Knight, R. J. & Lambiase, J. J. 1978 Bedforms and their hydraulic stability relationships in a tidal environment, Bay of Fundy. *Nature, Lond.* **275**, 100–104.

PHILOSOPHICAL TRANSACTIONS OF THE ROYAL SOCIETY A MATHEMATICAL, PHYSICAL & ENGINEERING SCIENCES

Dalrymple, R. W., Knight, R. J., Zaitlin, B. A. & Middleton, G. V. 1990 Dynamics and facies model of a macrotidal sand-bar complex, Cobequid Bay-Salmon River Estuary (Bay of Fundy). *Sedimentol.* **37**, 577–612.

Davis, R. A. & Flemming, B. W. 1991. Time-series study of mesoscale tidal bedforms, Martens Platte, Wadden Sea, Germany. *Can. Soc. Petrol. Geol. Mem.* **16**, 275–282.

De Boer, P. L., Oost, A. P. & Visser, M. J. 1989 The diurnal inequality of the tide as a parameter for recognizing tidal influences. *J. sedim. Petrol.* **59**, 912–921.

De Mowbray, T. & Visser, M. J. 1984 Reactivation surfaces in subtidal channel deposits, Oosterschelde, southwest Netherlands. *J. sedim. Petrol.* **54**, 811–824.

De Raaf, J. F. M. & Boersma, J. R. 1971 Tidal deposits and their sedimentary structures. *Geol. Mijnb.* **50**, 479–504.

Davies, J. L. 1964 A morphogenetic approach to world shorelines. *Z. Geomorph.* **8**, 127–142.

Ehlers, J. 1988 *The morphodynamics of the Wadden Sea.* Rotterdam: Balkema.

Eisma, D. & Kalf, J. 1979 Distribution and particle size of suspended matter in the Southern Bight of the North Sea and eastern Channel. *Neth. J. Sea Res.* **13**, 298–324.

Elliott, T. & Gardiner, A. R. 1981. Ripple, megaripple and sandwave bedforms in the macrotidal Loughor Estuary, South Wales, U.K. *Spec. Publs Int. Assoc. Sediment.* **5**, 51–64.

Flather, R. A. & Davies, A. M. 1978 On the specification of meteorological forcing in numerical models for North Sea storm surge prediction, with application to the surge of 2 to 4 January 1976. *Dt. Hydrogr. Z. Ergänzungsheft* A**15**, 1–51.

Fredsøe, J. 1975 The friction factor and height-length relation in flow over a dune-covered bed. *Prog. Rep. Inst. Hydrodyn. Hydraul. Engng Tech. Univ. Denmark* **37**, 31–36.

Fredsøe, J. 1982 Shape and dimensions of stationary dunes in river. *J. Hydraul. Div. Am. Soc. civ. Engrs* **108**, 932–947.

Führböter, A. 1967 Zur Mechanik der Strömungsriffel. *Mitt. Franzius Inst. Hannover* **29**, 1–35.

Gabel, S. L. 1993. Geometry and kinematics of dunes during steady and unsteady flows in the Calamus River, Nebraska, U.S.A. *Sedimentol.* **40**, 237–267.

Gee, D. M. 1975 Bed form response to unsteady flows. *J. Hydraul. Div. Am. Soc. civ. Engrs* **101**, 437–449.

Gleick, J. 1988 *Chaos.* New York: Viking Penguin.

Guy, H. P., Simons, D. B. & Richardson, E. V. 1966 Summary of alluvial channel data from flume experiments, 1956–61. *Prof. Pap. U.S. geol. Surv.* 461-I, 1–96.

Harding, J. & Binding, A. A. 1978 Windfields during gales in the North Sea and the gales of 3 January 1976. *Meteorol. Mag.* **107**, 164–181.

Hino, M. 1968 Equilibrium-range spectra of sand waves formed by flowing water. *J. Fluid Mech.* **34**, 565–573.

Jackson, R. G. 1976 Largescale ripples of the lower Wabash River. *Sedimentol.* **23**, 593–623.

Jain, S. C. & Kennedy, J. F. 1974 The spectral evolution of sedimentary bed forms. *J. Fluid Mech.* **63**, 301–314.

Jones, S. R. 1981 Ten years of measurement of coastal sea temperatures. *Weather* **36**, 48–55.

Jones, S. R. & Jeffs, T. M. 1991. Near-surface sea temperature in coastal waters of the North Sea, English Channel and Irish Sea. MAFF Directorate of Fisheries Research Lowestoft, Fisheries Research Data Report No. 24, 1–70.

Klein, G. deV. 1970 Depositional and dispersal dynamics of intertidal sand bars. *J. sedim. Petrol.* **40**, 1095–1127.

Kohsiek, L. H. M. & Terwindt, J. H. J. 1981 Characteristics of foresets and topset bedding in megaripples related to hydrodynamic conditions on an intertidal shoal. *Specl. Publs Int. Assoc. Sediment.* **5**, 27–37.

Kostaschuk, R. A., Church, M. A. & Luternauer, J. L. 1989 Bedforms, bed material, and bedload transport in a salt-wedge estuary: Fraser River, British Columbia. *Can. J. Earth Sci.* **26**, 1440–1452.

Langhorne, D. N. 1982 A study of the dynamics of a marine sandwave. *Sedimentol.* **29**, 571–594.

PHILOSOPHICAL TRANSACTIONS OF THE ROYAL SOCIETY A MATHEMATICAL, PHYSICAL & ENGINEERING SCIENCES

Langhorne, D. N., Malcolm, J. O. & Read, A. A. 1985 Observations of changes of intertidal bedforms over a spring-neap tidal cycle. *Rep. Inst. Oceanogr. Sci.* **203**, 1–101.

May, R. M. 1973 *Stability and complexity in model ecosystems.* Princeton University Press.

McCabe, P. J. & Jones, C. M. 1977 Formation of reactivation surfaces within superimposed deltas and bedforms. *J. sedim. Petrol.* **47**, 707–715.

McCave, I. N. 1971 Sand waves in the North Sea off the coast of Holland. *Marine Geol.* **10**, 199–225.

McIntyre, R. J. 1979 Analytical models for west coast storm surges, with application to events of January 1976. *Appl. math. Modelling* **3**, 89–98.

Nakagawa, A. H. & Tsujimoto, T. 1983 Time-lag appearing in unsteady flow with sand waves. *J. Hydrosci. Hydraul. Engng Japan Soc. civ. Engrs* **1**, 83–95.

Nakagawa, H., Tsujimoto, T. & Yada, A. 1978. On relation between bed configurations and sediment transport, and deformation processes of sand waves. *Annls Disaster Prev. Res. Inst. Kyoto Univ.* 21B-2, 385–405.

Nasner, H. 1974 Über des Verhalten von Transportkörpern im Tidegebiet. *Mitt. Franzius Inst. Hannover* **40**, 1–149.

NEDECO (Netherlands Engineering Consultants) 1959 *River studies and recommendations on improvement of Niger and Benue.* Amsterdam: North-Holland.

Nordin, C. F. 1971 Statistical properties of dune profiles. *Pap. U.S. geol. Surv.* 562F, 1–41.

Nordin, C. F. & Algert, J. H. 1966 Spectral analysis of sand waves. *J. Hydraul. Div. Am. Soc. civ. Engrs* **92**, 95–114.

O'Loughlin, E. M. & Squarer, D. 1967 Areal variations of bed-form characteristics in meandering streams. *Proc. 12th Congr. Int. Assoc. Hydraulics Res.* **2**, 118–127.

Peters, J. J. 1971 *La dynamique de la sédimentation de la region divagante du bief maritime du Fleuve Congo.* Borgerhout, Belgium: Labortoire de Recherche Hydrauliques.

Pratt, C. J. & Smith, K. V. H. 1972 Ripple and dune phases in narrowly graded sand. *J. Hydraul. Div. Am. Soc. civ. Engrs* **98**, 859–874.

Pretious, E. S. & Blench, T. 1951 Final report on special observations of bed movement in Lower Fraser River at Ladner Reach during 1950 freshet. Rep. Nat. Res. Council Canada, Fraser River Model, Vancouver, Canada.

Raichlen, F. & Kennedy, J. F. 1965 The growth of sediment bed forms from an initially flattened bed. *Proc. 11th Congr. Int. Assoc. Hydraulics Res.* **1**, 1–8.

Reineck, H. -E. 1963 Sedimentgefüge im Bereich der südlichen Nordsee. *Abh. senck. naturf. Ges.* **505**, 1–138.

Rossiter, J. R. 1954 The North Sea storm surge of 31 January and 1 February 1953. *Phil. Trans. R. Soc. Lond.* **A246**, 371–400.

Rubin, D. M. & McCullogh, D. S. 1980 Single and superimposed bedforms: a synthesis of San Francisco Bay and flume studies. *Sediment. Geol.* **26**, 207–331.

Sawai, K. 1988 Transformation of sand waves due to the time change of flow conditions. *J. Hydrosci. Hydraul. Engng Japan Soc. civ. Engrs* **5**, 1–14.

Shaw, M. S., Hopkins, J. S. & Caton, P. G. F. 1976 The gales of January 1976. *Weather* **31**, 172–183.

Shen, H. W. & Cheong, H. F. 1977 Statistical properties of sediment bed profile. *J. Hydraul. Div. Am. Soc. civ. Engrs* **103**, 1303–1321.

Shinohara, K. & Tsubaki, T. 1959 On the characteristics of sand waves formed upon the beds of open channels. *Rep. Res. Inst. Appl. Mech. Kyushu Univ.* **7**(25), 15–45.

Simons, D. B. & Richardson, E. V. 1962 Resistance to flow in alluvial channels. *Trans. Am. Soc. civ. Engrs* **127**, 927–953.

Simons, D. B., Richardson, E. V. & Nordin, C. F. 1965*a* Bedload equation for ripples and dunes. *Prof. Pap. U.S. geol. Surv.* 462-H, 1–9.

Simons, D. B., Richardson, E. V. & Nordin, C. F. 1965*b* Sedimentary structures generated by flow in alluvial channels. *Spec. Publs Soc. Econ. Pal. Mineral.* **12**, 34–52.

PHILOSOPHICAL TRANSACTIONS OF THE ROYAL SOCIETY A MATHEMATICAL, PHYSICAL & ENGINEERING SCIENCES

Southard, J. B. & Boguchwal, L. A. 1990*a* Bed configurations in steady unidirectional flows. Part 2. Synthesis of flume data. *J. sedim. Petrol.* **60**, 658–679.

Southard, J. B. & Boguchwal, L. A. 1990*b* Bed configurations in steady unidirectional water flows. Part 3. Effects of temperature and gravity. *J. sedim. Petrol.* **60**, 680–686.

Squarer, D. 1970 Friction factors and bed forms in fluvial channels. *J. Hydraul. Div. Am. Soc. civ. Engrs* **96**, 995–1017.

Steers, J. A., Stoddart, D. R., Bayliss-Smith, T. P., Spencer, T. & Durbridge, P. M. 1979 The storm of 11 January 1978 on the east coast of England. *Geogr. J.* **145**, 192–205.

Stein, R. A. 1965 Laboratory study of total load and apparent bed load. *J. geophys. Res.* **70**, 1831–1842.

Stewart, I. 1990 *Does God play dice? The mathematics of chaos*. London: Penguin Books.

Stride, A. H. 1982 *Offshore tidal sands*. London: Chapman & Hall.

Stückrath, T. 1969 Die Bewegung von Grossrippeln an der Sohle des Rio Paraná. *Mitt Franzius Inst. Hannover* **32**, 267–293.

Summers, D. 1978 *The East Coast floods*. Newton Abbot: David & Charles.

Suthons, C. T. 1963 Frequency of occurence of abnormally high sea levels on the east and south coasts of England. *Proc. Instn civ. Engrs* **25**, 433–450.

Taylor, B. D. 1971 Temperature effects in alluvial streams. Rep. W.M. Keck Lab. Hydraul. Wat. Res. Calif. Inst. Techn KH-R-27, 1–204.

Terwindt, J. H. J. 1975 Sequences in inshore tidal deposits. In *Tidal deposits* (ed. R.N. Ginsburg), pp. 85–89. Berlin: Springer-Verlag.

Terwindt, J. H. J. 1981 Origin and sequences of sedimentary structures in inshore mesotidal deposits of the North Sea. *Spec. Publs Inst. Assoc. Sediment.* **5**, 4–26.

Terwindt, J. H. J. 1988 Palaeo-tidal reconstructions of inshore tidal depositional environments. In *Tide-influenced sedimentary environments* (ed. P.L. De Boer, A. Van Gelder & S.-D. Nio), pp. 233–263. Dordrecht: Riedel.

Terwindt, J. H. J. & Brouwer, M. J. N. 1986 The behaviour of intertidal sandwaves during neap-spring tide cycles and the relevance for palaeoflow reconstructions. *Sedimentol.* **33**, 1–31.

Thompson, J. M. T. & Stewart, H. B. 1986 *Nonlinear dynamics and chaos*. Chichester: Wiley.

Tsujimoto, T. & Nakagawa, H. 1984 Unsteady behaviour of dunes. In *Channels and channel control structures* (ed. K.V.H. Smith), pp. 5-85 to 5-99. Berlin: Springer-Verlag.

Tucker, M. E. 1973 The sedimentary environments of tropical African estuaries: Freetown Peninsula, Sierra Leone. *Geol. Mijnb.* **52**, 203–215.

USWES (U.S. Waterways Experiment Station) 1935 Studies of river bed materials and their movement with special reference to the lower Mississippi River. *Pap. U.S. WatWays Expt. Stn* **17**, 1–161.

Van den Berg, J. H. 1982 Migration of large-scale bedforms and preservation of cross-bedded sets in highly accretionary parts of tidal channels in the Oosterschelde, SW Netherlands. *Geol. Mijnb.* **61**, 253–263.

Visser, M. J. 1980 Neap-spring cycles reflected in Holocene subtidal large-scale bedform deposits: a preliminary note. *Geol.* **8**, 543–546.

Visser, M. P. 1970 The turbidity of the southern North Sea. *Dt. hydrogr. Z.* **17**, 197–201.

Wijbenga, J. H. A. & Klaasen, G. J. 1983 Changes in bedform dimensions under unsteady flow conditions in a straight flume. Spec. Publs Int. Assoc. *Sediment.* **6**, 35–48.

Williams, G. P. 1970 Flume width and water depth effects in sediment transport experiments. *Prof. Pap. U.S. geol. Surv.* 562-H, 1–37.

Yalin, M. S. 1975 On the development of sand waves in time. *Proc. 16th Congr. Int. Assoc. Hydraul. Res.* **2**, 212–219.

Yalin, M. S. & Karahan, E. 1979 Steepness of sedimentary dunes. *J. Hydraul. Div. Am. Soc. civ. Engrs* **105**, 381–392.

Received 29 June 1992; accepted 21 May 1993

PHILOSOPHICAL TRANSACTIONS OF THE ROYAL SOCIETY A MATHEMATICAL, PHYSICAL & ENGINEERING SCIENCES

PHILOSOPHICAL TRANSACTIONS OF THE ROYAL SOCIETY A MATHEMATICAL, PHYSICAL & ENGINEERING SCIENCES

igure 2. Oblique aerial view of Lifeboat Station Bank looking north past the sea wall and ifeboat Station to Bob Hall's Sands (see also figure 1). The distance across the foreground easures about 300 m, and across the background about 1 km. Arrows show facing direction of edforms, as observed at low tide.

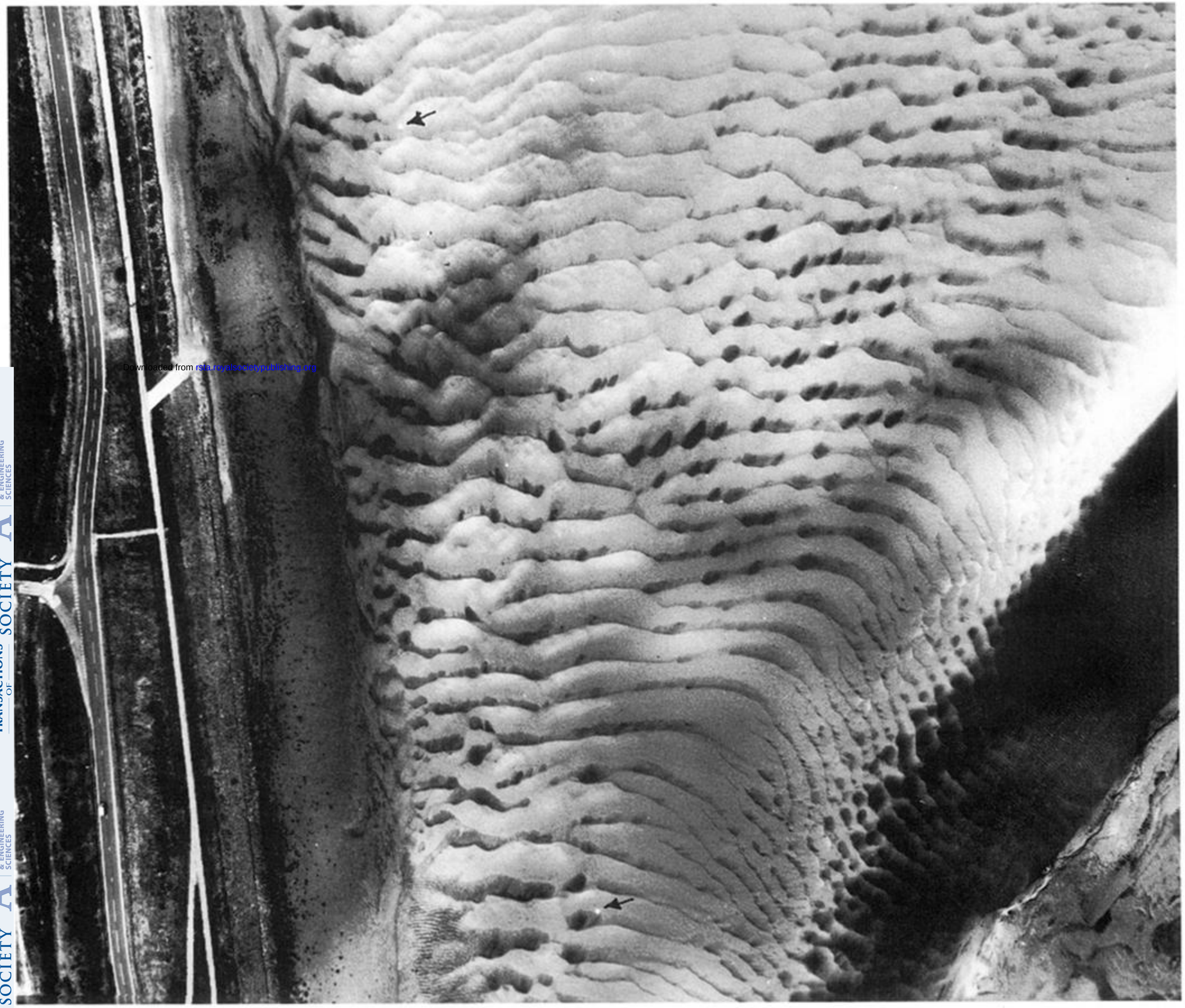

Figure 15. Vertical air photograph of dunes on the sampling range at Lifeboat Station Bank. The black discs (arrowed) mark the buoys at the ends of the range. The photograph shows an area measuring approximately 260m × 300m. See also figure 1.

PHILOSOPHICAL TRANSACTIONS OF THE ROYAL SOCIETY A MATHEMATICAL, PHYSICAL & ENGINEERING SCIENCES

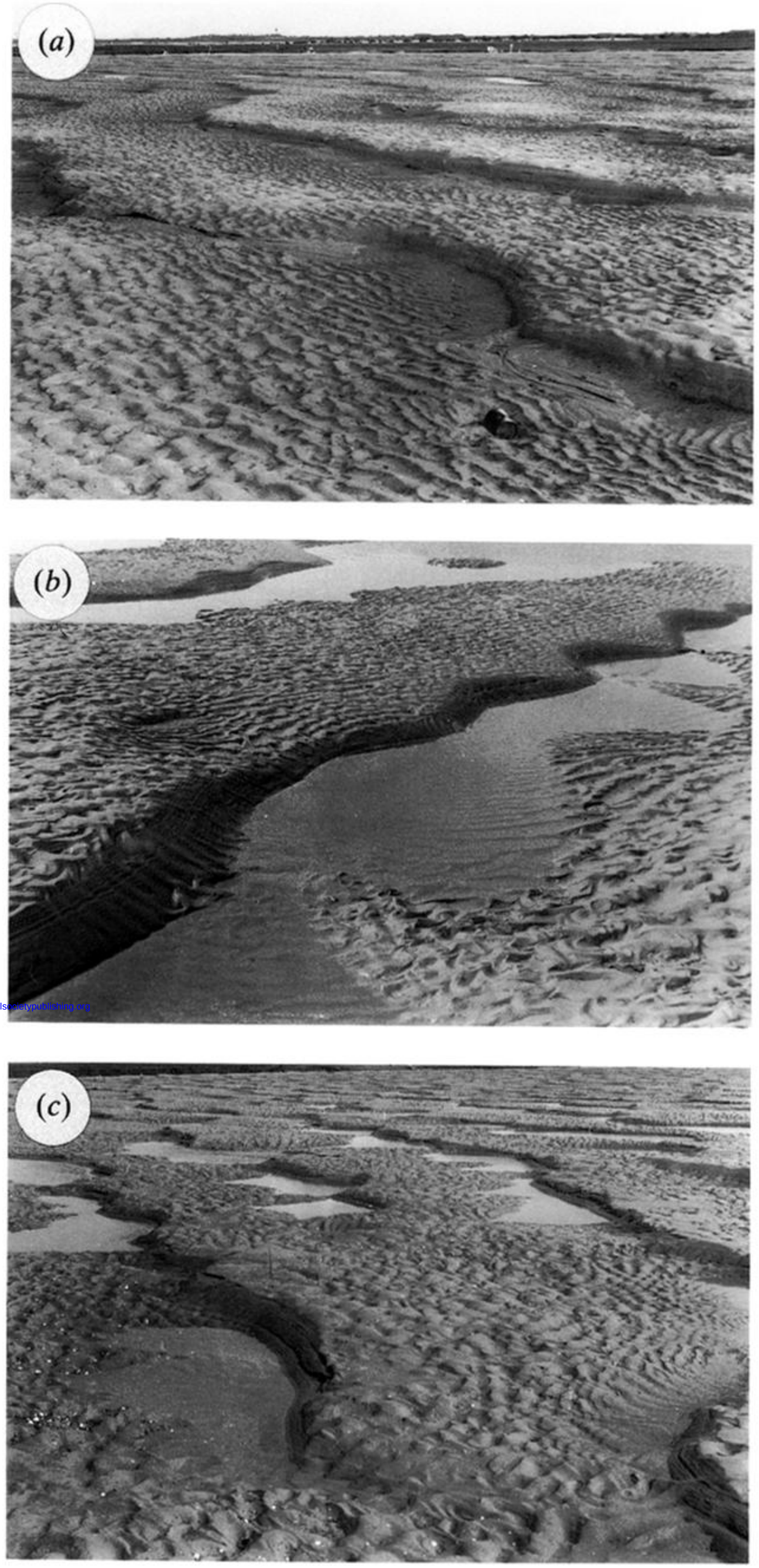

Figure 17. (*a*) Low-energy mature dunes. Flow from upper right. Current ripples have wavelength of about 0.15 m. (*b*) Low-energy mature dunes. Flow from upper left. Wavelength of current ripples about 0.15 m. (*c*) High-energy mature dunes. Flow from upper right. Wavelength of current ripples about 0.15 m.

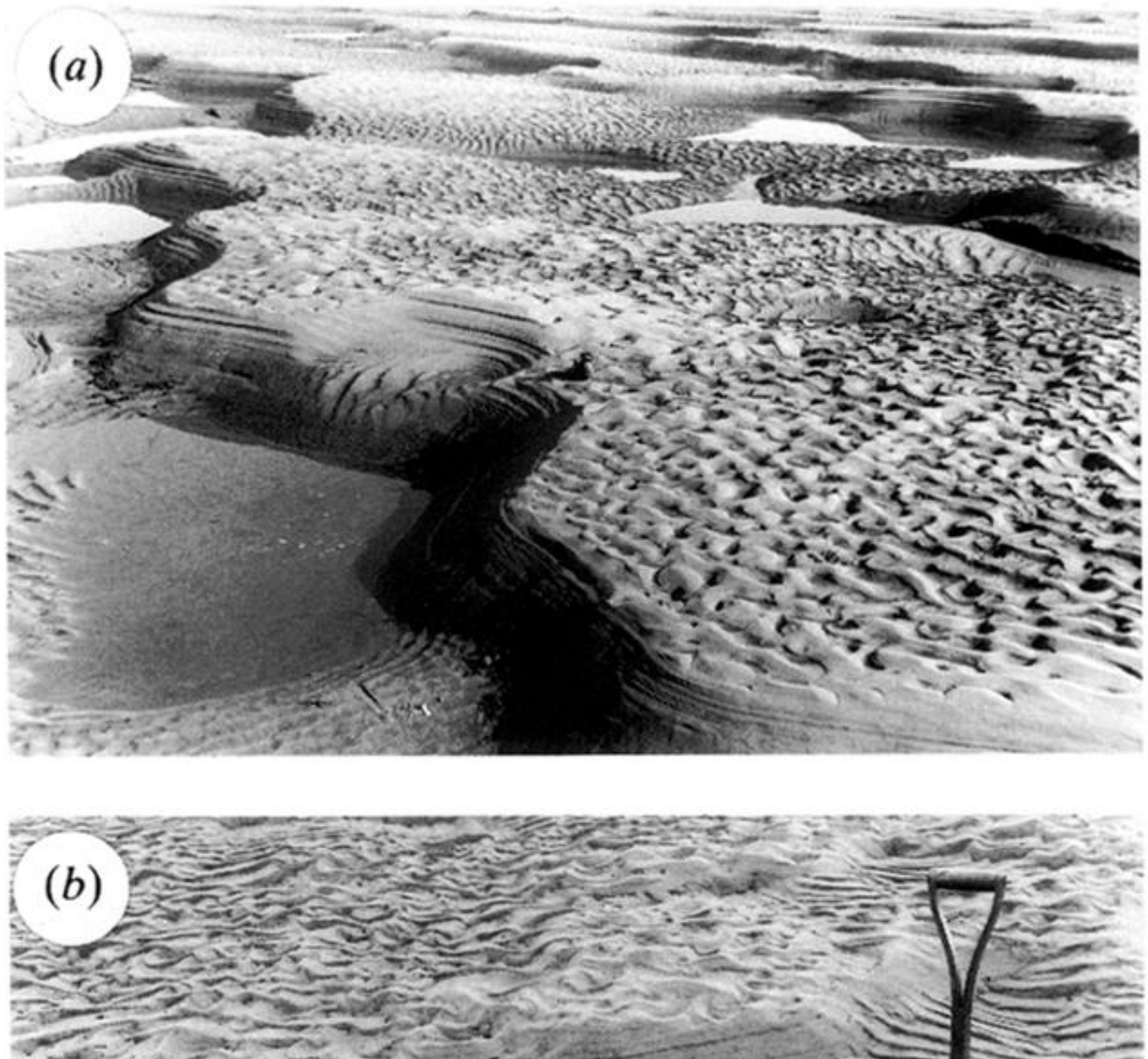

Figure 18. (*a*) High-energy mature dunes. Flow from upper right. Current ripples have wavelength of about 0.15 m. (*b*) Mature dune with a supplementary crest, viewed from leeward. Current from upper left. Spade about 0.9 m tall. (*c*) Mature dune with superimposed nascent forms, viewed from leeward. Flow toward observer. Spade about 0.9 m tall.

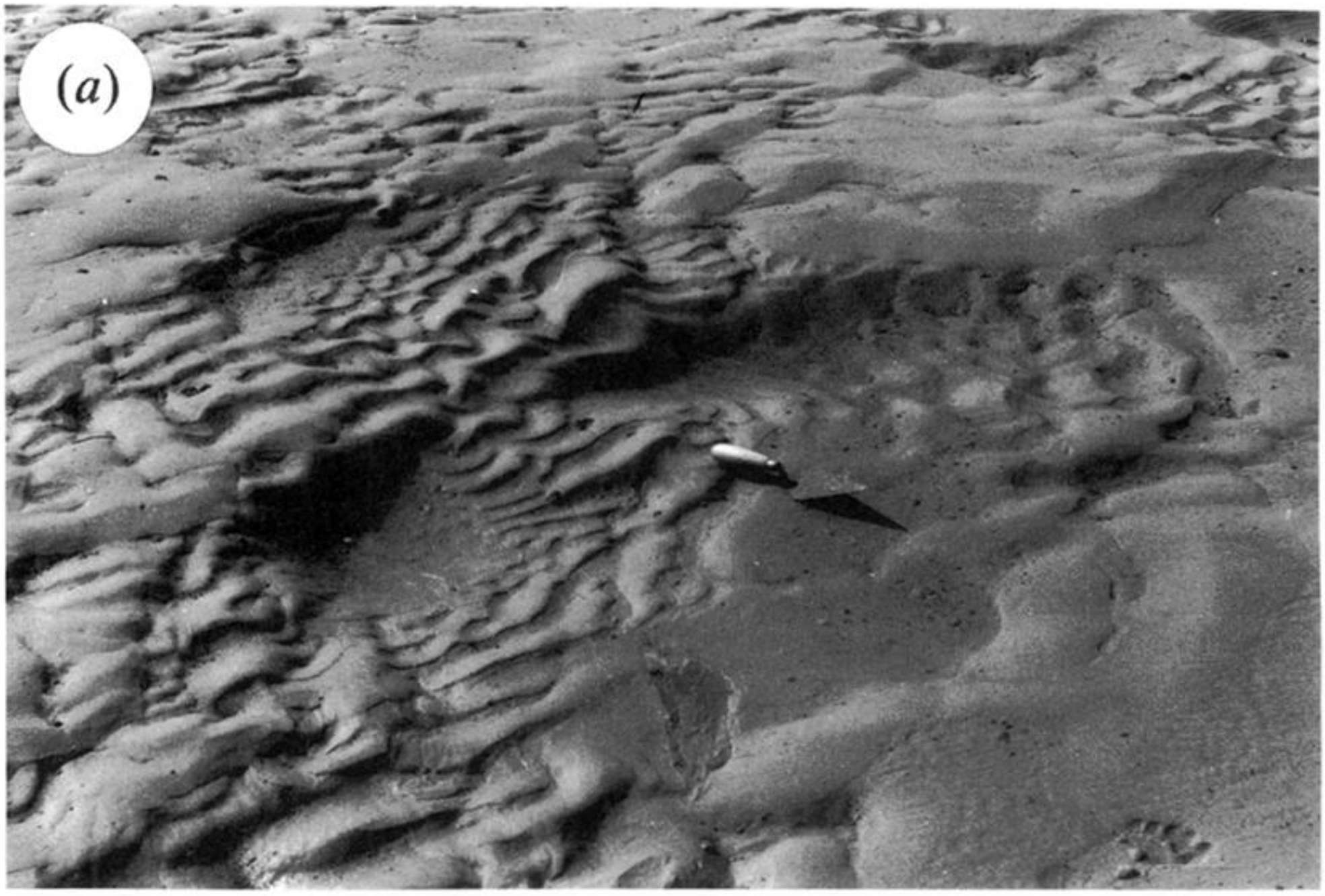

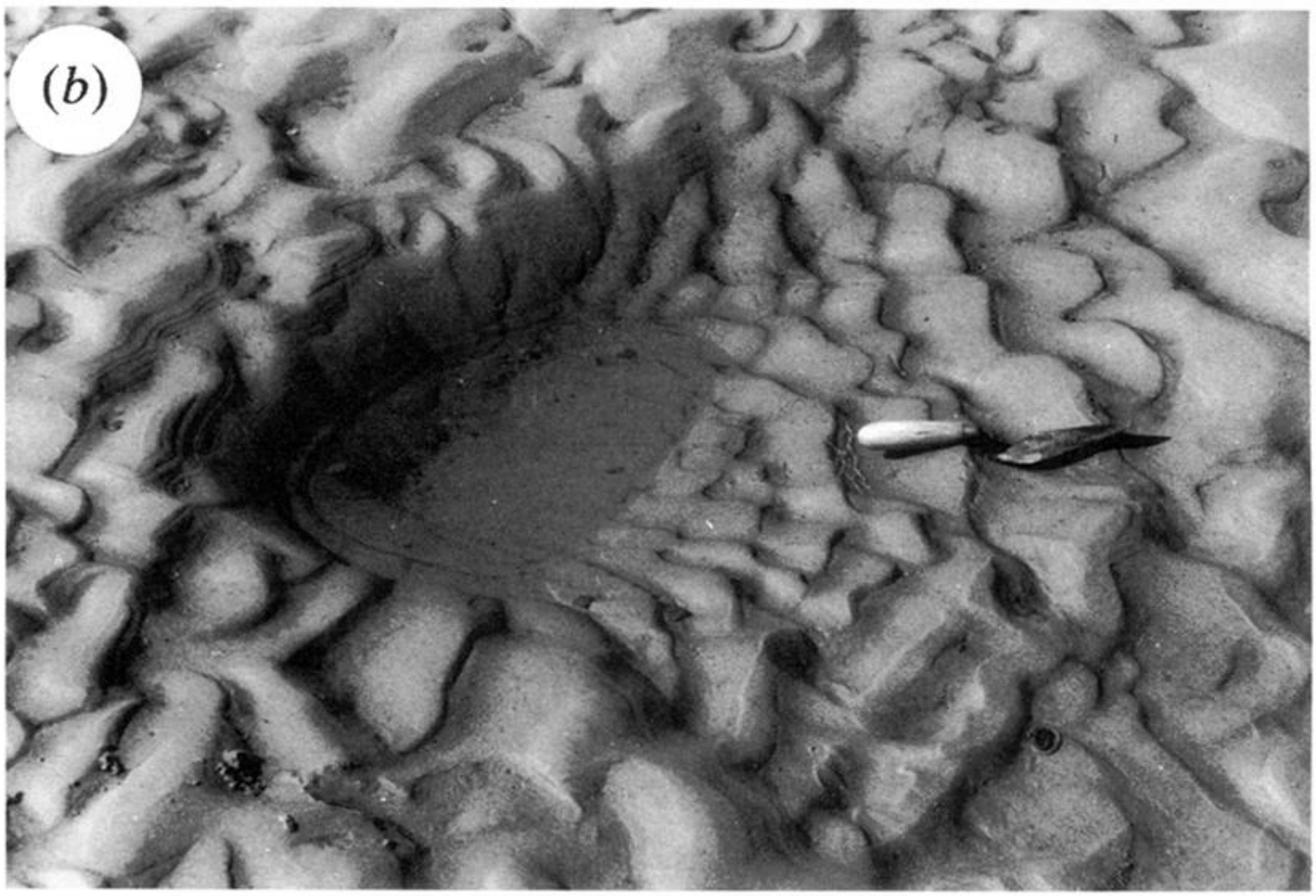

PHILOSOPHICAL TRANSACTIONS OF THE ROYAL SOCIETY A MATHEMATICAL, PHYSICAL & ENGINEERING SCIENCES

igure 19. Forms of nascent dune. Current from upper left in (a), (c), (d) and from left in (b). Trowel about 0.28 m long.

Figure 19. Continued.

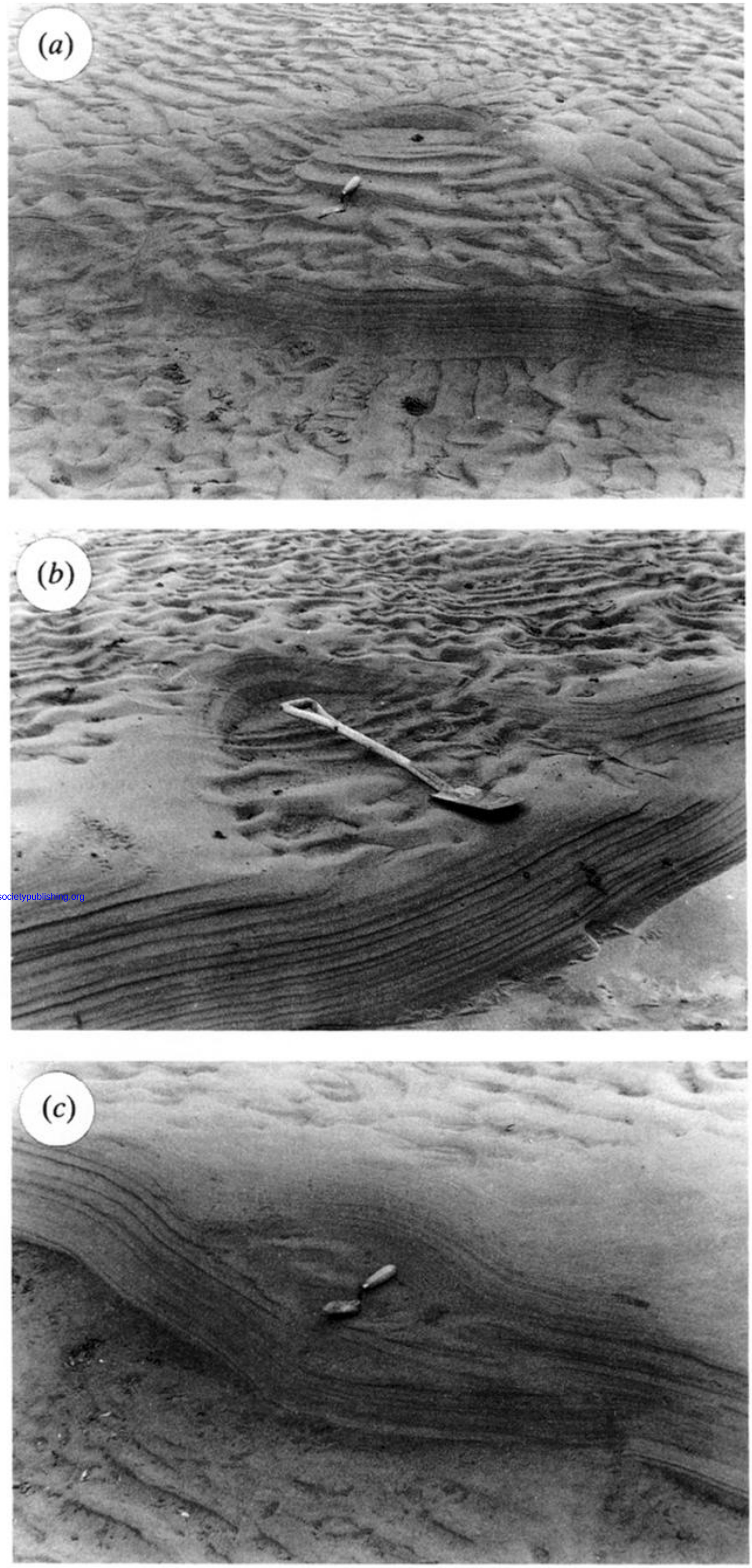

Figure 23. Photographs of selected nascent dunes to illustrate the progressive replacement of a portion of the crest of a mature dune by the crest of a nascent dune advancing upon it from upstream. See also figure 16*e*–*g*. Trowel (0.28 m) and spade (0.94 m) point in current direction.

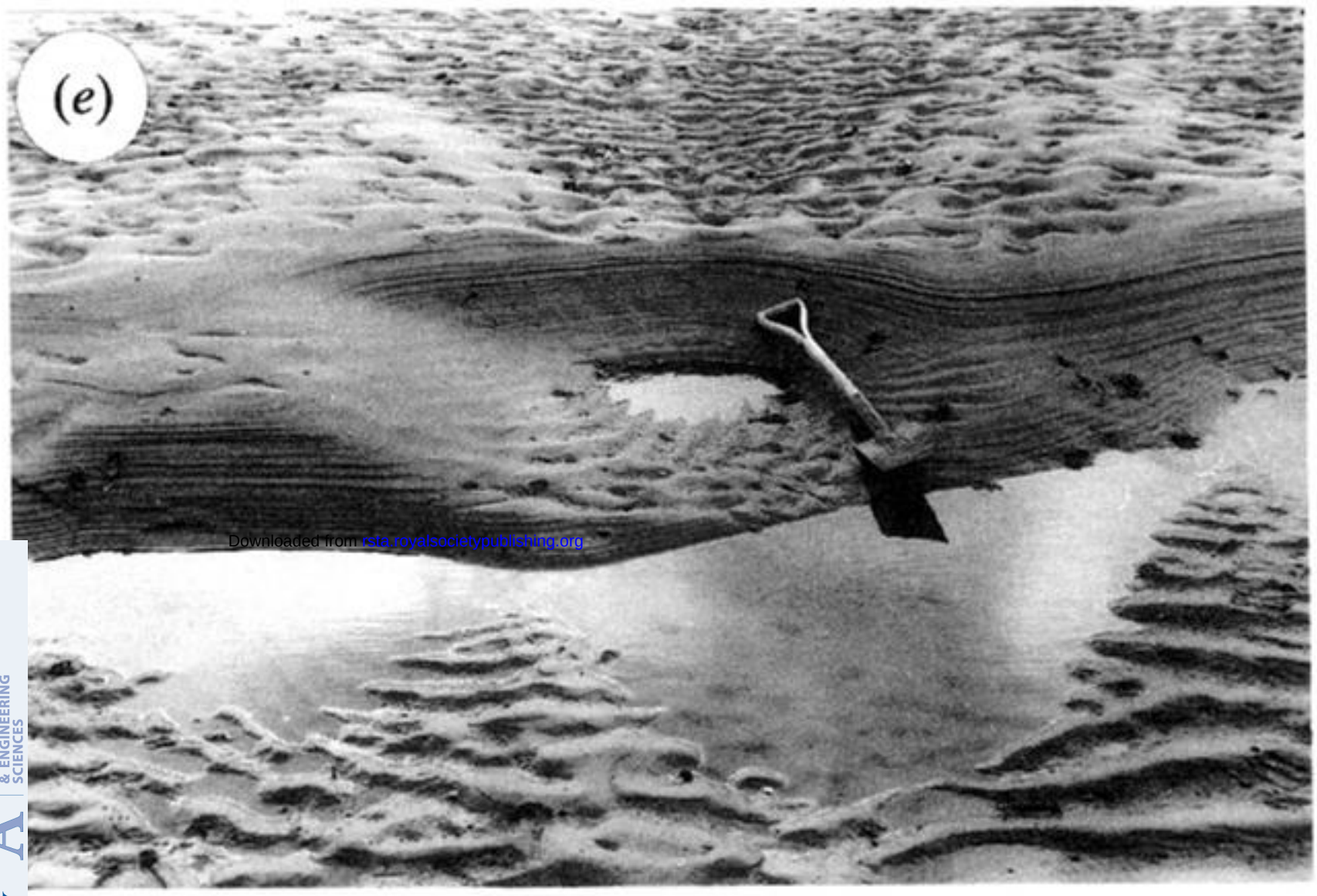

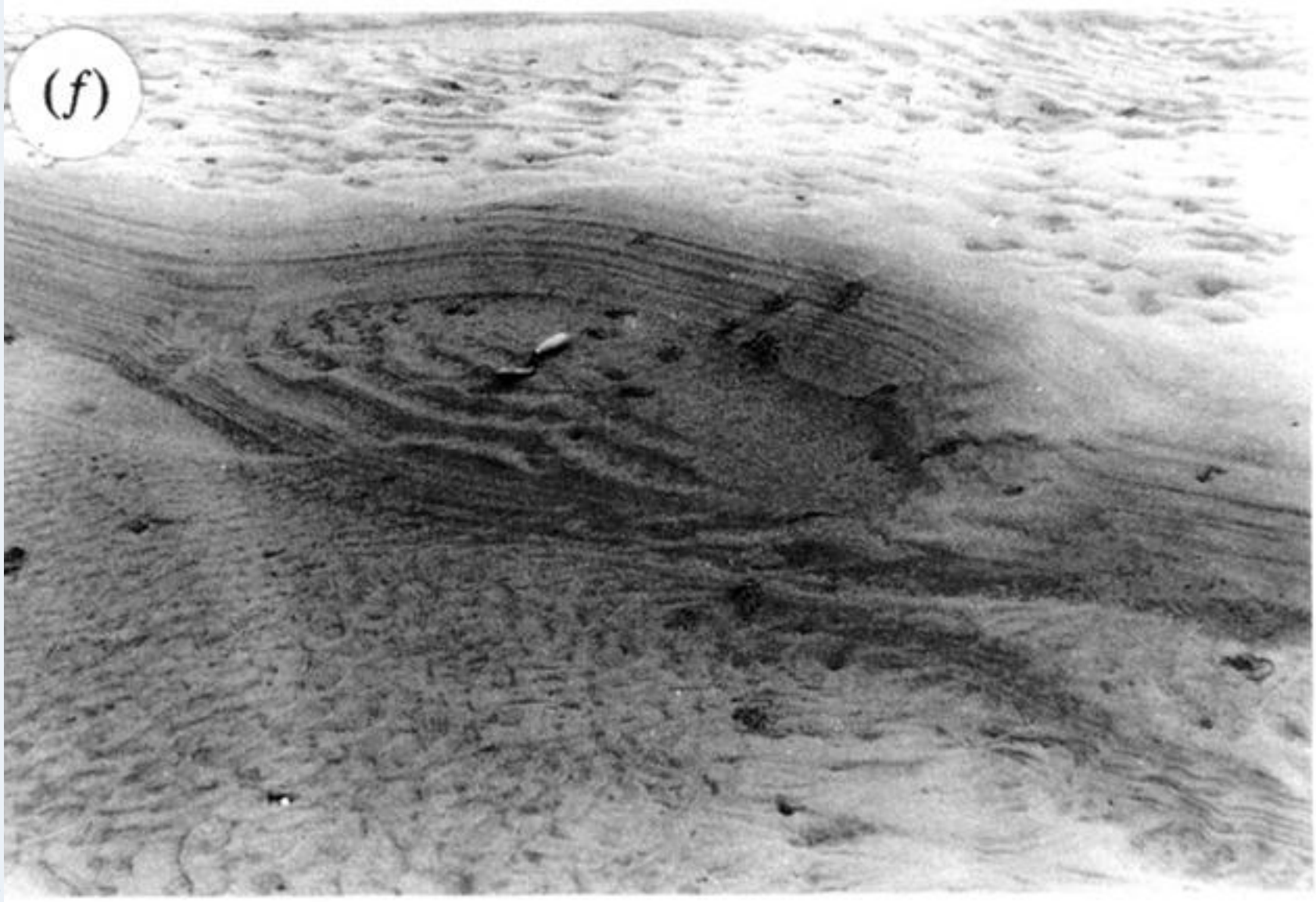

Figure 23. See opposite for caption.

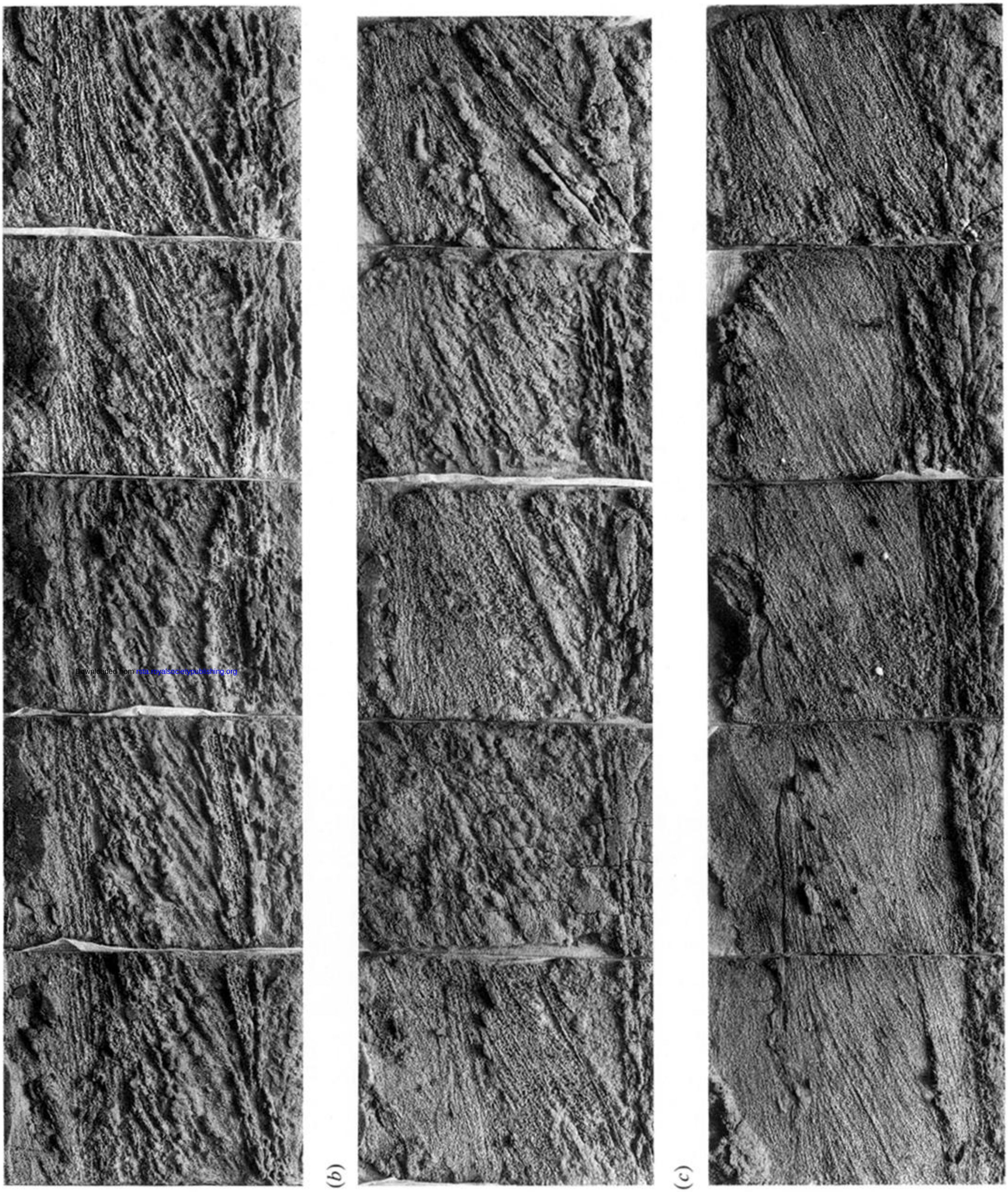

Figure 29. Sets of photographs of representative relief casts (to be read from left to right). (*a*) P4, (*b*) P8, (*c*) P12. Each composite peel is approximately 1.3 m long. See also figure 28.